



MATERIAL TRANSPORT ON OSCILLATING CONVEYORS

by

Howard A. Gaberson

B. S. M. E. , University of Michigan
(1955)

S. M. , Massachusetts Institute of Technology
(1957)

Submitted in Partial Fulfillment of the
Requirements for the Degree of

DOCTOR OF PHILOSOPHY

at the

MASSACHUSETTS INSTITUTE OF TECHNOLOGY

January, 1967

Signature of Author

Department of Mechanical Engineering,
January 9, 1967

Certified by.

Thesis Supervisor

Accepted by.

Chairman, Department Committee
on Graduate Students

ABSTRACTMATERIAL TRANSPORT ON OSCILLATING CONVEYORS

Howard A. Gaberson

Submitted to the Department of Mechanical Engineering on January 9, 1967 in partial fulfillment of the requirement for the degree of Doctor of Philosophy.

Abstract

This thesis presents a theory that predicts the motion of particles on an important class of practical oscillating conveyors. The trough of these conveyors undergoes a straight-line harmonic translational oscillation in a direction inclined to the trough. The trough may be inclined to the horizontal. The thesis considers operating conditions in which the amplitude of the oscillation is great enough to cause small flights of the particles once each cycle, which conditions are met in most practical conveyors. Experimental evidence, over a wide range of operating conditions, is presented, and it verifies the theory. Thus far, only a very few, over-simplified analyses of specific cases have been presented in the literature.

Most of the theoretical work is concentrated on a single particle on an oscillating plane. The coordinate system is oriented to the plane which permits separation of the two motion components regardless of plane inclination, (Fig. 1, page 19). The motion perpendicular to the plane has only two forms; it is either on the plane or off the plane and flying. This perpendicular motion is defined by Eq. (11b) on page 25. The motion parallel to the plane has four forms: sliding forward and backward, riding, and flying. As the operating conditions vary, the solutions are comprised of many different combinations of these four motion forms. Every solution is piecewise linear. The difficulties arise in matching the boundary conditions between the linear segments of the solution. A set of rules and conditions is developed restricting the possible combinations, Section 2.8.13. Finally, a set of solution routines are developed and programmed for computation on a digital computer. They test the operating conditions to see if one of nine combinations of motion forms yield a solution. Six of these combinations have been found adequate to describe the motions of all systems having parameters in the practical range, i. e., $-5^{\circ} < \beta < 5^{\circ}$; $30^{\circ} < \alpha < 47^{\circ}$; $0.2 \leq \mu < 1.0$; $0 \leq \epsilon < 1.0$; $1.15 \leq A \leq 2.0$; where the meaning of the notations is shown on page 9.

The coefficient of friction, μ , was a significant factor greatly affecting the theoretical solution. However, the need for another parameter became apparent upon analysis of the experimental data. To obtain satisfactory agreement between theory and experiment, a separate different "impact coefficient of friction, $\epsilon \mu$ ", had to be used in addition to the "sliding coefficient of friction, μ ". Interestingly enough, no separate "static coefficient of friction" was found necessary to explain the data. A zero coefficient of restitution in impact proved sufficiently accurate to predict the experimental results.

A general conveyor motion simulator was built to test the theory, (Figs. 10 and 11, pages 69, 70). It provided the oscillating plane for the single particle study and was fitted with a transparent fronted channel for the study of granular materials (Figs. 12 and 13, page 71). Data was taken photographically by a multiple flash technique which was capable of recording 30 points per cycle of one-third second duration, providing quite detailed information about the particle motion. (Figs. 14, a, b, c, d, e, page 73).

Many experiments were run on single particles and on granular materials for a wide range of operating conditions. The agreement between theory and experiment is very good; the transition between motion forms occurs as predicted. The coefficient of sliding friction was measured by noting the minimum static angle of the plane for which the particles remained sliding at constant speed.

Experimentally the bed of granular material was found to move essentially as a slug. It appeared to differ from a single particle only in having increased friction because of the walls of the channel. Hence, the theory developed in thesis for a single particle is applicable directly to beds of granular material.

Thesis Supervisor: J. P. Den Hartog
Title: Professor of Mechanical Engineering

ACKNOWLEDGEMENTS

I am indebted to Professor J. P. Den Hartog, the Chairman of my Thesis Committee, for his suggestion of this topic and for his patient help and encouragement throughout this study. I am also grateful to Professors N. C. Dahl and R. W. Mann, who helped me by serving on my thesis committee and offering advice in the direction of my research. Thanks are also due to Mr. J. M. Morris of the Carrier Division of Rex Chainbelt, Inc., Louisville, Kentucky, who spent a great deal of time with me explaining the practical industrial applications of these machines. In addition, I would like to thank Professors W. M. Murray and W. M. Rohsenow who many times have offered encouragement and assistance when problems arose.

I must acknowledge the support of the National Science Foundation who supported my study for 19 months by awarding me two Science Faculty Fellowships. I have also received generous support from the Mechanical Engineering Department in the form of a Wilfred Lewis Fellowship. I also acknowledge the support of the staff in the Computer Room of the M. I. T. Aeroelastic and Structures Research Laboratory, where all of the numerical calculations were carried out.

Finally I must acknowledge the wonderful help given me in the final preparation of this report. Mr. Domenic Leone prepared the drawings and photographs, as well as guided the final assembly of the report. Miss Carol Laverdiere and Mrs. Jane Benson did much of the nontechnical typing as well as the proof reading. Mrs. Nancy Jordan did the technical typing.

TABLE OF CONTENTS

| | Page |
|---|------|
| Abstract | 2 |
| Acknowledgements | 4 |
| Table of Contents | 5 |
| List of Figures | 7 |
| List of Tables | 9 |
| List of Symbols | 10 |
| Chapter I | |
| Introduction | 14 |
| Chapter II | |
| Theoretical Analysis | 18 |
| 2.1 The Scope of the Study | 18 |
| 2.2 The Model and the Coordinate Systems | 19 |
| 2.3 The Dynamic Equilibrium of the Particle | 20 |
| 2.4 The Necessary Range of the Angles α and β | 22 |
| 2.5 Initial Observations | 24 |
| 2.6 The Y Motion of the Particle | 24 |
| 2.7 X Motion of the Particle | 31 |
| 2.8 Rules and Conditions for Predicting Transitions Between X Motion Forms | 36 |
| 2.9 General Observations about the Solutions | 47 |
| 2.10 Solutions without a Ride | 50 |
| 2.11 Solutions with a Ride | 58 |
| 2.12 Further Comments on the Computations | 60 |
| 2.13 The Application of the Single Particle Theory to Granular Solids in Troughs | 64 |

TABLE OF CONTENTS

| | Page |
|--|------|
| Chapter III | |
| Experimental Analysis | 68 |
| 3. 1 Description of the Apparatus | 68 |
| 3. 2 Experimental Procedure | 74 |
| 3. 3 Processing the Data | 77 |
| 3. 4 Final Comments on the Experimental Analysis | 79 |
| Chapter IV | |
| A Comparison of the Theoretical and Experimental Analyses | 80 |
| 4. 1 Introductory Comments | 80 |
| 4. 2 The Comparison | 81 |
| 4. 3 Final Comments on the Comparison | 102 |
| Chapter V | |
| Concluding Remarks, Comparisons, Recommendations for Further Research | 103 |
| Appendix A1 | |
| Theoretical Details | 106 |
| Appendix A2 | |
| The Fortran Programs of the Solution Routines | 130 |
| Appendix A3 | |
| Details of Experimental Apparatus | 155 |
| Bibliography | 162 |
| Biographical Note | 164 |

LIST OF FIGURES

| | | Page |
|-----|--|------|
| 1. | The Coordinate Systems and the Angles | 19 |
| 2. | Free Body Diagram of Particle | 20 |
| 3. | $\alpha < \beta$, $\alpha > \beta$. | 22 |
| 4. | Time of Flight (τ_1) and Time of Impact (τ_2) as Functions of the Generalized Amplitude, Λ . | 23 |
| 5. | Diagram Depicting the Results of an Impact on X Motion. | 45 |
| 6. | Displacement as a Function of Time for Various Values of ϵ . | 60 |
| 7. | Distribution of Solution Forms with A and ϕ for $\zeta = 1.0$, $\epsilon = 1.0$. | 62 |
| 8. | Distribution of Solution Forms with A and ϕ for $\zeta = 1.0$, $\epsilon = 0.5$. | 63 |
| 9. | Diagram of Coordinates and Dimensions of a Bed of Granular Material. | 65 |
| 10. | Conveyor Motion Simulator. | 69 |
| 11. | Oblique View of Conveyor Motion Simulator. | 70 |
| 12. | The Transparent-Fronted Channel Filled with Rice, showing the Dyed Marking Grains. | 71 |
| 13. | Looking Down on the Transparent-Fronted Channel. | 71 |
| 14. | Typical Data Photographs. | 73 |
| 15. | Experimental Case 1. | 83 |
| 16. | Experimental Case 2. | 85 |
| 17. | Experimental Case 3. | 87 |
| 18. | Experimental Case 4. | 89 |

LIST OF FIGURES

| | Page |
|---------------------------|------|
| 19. Experimental Case 5. | 89 |
| 20. Experimental Case 6. | 92 |
| 21. Experimental Case 7. | 94 |
| 22. Experimental Case 8. | 96 |
| 23. Experimental Case 9. | 98 |
| 24. Experimental Case 10. | 100 |

LIST OF TABLES

| | | Page |
|----------|--|------|
| Table 1 | Non-Dimensionalized Operating Conditions | 32 |
| Table 2 | Summary of Particles | 74 |
| Table 3 | Data Summary | 82 |
| Table A1 | | 106 |

List of Symbols

| | |
|---------------------|---|
| a | displacement amplitude of plane oscillation |
| A | generalized amplitude Eq. (11b) |
| F | friction force Eq. (2b) |
| F_{ag} | Force available for a Slide G Eq. (33a) |
| \overline{F}_{ag} | $\frac{F_{ag}}{m a \omega^2}$ |
| F_{al} | Force available for a Slide L Eq. (34a) |
| F_r | Required force Eq. (32a) |
| \overline{F}_r | $\frac{F_r}{m a \omega^2}$ |
| $F(x)$ | a function of x, Eq. (44b) |
| $F'(x)$ | $\frac{d(F(x))}{dx}$ |
| g | acceleration of gravity |
| h | height of bed of granular material |
| l | length of bed of granular material |
| m | mass of particle |
| N | normal force Eq. (2a) |
| p | pressure in bed of granular material |

List of Symbols

| | |
|----------------------|--|
| R | T_2/T_1' - Eq. (A1. 6) |
| t | time |
| T | period of oscillation |
| t_1 | time of flight Eq. (11a) |
| T_1 | $\tau_1 - \pi/2$ |
| T_2 | $\tau_2 - \pi/2$ |
| t_1' | time at end of fly definite zone Eq. (12b) |
| T_1' | $\tau_1' - \pi/2$ |
| w | width of bed of granular material |
| X | x/a |
| \dot{X} | $\dot{x}/a\omega$ |
| \ddot{X} | $\frac{\ddot{x}}{a\omega^2}$ |
| \dot{x}_{avg} | average x velocity |
| x, y | displacements of particle - Fig. 1 |
| \dot{x}, \dot{y} | velocities of particle |
| \ddot{x}, \ddot{y} | accelerations of particle |
| X_i | initial non dimensional x displacement |
| \dot{X}_i | initial non dimensional x velocity |
| x_{new} | new value of x in iterative solution Eq. (44b) |
| X' | x'/a |
| \dot{X}' | $\frac{\dot{x}'}{a\omega}$ |
| \ddot{X}' | $\frac{\ddot{x}'}{a\omega^2}$ |

List of Symbols

| | |
|------------------------|---|
| x', y' | displacements of plane - Fig. 1 |
| \ddot{x}', \ddot{y}' | accelerations of plane |
| \dot{x}', \dot{y}' | velocities of plane |
| Y | $y'/a \omega^2$ |
| \dot{Y}' | \dot{y}'/a |
| \ddot{Y}' | $\ddot{y}'/a \omega$ |
| α | angle of oscillation - Fig. 1 |
| β | angle of plane inclination - See Fig. 1 |
| γ | angle used in GFGL Solution Eq. (44c) |
| δ | angle used in GFGL Solution Eq. (44d) |
| Δx | x displacement per cycle |
| $\Delta \dot{x}$ | change of x velocity during impact Eq. (40a) |
| $\Delta \dot{X}$ | $\Delta \dot{x}/a \omega$ |
| $\Delta \dot{Y}$ | change of non dimensional y velocity at impact Eq. (22) |
| ζ | generalized table inclination Table 1, Appendix A1. 2 |
| ϵ | impact friction multiplier |
| η | distance coordinate - Fig. 9 |

List of Symbols

| | |
|--------------|---|
| μ | coefficient of friction |
| μ_e | external coefficient of friction of granular materials |
| μ_{eff} | effective coefficient of friction of granular materials Eq. (58b) |
| ρ | density of granular material |
| τ | ωt nondimensional time |
| τ_{bgd} | nondimensional time at the beginning of the G Definite Zone Eq. (35) |
| τ_{bld} | nondimensional time at the beginning of the L Definite Zone Eq. (36b) |
| τ_{egd} | nondimensional time at the end of G Definite Zone Eq (37b) |
| τ_{eld} | nondimensional time at end of L Definite Zone Eq. (38c) |
| τ_i | initial nondimensional time |
| τ_{tg} | nondimensional time at termination of a Slide G |
| τ_{tl} | nondimensional time at termination of a Slide L |
| τ_1 | ωt_1 |
| τ_1' | $\omega t_1'$ |
| τ_2 | nondimensional time of impact Eqs. (16) |
| τ_2^* | τ_2 but refers to velocity immediately following impact |
| ϕ | generalized friction Table 1, Appendix A1.2 |
| ψ | constant Table 1, Appendix A1.2 |
| ω | angular velocity |

CHAPTER I

INTRODUCTION

1.1 Problem Statement

This thesis presents a theory that predicts and explains the motion of particles on the important practical class of oscillating conveyors in which the motion is sinusoidal in a straight line, inclined to the conveyor trough, and of a magnitude great enough to cause small flights of the particles once each cycle. The thesis also presents experimental evidence proving the theory over a wide range of practical values.

1.2 Description of Machines

These conveyors are generally in the form of long troughs mounted on springs or links that constrain the trough motion to a pure translation in a straight line usually inclined to the trough. Within limits, the trough need not be horizontal, and many of these conveyors are designed to transport material uphill quite efficiently. A very striking example of the uphill conveyor has the trough in the form of a tall spiral, whose only function is to lift material.

1.3 Advantages

The oscillating conveyor has many advantages. It can be totally enclosed protecting either the conveyed material or the environment. Its oscillatory motion makes it self-cleaning and non-clogging. The machinery need have far fewer rotating parts; in fact, the spring-supported trough merely moves on its springs which never require maintenance or lubrication. The oscillatory motion is comparatively easy to drive, electromagnetically or mechanically by means of a rotating eccentric.

1.4 Different Types of Oscillatory Conveyors

A broad class of these machines are those in which the oscillation is in the plane of the trough. A sinusoidal oscillation of the trough in these machines can only cause a downhill motion of the particles. Thus, to obtain horizontal or uphill particle motion, one must have the trough accelerate slowly in the forward direction and then quickly jerk back, leaving a net displacement of the particle. Interest has waned in these conveyors because of the necessary friction and inherent loss of efficiency. Also a durable efficient quick-return mechanism is comparatively expensive.

However, when the oscillation vector is inclined to the trough, the oscillation can be sinusoidal because the normal, and hence, the frictional force on the particle is greater on the forward stroke and reduced on the return stroke. Sinusoidal motion is very easy to produce, e.g., the trough is supported elastically such that its lowest mode of vibration is a translation in the desired direction and then a rotating eccentric or an electromagnet can easily drive it. Increasing the amplitude brings even more favorable results, for as the amplitude is increased, the particle begins to "fly" for some portion of the cycle, thus traveling completely without friction for that interval. As expected, these conveyors are the most efficient and, hence, the most popular of this class.

There have been studies where a general two-dimensional motion is given to the trough, going so far as to employ Calculus of Variations to the possible path, but the motion becomes so complicated that the machinery is uneconomical to produce.

1.5 History

Quoting from Guthrie and Morris, (Ref. 21), "As such, vibrating equipment in the form of screens or grasshopper-type feeders have existed for over 100 years in this country and there are indications

to believe that ancient civilizations, such as the Greeks and the Romans, made some use of these products."

More recently, investigations and analyses of the conveyors in which the oscillation direction is in the plane of the trough have been conducted by Blekhman and Dzhanelidze (Ref. 1), Bolz (Ref. 4), Wolff (Ref. 9), and Gutman (Ref. 10).

The class of conveyors with an inclined oscillation vector have received serious analytical treatment by Blekhman and Dzhanelidze (Ref. 1), Berry (Ref. 6), Burton (Ref. 11), and Taniguchi, et al., (Ref. 2). Booth and McCallion (Ref. 5), have presented a digital computer technique for analyzing this problem, together with an experimental verification, but only measuring average conveying velocity. Shertz and Hazen (Ref. 8) treat this problem on an analog computer and offer fine experimental support for their findings.

Studies of general two-dimensional trough motion of constant contact conveyors are analytically presented by Blekhman (Ref. 1), and Troitskii (Ref. 7), the latter employing Calculus of Variations to demonstrate the optimum trough trajectories. Shertz and Hazen (Ref. 8) have also used the analog computer in studying elliptical trough trajectories, their straight line analysis being a special case of the general attack.

The conveyors which are the subject of this report, i.e., those with an inclined oscillation vector and amplitudes great enough to cause flights, are not adequately analyzed in the literature. Rachner and Jungk (Ref. 13) present a logic that concludes that the trough velocity at the time of particle flight is a reasonable approximation of the conveying velocity. Paz (Ref. 3) has presented a very simplified analysis of a particular case. Taniguchi, et al., (Ref. 2) over simplified

in neglecting the effect of impact, and restricting themselves to very low oscillation angles (less than 20°) so that while their solution is reasonably close to the truth for their case, they have mistakenly assumed that what will be called the FGL solution in this study applies to all operating conditions. Because of their neglect of impact, they could not obtain adequate experimental verification.

All of these investigators have realized the need for utilizing a zero coefficient of restitution. Ref. 1 introduced the idea of different behavior at impact. All of the investigators have used the coordinate system used in this analysis.

Since none of the investigators have had any general success with single particles experimentally, little has been attempted in the predicting of the motion of granular materials; the problem has appeared formidable. In this analysis which does present the single particle theory, it is shown that the proper single particle analysis can indeed be extended to the study of granular materials.

1.6 Description of Study

A thorough study of single particle dynamics is undertaken which leads to a general theory and computer programs to find solutions for operating conditions. Complicated nondimensional parameters become evident that reduce the number of variables. An experimental program verifies the theory. The extension of this single particle theory to granular material is presented and experimentally verified.

CHAPTER II

THEORETICAL ANALYSIS

2.1 The Scope of the Study

The most popular of the oscillating conveyors is the one that oscillates harmonically in a straight line with the oscillation vector inclined to the horizontal. A number of analyses are available on the transport of material on conveyors which operate in this way, but at so low an amplitude that the particle does not leave the plane. (Refs. 1, 5, 6, 9, 10, 11, and 2). Generally however, in the interest of efficient operation, conveyors are such that a definite flight of the particle occurs each cycle. The present analysis is therefore restricted to consideration of cases in which the particle leaves the plane at some point in the cycle. This case has not yet been satisfactorily analyzed in the literature.

The coefficient of restitution is taken equal to zero in the analysis that follows. This is a good approximation for most cases of practical interest. Consider dropping a small flat board, or a box, or some loose granular material onto a flat surface. For small drop heights these items will not rebound at all. In general, as the amplitude of oscillations of a conveyor is increased to the point where rebounding might appear, the impacts become severe and damaging, and the particle motion becomes non-steady-state and unstable. A board will begin to tumble and toss irregularly, and finally bounce out of the trough. Thus for any practical conveying device a zero coefficient of restitution is actually attained.

2.2 The Model and the Coordinate Systems

Figure 1 shows a plane inclined to the horizontal at angle β . The plane is undergoing translational harmonic oscillations in the direction α to the horizontal. On this plane rests a particle of mass m that is flat enough to inhibit any rolling. Two coordinate systems are used. The $x' - y'$ coordinate system refers to the position of the plane. The system is considered fixed to earth, and x' and y' are taken zero at the mean position of the oscillation.

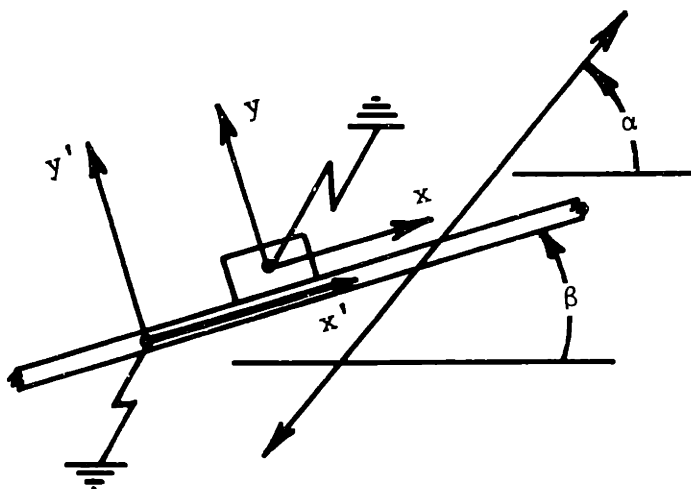


Figure 1 - The Coordinate Systems and the Angles

The x - y coordinate system refers to the position of the particle. The system is considered fixed to earth in such a way that $y = y'$ when the particle is resting on the plane. The $x = 0$ position is not important and will be set as a matter of convenience during integration of the equations of motion. The x axes are directed parallel to the plane at all times, and the y axes perpendicular to the plane as shown on Figure 1.

Given the above, the motion of the plane may be written as follows:

$$x' = a \cos (\alpha - \beta) \sin \omega t, \quad (1a)$$

$$\dot{x}' = a \omega \cos (\alpha - \beta) \cos \omega t, \quad (1b)$$

$$\ddot{x}' = -a \omega^2 \cos (\alpha - \beta) \sin \omega t, \quad (1c)$$

$$y' = a \sin (\alpha - \beta) \sin \omega t, \quad (1d)$$

$$\dot{y}' = a \omega \sin (\alpha - \beta) \cos \omega t, \quad (1e)$$

$$\ddot{y}' = -a \omega^2 \sin (\alpha - \beta) \sin \omega t. \quad (1f)$$

where dots over the variables indicate differentiation with respect to time, a is the displacement amplitude of the oscillations, and ω is the frequency.

2.3 The Dynamic Equilibrium of the Particle

Consider the free body diagram of the particle on the plane shown in Figure 2.

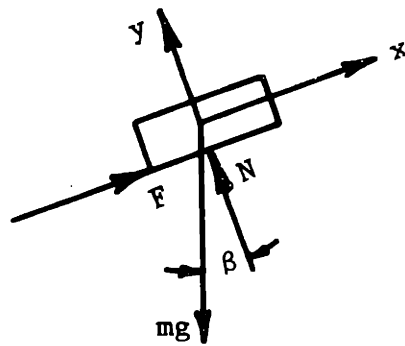


Figure 2 - Free Body Diagram of Particle

In Fig. 2, F is the frictional force, N is the normal force, and mg is the force of gravity. Dynamic equilibrium in the x and y directions requires that

$$m\ddot{y}' = N - mg \cos \beta, \quad (2a)$$

$$m\ddot{x}' = F - mg \sin \beta. \quad (2b)$$

The frictional force, F , and the normal force, N , in Eqs. (2a) and (2b) have unusual character which adds to the complexity of the problem. Note that the normal force N cannot be negative. It is positive when the particle is on the plane, and zero whenever the particle is off the plane, that is, for $y > y'$. The relationship between the frictional force F , and the normal force N requires special consideration. When the particle slides on the plane the frictional force is found in the usual manner, i. e., it is the product of the coefficient of friction μ and the normal force. However, during the impact, when pressures are apt to be extremely large and local bouncing may occur, the friction coefficient will be different from μ . To account for this, an impact friction multiplier, ϵ , is introduced that effectively changes the coefficient of friction at this point. On the other hand, a different, static, coefficient of friction is not necessary.

Professor Rabinowicz (Ref. 14) has shown that a certain finite time interval is required for static friction to be developed. Thus, no static coefficient is required when the particle instantaneously changes its relative sliding direction, even though an instant of zero relative velocity exists. Also, for the cases in which a short interval of zero relative velocity does exist, in practice machine vibration will inhibit the attainment of truly static conditions. Finally, when the particle has the same velocity as the plane, the friction force will take on the value required to maintain particle velocity. The relationships between F and N are thus

$$F = \mu N \quad \text{when } x < x', \quad (3a)$$

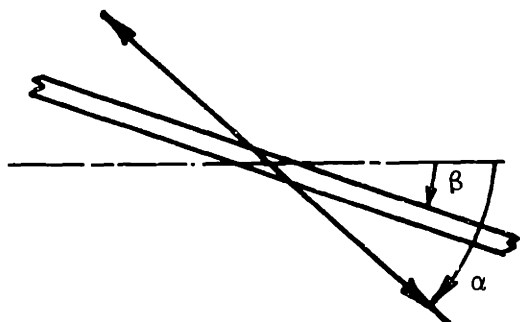
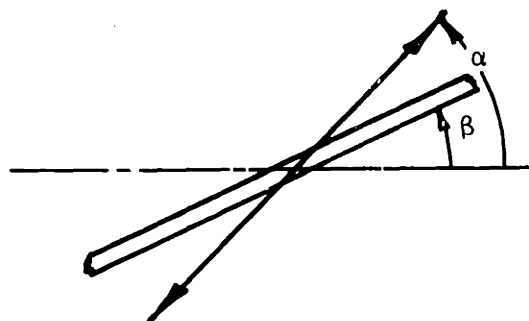
$$F = -\mu N \quad \text{when } x > x', \quad (3b)$$

$$F = \pm \epsilon \mu N \quad \text{during impact, and} \quad (3c)$$

$$-\mu N \leq F \leq +\mu N \quad \text{when } x = x'. \quad (3d)$$

Needless to say, the above require F to be zero whenever N is zero.

Let us consider the ranges of α and β that must be considered in order to assure that the theory covers all cases of interest. In the first place the angle of inclination β of the plane and the angle of oscillation α have a range between $\pm 90^\circ$. Also we need only consider the case where $\alpha > \beta$. Consider the situation where $\alpha < \beta$ shown in Fig. 3a. We see that this case is the same as

Figure 3a - $\alpha < \beta$ Figure 3b - $\alpha > \beta$

the case shown in Fig. 3b, where $\alpha > \beta$, except that the direction of the x axis is reversed. In addition, the case of $\alpha = \beta$ is covered in the Introduction, and is of no interest. Thus, all possible cases are included for α and β within the limits

$$\beta < \alpha < \frac{\pi}{2}. \quad (4)$$

One would also expect that β is limited by the angle of friction, and indeed, this is the case. In Fig. 2 only the two forces N and $mg \cos \beta$ act in the y direction. Since the particle has identical y velocities at the beginning and end of a cycle of period T , the impulse from the normal force must be equal and opposite to that of the gravitational force, or

$$\int_0^T N \, dT = mgT \cos \beta. \quad (5)$$

The maximum x impulse that friction can offer is the product of the coefficient of friction and this value, or

$$\int_0^T F \, dT = \mu mgT \cos \beta. \quad (6)$$

Again from Fig. 2, there are only the two forces F and $mg \sin \beta$ in the x direction. For periodic motion, the x velocities must be equal at the beginning and end of this cycle of period T . Hence, the x impulse from gravity can never be greater than the maximum x impulse available from friction. Therefore,

$$mgT \sin \beta \leq \mu mgT \cos \beta. \quad (7)$$

and

$$\tan \beta \leq \mu. \quad (8)$$

using an identical argument for sliding in the other direction, we find the permissible range of values of β is defined by

$$-\mu \leq \tan \beta \leq +\mu. \quad (9)$$

2. 5 Initial Observations

As will be seen, because the axes have been oriented to the plane, the x and y motions will separate; the two sets of equations of motions can be integrated and analyzed separately. The y motion is the simpler of the two, because there are only two possible forms; the particle is either on the plane, riding with the y motion of the plane, or off the plane and flying. The x motion is more complicated; it has four forms. The particle can be on the plane and sliding forward, sliding backward, or riding with the same relative velocity as the plane. Also, it can be off the plane and flying. No difficulty is encountered in deriving the equations of motion for any one of these different forms. The problem is, for a given set of operating conditions, to determine the correct sequence and phasing of the motion forms, so that the various equations can be assembled to find the displacement during the cycle. As will be seen, many combinations are possible. A set of rules, conditions, and equations must be developed to reduce the number of possibilities. Finally, by requiring periodicity the solutions of practical importance are obtained. Even with the theory, the calculations to obtain an actual solution are quite lengthy, thus they have been programmed for computation on a digital computer. Several calculated examples are presented which will be later compared to experimental results which verify the theory.

2. 6 The Y Motion of the Particle

2. 6. 1 The Time of Flight

Just prior to a flight, the particle has the same y velocity, displacement, and acceleration as the plane. Furthermore, the normal force acting on the particle is positive and is becoming smaller; the time at which the normal force becomes zero is the time of initiation of a flight. Since the particle is on the plane prior to the flight and has the y acceleration of the plane at that time, the expression for the normal force prior to flight is obtained by substituting the y acceleration of the plane (Eq. (1f)) in the y equilibrium equation (Eq. (2a)), giving

2.5 Initial Observations

As will be seen, because the axes have been oriented to the plane, the x and y motions will separate; the two sets of equations of motions can be integrated and analyzed separately. The y motion is the simpler of the two, because there are only two possible forms; the particle is either on the plane, riding with the y motion of the plane, or off the plane and flying. The x motion is more complicated; it has four forms. The particle can be on the plane and sliding forward, sliding backward, or riding with the same relative velocity as the plane. Also, it can be off the plane and flying. No difficulty is encountered in deriving the equations of motion for any one of these different forms. The problem is, for a given set of operating conditions, to determine the correct sequence and phasing of the motion forms, so that the various equations can be assembled to find the displacement during the cycle. As will be seen, many combinations are possible. A set of rules, conditions, and equations must be developed to reduce the number of possibilities. Finally, by requiring periodicity the solutions of practical importance are obtained. Even with the theory, the calculations to obtain an actual solution are quite lengthy, thus they have been programmed for computation on a digital computer. Several calculated examples are presented which will be later compared to experimental results which verify the theory.

2.6 The Y Motion of the Particle

2.6.1 The Time of Flight

Just prior to a flight, the particle has the same y velocity, displacement, and acceleration as the plane. Furthermore, the normal force acting on the particle is positive and is becoming smaller; the time at which the normal force becomes zero is the time of initiation of a flight. Since the particle is on the plane prior to the flight and has the y acceleration of the plane at that time, the expression for the normal force prior to flight is obtained by substituting the y acceleration of the plane (Eq. (1f)) in the y equilibrium equation (Eq. (2a)), giving

$$N = m [-a\omega^2 \sin(\alpha - \beta) \sin\omega t + g \cos \beta] \quad (10)$$

Equating this expression to zero yields the time of flight, t_1 , as follows:

$$\sin \omega t_1 = 1/A, \quad (11a)$$

where

$$A \equiv \frac{\sin(\alpha - \beta)}{\cos \beta} \frac{a\omega^2}{g} \quad (11b)$$

The quantity, A , will be seen to be a very important parameter. Examination of (1f) shows A to be the ratio of the y component of the maximum plane acceleration to the y component of the acceleration of gravity. It can be thought of as the relative y acceleration. Equations (4) and (9) reveal that A is always a positive number, and (11a) shows that A must be greater than unity. This last restriction comes about because the study is limited to cases in which a flight occurs.

Note that Eq. (11a) yields two values of t_1 in an interval of one cycle, one in the first quadrant and one in the second. These will be denoted as t_1 and t_1' ; by utilizing principal value notation, these may be written:

$$\omega t_1 = \text{Sin}^{-1} (1/A) \quad (12a)$$

$$\omega t_1' = \pi - \text{Sin}^{-1} (1/A). \quad (12b)$$

From Eq. (10), one can show that the time interval between t_1 and t_1' requires a negative N for the particle to remain on the plane. A negative N is impossible so this interval is a "definite fly zone", a zone in which the particle cannot remain on the plane. Since N , in Eq. (10),

is decreasing just prior to t_1 , t_1 is the time at which the particle will begin its flight. The second value, t_1' , is a limiting value. If the impact after the flight occurs prior to t_1' , the particle will instantly fly again; if the impact occurs after t_1' , the particle remains on the plane.

2. 6. 2 Nondimensional Displacement and Time

For convenience we shall use a time variable τ non-dimensionalized with respect to ω , and displacements, expressed in capital letters nondimensionalized with respect to a . Thus, $\tau = \omega t$, and $X = x/a$, and $Y = y/a$. Dots over the capital letters will denote differentiation with respect to τ . The new symbols are listed in the symbols table. Utilizing these new variables, the y velocity, displacement, and acceleration of the plane become

$$\dot{Y}' = \sin(\alpha - \beta) \sin \tau \quad (13a)$$

$$\ddot{Y}' = \sin(\alpha - \beta) \cos \tau \quad (13b)$$

$$\ddot{\ddot{Y}}' = -\sin(\alpha - \beta) \sin \tau. \quad (13c)$$

Finally, Eqs. (11) and (12) become

$$\tau_1 = \text{Sin}^{-1}(1/A) \quad (14a)$$

$$\tau_1' = \pi - \text{Sin}^{-1}(1/A) \quad (14b)$$

where:
$$A \equiv \frac{a \omega^2 \sin(\alpha - \beta)}{g \cos \beta} \quad (14c)$$

2. 6. 3 Y Motion During a Flight

The y acceleration during a flight is found from Eq. (2a), with N set equal to zero, yielding

$$\frac{a \omega^2 \ddot{Y}}{g \cos \beta} = -1. \quad (15a)$$

Equation (15a) is integrated with respect to τ , the integration constant being evaluated by the condition that the particle velocity equals the plane velocity at τ_1 . The integration yields:

$$\frac{a \omega^2 \dot{Y}}{g \cos \beta} = \tau + \tau_1 + A \cos \tau_1. \quad (15b)$$

Equation (15b) is again integrated with respect to τ , the constant being evaluated with the condition that the displacement of the particle at τ_1 , equals that of the plane at τ_1 . This yields:

$$\frac{a \omega^2 Y}{g \cos \beta} = -1/2 (\tau - \tau_1)^2 + A \cos \tau_1 (\tau - \tau_1) + 1. \quad (15c)$$

2. 6. 4 The Termination of the Flight

The flight began with equal y displacement of the particle and the plane, and the flight terminates when these two displacements are again equal. Thus, the time of impact, τ_2 , is found by equating Eq. (15c) and Eq. (13a), at the time τ_2 . After some manipulation, the following transcendental equation is obtained:

$$\sin \tau_2 = B \tau_2^2 + C \tau_2 + D \quad (16a)$$

$$\text{where } B \equiv -1/2 \sin \tau_1 \quad (16b)$$

$$C \equiv \tau_1 \sin \tau_1 + \cos \tau_1 \quad (16c)$$

$$D \equiv -1/2 \tau_1^2 \sin \tau_1 - \tau_1 \cos \tau_1 + \sin \tau_1. \quad (16d)$$

Thus, it is seen that both τ_1 and τ_2 are functions of A alone. They are plotted as functions of A in Fig. 4; Table A1 in the appendix lists some values of τ_1 , τ_2 , and τ_1' , for various A 's.

In Appendix A 1.1, it is proved that τ_2 definitely lies outside the definite fly range, i. e., $\tau_2 > \tau_1'$. Thus it is assured that a particle with a zero coefficient of restitution, undergoing once per cycle periodic behavior, will always fly at τ_1 as given by Eq. (14a) and remain flying (with $Y > Y'$) until τ_2 as given by Eqs. (16); throughout the rest of the cycle the particle will be on the plane with $Y = Y'$.

2.6.5 Limiting Amplitude for Once Per Cycle Periodic Solutions

As was mentioned above, this analysis is only concerned with steady state solutions, that are once per excitation cycle periodic. This once per cycle limitation leads to an upper limit on the relative y acceleration, A , which will in general be referred to as the amplitude. Clearly, for once per cycle periodic behavior, the termination of the flight must come before the next time of flight, and in the limiting case the time of impact will occur just at the next time of flight. For this particular case

$$\tau_2 - \tau_1 = 2\pi, \quad (17)$$

and

$$\sin \tau_2 = \sin \tau_1 = 1/A. \quad (18)$$

The cosine will be

$$\cos \tau_1 = \frac{\sqrt{A^2 - 1}}{A} \quad (19)$$

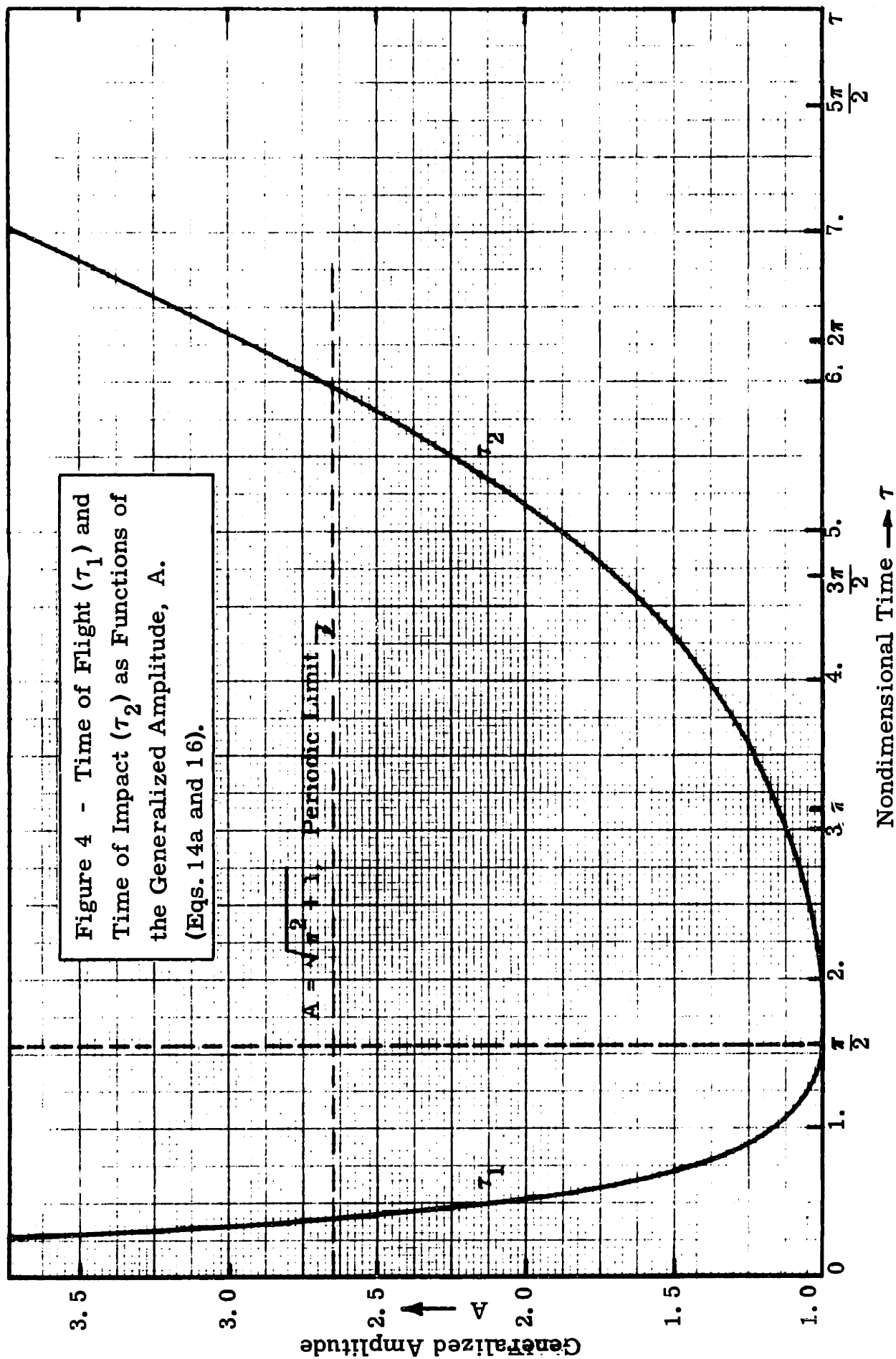


Figure 4 - Time of Flight (τ_1) and Time of Impact (τ_2) as Functions of the Generalized Amplitude, A. (Eqs. 14a and 16).

By substituting (17), (18) and (19), in Eqs. (16), the limiting amplitude is found to be

$$A_{\text{lim}} = \sqrt{\pi^2 + 1} \approx 3.297 \quad (20)$$

This limiting value of A is shown as a horizontal dotted line in Fig. 4. Therefore, this analysis will be concerned with a range of amplitudes, A, greater than unity to assure a flight and less than $\sqrt{\pi^2 + 1}$ to assure periodic once per cycle behavior, or in symbols

$$1.0 \leq A \leq \sqrt{\pi^2 + 1} \quad (21)$$

2. 6. 6 The Impact After the Flight

In order to compute the frictional x impulse during the impact, the y velocity change during impact must be computed. The y velocity of the particle just prior to the impact is given by the flight equation, Eq. (15b) and since the coefficient of restitution is zero, the velocity of the particle just following the impact will equal the plane velocity at that time. Define:

$$\Delta \dot{Y} \equiv \dot{Y}(\tau_2) - \dot{Y}'(\tau_2). \quad (22)$$

$\dot{Y}(\tau_2)$ is obtained from Eq. (15b) and $\dot{Y}'(\tau_2)$ is obtained from (13b) both evaluated at τ_2 , obtained from Eqs. (16). Thus, Eq. (22) becomes:

$$\frac{\Delta \dot{Y}}{\sin(\alpha - \beta)} = \frac{-1}{A} (\tau_2 - \tau_1) + \cos \tau_1 - \cos \tau_2. \quad (23)$$

It might be pointed out that $\Delta\dot{Y}$ is definitely a negative quantity, otherwise the particle could not reach the plane.

2.7 X Motion of the Particle

2.7.1 The Nondimensional Quantities ϕ , ζ , and ψ

It is convenient to now introduce three additional nondimensional quantities which simplify manipulation and reduce the number of variables by one. The discussion of their range of permissible values is given in Appendix A1.2, the results of which are summarized in Table 1, which collects all the nondimensional operating conditions.

2.7.2 Introductory Comments on the X Motion

The particle y motion, having been thoroughly deduced (i. e. the particle definitely leaves the plane and flies at τ_1 , continues this flight until τ_2 , at which times it suffers an inelastic impact and then remains on the plane until $\tau_1 + 2\pi$), the more complicated x motion must now be considered. For x motion there exist four possibilities: riding with no relative x velocity, flying, sliding forward, and sliding backward. Specifically defining these four possibilities, we have

Ride motion when

$$Y = Y', \text{ and} \tag{24a}$$

$$\dot{X} = \dot{X}'; \tag{24b}$$

Fly motion when

$$Y > Y'; \tag{25}$$

Slide G (slide greater; sliding forward; particle velocity greater than plane velocity) motion when

$$Y = Y', \text{ and} \tag{26a}$$

$$\dot{X} > \dot{X}'; \tag{26b}$$

Table 1

NON-DIMENSIONALIZED OPERATING CONDITIONS

| SYMBOL | DEFINITION | RANGE | EQS. NOS. |
|---|---|--|--------------------|
| A (amplitude) | $\frac{a\omega^2}{g} \frac{\sin(\alpha - \beta)}{\cos \beta}$ | $1 \leq A \leq \sqrt{\pi^2 + 1}$ (≈ 3.3) | (11b) (21) |
| ϵ (impact friction multiplier) | experimentally determined | $0 \leq \epsilon < \infty$ | |
| ϕ (ND friction) | $\frac{\mu + \cot(\alpha - \beta)}{\mu + \tan \beta}$ | $1 \leq \phi < \infty$ (and only for $\alpha = \pi/2$ can $\phi = 1$.) | (A1.9) (A1.15) |
| ξ (ND plane tilt) | $\frac{\mu}{\mu + \tan \beta}$ | $0.5 < \xi < \infty$ ($\xi = 1$ for $\beta = 0$) | (A1.10) (A1.21) |
| ψ (multiplier) | $(\mu + \tan \beta) \sin(\alpha - \beta)$ | $0 < \psi < 2\mu$ | (A1.11) (A1.23) |

Slide L (slide less; sliding backward; particle velocity less than plane velocity) motion when

$$Y = Y', \text{ and} \tag{26c}$$

$$\dot{X} < \dot{X}'. \tag{26d}$$

The following paragraphs derive the x equations of motion applicable during each type of motion.

2.7.3 Slide G Motion

The normal force acting on the particle when the particle is on the plane has been given in Eq. (10). When the particle is sliding forward the frictional force, F , must act in the negative direction on the particle as was noted in Eq. (3b). Thus, substituting N from Eq. (10) into (3b) to obtain F , and in turn substituting the resulting F into Eq. (2b), yields the x acceleration during this type of motion to be:

$$\ddot{x} = -\mu g \cos \beta + \mu a \omega^2 \sin(\alpha - \beta) \sin \omega t - g \sin \beta. \tag{27a}$$

Utilizing the nondimensional variables of Table 1, this becomes more simply:

$$\frac{\ddot{X}}{\Psi} = \frac{-1}{A} + \zeta \sin \tau. \tag{27b}$$

Integration of Eq. (27b) with the initial condition that $\dot{X} = \dot{X}_i$, at $\tau = \tau_i$, yields the velocity to be

$$\frac{\dot{X}}{\Psi} = \frac{-1}{A} (\tau - \tau_i) - \zeta (\cos \tau - \cos \tau_i) + \frac{\dot{X}_i}{\Psi}. \tag{27c}$$

Integration of Eq. (27c), with the initial condition that $X = X_i$, when $\tau = \tau_i$, yields the displacement to be

$$\frac{X}{\Psi} = \frac{-1}{2A} (\tau - \tau_i)^2 - \zeta (\sin \tau - \sin \tau_i) + \left(\zeta \cos \tau_i + \frac{X_i}{\Psi} \right) (\tau - \tau_i) + \frac{X_i}{\Psi}. \quad (27d)$$

2.7.4 Slide L Motion

Again the normal force is given by Eq. (10). However, since the particle is sliding backward, the frictional force must be taken to be positive as is indicated in Eq. (3a). Combining (10), and (3a) in (2b) yields the acceleration to be

$$\ddot{x} = \mu g \cos \beta - \mu a \omega^2 \sin(\alpha - \beta) \sin \omega t - g \sin \beta. \quad (28a)$$

Casting this in nondimensional form yields:

$$\frac{\ddot{X}}{\Psi} = \frac{1}{A} (2\zeta - 1) - \zeta \sin \tau. \quad (28b)$$

Integration of (28b) with the initial condition that $\dot{X} = \dot{X}_i$, when $\tau = \tau_i$, yields the velocity to be

$$\frac{\dot{X}}{\Psi} = \frac{1}{A} (2\zeta - 1) (\tau - \tau_i) + \zeta (\cos \tau - \cos \tau_i) + \frac{\dot{X}_i}{\Psi}. \quad (28c)$$

Finally, integration of (28c) utilizing the condition that $X = X_i$, when $\tau = \tau_i$ yields the displacement

$$\frac{X}{\Psi} = \frac{1}{2A} (2\zeta - 1) (\tau - \tau_i)^2 + \zeta (\sin \tau - \sin \tau_i) + \left(\frac{\dot{X}_i}{\Psi} - \zeta \cos \tau_i \right) (\tau - \tau_i) + \frac{X_i}{\Psi}. \quad (28d)$$

2.7.5 Ride Motion

When a ride is occurring the x velocity of the particle is identical with that of the plane. In terms of the nondimensional variables Eqs. (1d), (1e), (1f) for the x motion of the plane may be written:

$$\frac{X'}{\Psi} = (\phi - \zeta) \sin \tau, \quad (29a)$$

$$\frac{\dot{X}'}{\Psi} = (\phi - \zeta) \cos \tau, \quad (29b)$$

$$\frac{\ddot{X}'}{\Psi} = -(\phi - \zeta) \sin \tau. \quad (29c)$$

Hence, the acceleration and velocity of the particle during a ride may be written

$$\frac{\ddot{X}}{\Psi} = -(\phi - \zeta) \sin \tau, \quad (30a)$$

$$\frac{\dot{X}}{\Psi} = (\phi - \zeta) \cos \tau. \quad (30b)$$

Integration of Eq. (30b), with the initial condition that when $\tau = \tau_i$, $X = X_i$, yields the displacement to be

$$\frac{X}{\Psi} = (\phi - \zeta) (\sin \tau - \sin \tau_i) + \frac{X_i}{\Psi}. \quad (30c)$$

2.7.6 Fly Motion

During a flight the normal force and hence the frictional force acting on the particle are zero. The acceleration of the particle can be taken from Eq. (2b) with F taken zero. This gives:

$$x = -g \sin \beta. \quad (31a)$$

Utilization of the nondimensional variables permits the above to be written as:

$$\frac{\ddot{X}}{\Psi} = -\frac{1}{A} (1 - \zeta). \quad (31b)$$

Integration of (31b) with the initial condition that $X = X_i$, at $\tau = \tau_i$ yields the velocity to be

$$\frac{\dot{X}}{\Psi} = -\frac{1}{A} (1 - \zeta) (\tau - \tau_i) + \frac{\dot{X}_i}{\Psi}. \quad (31c)$$

Finally integration of (31c) taking $X = X_i$, at $\tau = \tau_i$, yields the displacement as

$$\frac{X}{\Psi} = -\frac{1}{2A} (1 - \zeta) (\tau - \tau_i)^2 + \frac{\dot{X}_i}{\Psi} (\tau - \tau_i) + \frac{X_i}{\Psi}. \quad (31d)$$

2.8 Rules and Conditions for Predicting Transitions Between X Motion Forms

2.8.1 The Required and Available Friction Force

Two useful concepts are introduced in this section; they are the available and the required frictional force. Their main use is in the determination of the times of transition between the various types of motion.

When a particle is on the plane, a certain minimum frictional force is required for the particle to maintain a ride, i. e. maintain the acceleration of the plane. This is called the required friction force and is symbolized as F_r . Its value is obtained from Eq. (2b), the x equilibrium equation, with the x acceleration being taken equal to the x acceleration of the plane, Eq. (1c). This yields:

$$F_r \equiv mg \sin \beta - ma \omega^2 \cos (\alpha - \beta) \sin \omega t. \quad (32a)$$

Manipulating with the nondimensional variables and introducing a nondimensional \bar{F}_r , (32a) becomes

$$\frac{\bar{F}_r}{\psi} = \frac{1 - \zeta}{A} - (\phi - \zeta) \sin \tau, \quad (32b)$$

where

$$\bar{F}_r \equiv \frac{F_r}{ma \omega^2}. \quad (32c)$$

When the particle is resting on the plane, the coefficient of friction times the normal force yields the maximum frictional force attainable at any given time. This is called the available frictional force. Since this maximum can act in either direction, two values of force are obtained. That value corresponding to a Slide G, a slide with $\dot{X} > \dot{X}'$, is called the available force for a Slide G, and is denoted F_{ag} . The value corresponding to a Slide L, a slide with $\dot{X} < \dot{X}'$, is the available force for a Slide L and is denoted F_{al} .

F_{ag} is obtained from Eq. (10), the equation for the normal force, multiplied by a negative μ since in this case the frictional force acts in the negative direction. This yields:

$$F_{ag} = -\mu mg \cos \beta + \mu ma \omega^2 \sin(\alpha - \beta) \sin \omega t. \quad (33a)$$

Utilizing the nondimensional variables and defining a nondimensional F_{ag} , Eq. (33a) is written as:

$$\frac{\bar{F}_{ag}}{\psi} = -\frac{\zeta}{A} + \zeta \sin \tau, \quad (33b)$$

where

$$\bar{F}_{ag} \equiv \frac{F_{ag}}{ma \omega^2}. \quad (33c)$$

To obtain F_{al} , the available force for a Slide L, the only difference being that friction acts in the opposite direction, all one need do is reverse the signs on the right hand side of (33b). This yields:

$$\frac{\bar{F}_{al}}{\psi} = \frac{\zeta}{A} - \zeta \sin \tau, \quad (34a)$$

where

$$\bar{F}_{al} \equiv \frac{F_{al}}{ma \omega^2}. \quad (34b)$$

2.8.2 Terminating A Ride

The first of the transitions to be studied are the terminations

of a Ride, except that it has been proved that a flight will definitely initiate at τ_1 , and terminate at τ_2 . Given that a ride is occurring, $\dot{X} = \dot{X}'$, the available force for a Slide G is more negative than the required force, and similarly the available force for a Slide L is more positive than the required force. Two different terminations must be considered.

2. 8. 3 A Ride Terminating in a Slide G

In Appendix A. 1. 3 by comparing \bar{F}_r and \bar{F}_{ag} , it is proved that a Ride can only terminate in a Slide G at one time during each cycle. This time, which is in the first quadrant, is called τ_{bgd} and is given by:

$$\tau_{bgd} = \text{Sin}^{-1} \left(\frac{1}{A\phi} \right). \quad (35)$$

Further, it is shown that except for the special case where $\alpha = \frac{\pi}{2}$, and $\phi = 1$, $\tau_{bgd} < \tau_1$; i. e., virtually every ride that is occurring prior to the time of flight must terminate in a Slide G before the flight.

2. 8. 4 A Ride Termination in a Slide L

In Appendix A. 1. 4, by comparing \bar{F}_r and \bar{F}_{al} , it is proved that a Ride can terminate in a Slide L, only if

$$2 \zeta - \phi < 0, \quad (36a)$$

and that this termination can only occur in the third quadrant at a time τ_{bld} , given by

$$\tau_{bld} = \text{Sin}^{-1} \left(\frac{2 \zeta - 1}{\phi - 2 \zeta} \frac{1}{A} \right) + \pi. \quad (36b)$$

Thus, virtually all Rides terminate in slides. If a Ride is occurring in the first quadrant it must terminate in a Slide G at τ_{bgd} given in Eq. (35). If a Ride is occurring in the third quadrant and condition (36a) is met, it must terminate in a Slide L at τ_{bld} given in Eq. (36b).

2. 8. 5 Decision Times

Another concept useful in discussing the solutions, is that of the Decision Time. Specifically, this is any time when the particle is on the plane and has the same x velocity as the plane. Given this definition, a Ride is then a sequence of Decision Times, but this is not important in what follows. The usefulness of the concept can be appreciated by considering that the most common way in which the slides will terminate will be at Decision Times. These points can also occur following an impact. These are the only times in analyzing solutions when any further rules for defining the type of transition will be needed.

2. 8. 6 The Definite Slide Zones

As has probably been inferred there are certain time intervals in each cycle when the Force Required to maintain a Ride, exceeds that available from friction. Inside these intervals a Ride is impossible, and should a particle reach a Decision Time within one of these intervals, an appropriate slide will initiate. Generally, two such zones exist. One each for the Slide G and the Slide L. However, for a definite range of operating conditions, no Slide L Definite Zone is possible.

2. 8. 7 G Definite Zone

In Appendix A. 1. 5, by noting the interval when $\bar{F}_r < \bar{F}_{ag}$, it is proved that a Slide G Definite Zone exists in the first and second quadrants between the times τ_{bgd} (time at the beginning of G definite) and τ_{egd} (time at the end of G definite). These times are expressed as:

$$\tau_{bgd} = \text{Sin}^{-1} \left(\frac{1}{A\phi} \right) \quad (37a)$$

$$\tau_{egd} = \pi - \text{Sin}^{-1} \left(\frac{1}{A\phi} \right). \quad (37b)$$

Except for the trivial case of $\alpha = \frac{\pi}{2}$, when $\phi = 1$, the beginning of this zone, τ_{bgd} always precedes the time of flight, τ_1 . Only for cases of very low amplitude ($A < 1.15$) is it possible for the end of this zone, τ_{egd} , to extend beyond the size of impact, τ_2 . These cases will admit complications which will be mentioned later, but such low amplitudes will seldom be encountered in practice. No such cases were computed in this study.

2.8.8 L Definite Zone

In Appendix A. 1. 6, by noting the possible interval when $F_r > F_{al}$, it is proved that an L Definite Zone will exist only if the following condition is met

$$\frac{1 - 2\xi}{A} - (2\xi - \phi) > 0. \quad (38a)$$

If the L Definite Zone exists, it will lie in the third and fourth quadrants between τ_{bld} (time at the beginning of L Definite) and τ_{eld} (time at the end of L Definite). These times are expressed as follows:

$$\tau_{bld} = \pi - \text{Sin}^{-1} \left[\frac{2\xi - 1}{2\xi - \phi} \cdot \frac{1}{A} \right] \quad (38b)$$

$$\tau_{eld} = 2\pi + \text{Sin}^{-1} \left[\frac{2\xi - 1}{2\xi - \phi} \cdot \frac{1}{A} \right]. \quad (38c)$$

2. 8. 9 The Termination of a Slide in General

Any slide will terminate in one of two ways. Clearly, any slide that is occurring just prior to the time of flight terminates at the time of flights. All other slides terminate when the particle velocity becomes equal to the plane velocity, i. e., at a Decision Time. Given that a slide is occurring, it will terminate at the very next Decision Time, except for the special terminations at the time of flight.

2. 8. 10 Neither Slide can Terminate in its Corresponding Definite Zone

A very useful fact for predicting the character of the solutions is the fact that no slide may terminate in the corresponding Definite Zone, except the Slide G at the time of flight, since the time of flight takes priority over all other behavior. This certainly appears intuitively true, and is proved in Appendix A1. 7.

2. 8. 11 The Slide Termination Equations

The relationships for determining the time of termination of a slide are obtained by equating the velocity of the particle during that slide with the velocity of the plane. The time of termination of a Slide G, τ_{tg} , is obtained by equating Eq. (27c), with Eq. (29b) which yields:

$$\cos \tau_{tg} + \frac{1}{A\phi} \tau_{tg} - \frac{1}{\phi} \left[\frac{\tau_i}{A} + \zeta \cos \tau_i + \frac{\dot{X}(\tau_i)}{\psi} \right] = 0 \quad (39a)$$

The time of termination for a Slide L, τ_{tl} , is obtained by equating Eq. (28c), with Eq. (29b) which yields:

$$\cos \tau_{tl} + \frac{1}{A} \left[\frac{2\zeta - 1}{2\zeta - \phi} \right] \tau_{tl} + \frac{1}{(2\zeta - \phi)} \left[- \frac{(2\zeta - 1) \tau_i}{A} - \zeta \cos \tau_i + \frac{\dot{X}(\tau_i)}{\psi} \right] = 0. \quad (39b)$$

2. 8. 12 The Results of the Impact on the X Motion

The impact will be considered to take place in zero time. This leads to the conclusion that no displacement takes place during the impact and that the particle suffers an instantaneous y velocity change as well as a possible x velocity change. In general, just prior to impact, the x velocity of the particle will differ from the x velocity of the plane. The frictional impulse during impact will act so as to decrease the magnitude of the relative velocity between the particle and the plane. The pressures during impact will be very high. It is probable that the pressures become so great that the simple friction law is really no longer applicable. However, this possibility can be conveniently introduced later, and so the simple friction law is considered applicable for the moment.

The product of the mass of the particle and the x velocity change, the change of the x momentum of the particle, will equal the impulse from the frictional force.

$$m \Delta \dot{x} = \int F dt. \quad (40a)$$

If the particle does not attain the velocity of the plane during the impact, the frictional force will be at its maximum value throughout the impact and F will equal the product of μ and the normal force, hence

$$m \Delta \dot{x} = \mu \int N dt. \quad (40b)$$

The $\int N dt$, is the y impulse during impact and is equal to the y momentum change during impact, thus

$$m \Delta \dot{x} = \mu m \Delta \dot{y}. \quad (40c)$$

Now, Eq. (23) is substituted into Eq. (40c) to obtain

$$\frac{\Delta \dot{X}}{\mu \sin(\alpha - \beta)} = \frac{1}{A} (\tau_2 - \tau_1) + \cos \tau_2 - \cos \tau_1. \quad (40d)$$

The negative of Eq. (23) was used in the above so the $\Delta \dot{X}$ will be a positive quantity here. Its sign in actual use will depend upon the sign of $(\dot{X} - \dot{X}')$ prior to the impact. Utilizing the nondimensional variables of Table 1, Eq. (40d) becomes

$$\frac{\Delta \dot{X}}{\psi} = \zeta \left[\frac{1}{A} (\tau_2 - \tau_1) + \cos \tau_2 - \cos \tau_1 \right]. \quad (41)$$

The probability that the friction law and the coefficient of friction are more complicated than has been assumed can now be introduced in the form of an impact friction multiplier ϵ on Eq. (41). It is assumed that the actual frictional velocity change attained during impact is obtained by multiplying the velocity change computed from the simple theory Eq. (41) by a complicated quantity, ϵ , the impact friction multiplier. This change in impact friction has been suggested by Blekhman (Ref. 1).

Another symbolism must be explained. The quantity τ_2 , represents the nondimensional time at impact and will be used to refer to velocities just prior to impact, while the quantity τ_2^* , represents this same time, but when used in connection with velocity will refer to the velocity at that time, but just following the impact.

Finally, the impact velocity change, $\epsilon \Delta \dot{X} / \psi$ is the maximum velocity change that can occur. It is only possible as long as a relative velocity exists between the particle and the plane throughout the impact. If the two velocities become equal during the impact something less than $\epsilon \frac{\Delta \dot{X}}{\psi}$ is attained, and the particle will have the velocity of the plane following the impact.

Let us summarize the above with the aid of the diagram in Fig. 5. Imagine that the horizontal line represents X velocity.

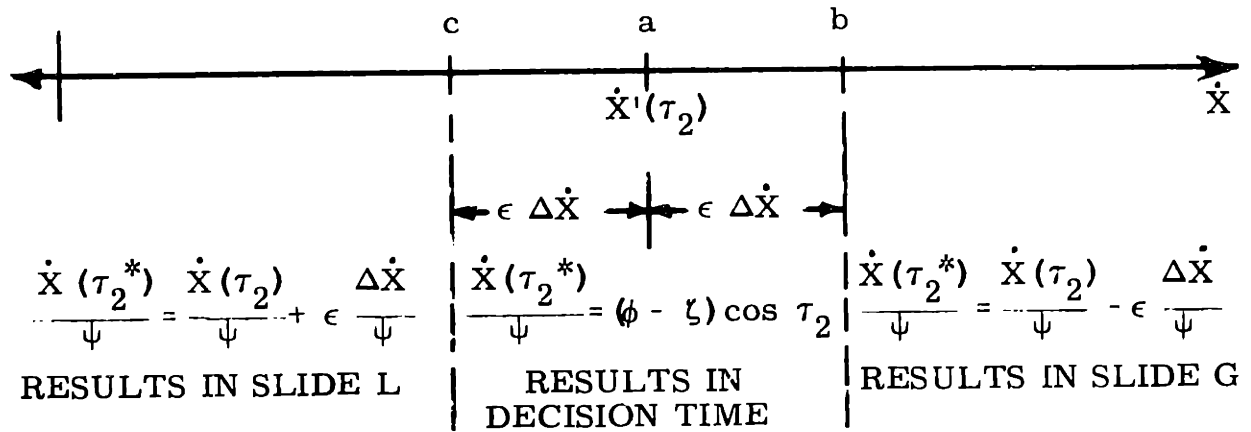


Figure 5 - Diagram Depicting the Results of an Impact on X Motion

$\epsilon \Delta \dot{X}$ is the greatest amount that friction is able to change the x velocity during the impact. Point a represents the velocity of the plane. Points c and b, both $\epsilon \Delta \dot{X}$ either side of point a, represent the extremes of particle velocity prior to impact, for which the particle will attain the velocity of the plane following impact. Within these limits the impact results in a Decision Time. For initial impact velocities in excess of Point b, the particle velocity is reduced by the maximum amount and the impact results in a Slide G. For initial impact velocities less than Point c, the particle velocity is increased the maximum amount and the impact results in a Slide L. In summary, then, the results of impact on the X motion may be stated as follows:

If

$$\dot{X}(\tau_2) > \dot{X}'(\tau_2) + \epsilon \Delta \dot{X} \quad (42a)$$

then

$$\dot{X}(\tau_2^*) = \dot{X}(\tau_2) - \epsilon \Delta \dot{X}, \quad (42b)$$

and a Slide G results.

If

$$\dot{X}'(\tau_2) - \epsilon \Delta \dot{X} \leq \dot{X}(\tau_2) \leq \dot{X}'(\tau_2) + \epsilon \Delta \dot{X}, \quad (42c)$$

then

$$\dot{X}(\tau_2^*) = \dot{X}'(\tau_2), \quad (42d)$$

and a Decision Time results.

If

$$\dot{X}(\tau_2) < \dot{X}'(\tau_2) - \epsilon \Delta \dot{X}, \quad (42e)$$

then

$$\dot{X}(\tau_2^*) = \dot{X}'(\tau_2) + \epsilon \Delta \dot{X}, \quad (42f)$$

and a Slide L results.

2.8.13 A Brief Summary of the Theory Thus Far

Before proceeding to the solutions, let us quickly list the various facts that have been presented.

The coefficient of restitution is zero, and the motion of the plane is described by (1).

The axes are ordered such that (4) is met. β must lie within the limits set by (9).

The operating conditions are used to compute the nondimensional variables of Table 1.

For the motion to be "once-per-rev" periodic and contain a Flight, A, must satisfy (21).

The particle definitely flies at τ_1 given by (14) and definitely lands at τ_2 given by (16). At all other times it is on the plane.

In nondimensional variables the motion of the plane is given by (29).

There are four possible forms the X motion can take; these are a Slide G, Slide L, Ride, and Flight, and the corresponding equations of motion are (27), (28), (30), and (31), respectively.

The limits of the Slide G Definite Zone are τ_{bgd} and τ_{egd} , as given by (37).

For a Slide L Definite Zone to exist, (38a) must be met.

If a Slide L Definite Zone exists, its limits are τ_{bld} and τ_{eld} , as given by (38).

Rides only occur between the Definite Slide Zones and must terminate at the beginning of the next Slide Zone in the corresponding slide.

It is possible when the amplitudes are very low, for τ_{bgd} to exceed τ_2 ; this causes complications.

Slides must terminate at the time of flight τ_1 , or at Decision Times given by (39).

The impact causes a velocity change and results in either a slide or a Decision Time as given by (42).

If a Decision Time occurs in a Definite Slide Zone, the corresponding slide ensues: If not a Ride ensues.

Now, we proceed to the solution.

2.9 General Observations about the Solutions

2.9.1 The Maximum Number of Slides and Rides

It is possible to make some observations as to the maximum

number of transitions that may be expected in any given cycle. Four distinct situations can be envisioned.

For the case of Slide L possible (the satisfaction of (38a)) and τ_{egd} less than τ_2 , the more normal case, there will be two definite slide zones; thus a Slide G and a Slide L could occur, and the flight could terminate in a Slide G or L. Two zones in which a ride could initiate are present. Thus, this case could be as complicated as three slides, two rides, and a flight. It might proceed Ride, Slide G, Flight, Slide G, Ride, and Slide L, or RGFGRL. This type of solution has been observed. The second Slide G could have been a Slide L.

For the above case, when τ_{egd} is greater than τ_2 , the situation is even more complicated. The flight could terminate in a Slide L, and then this Slide L in turn terminate still within the G Definite Zone. Thus, this case could conceivably be as complicated as RGFLGRL.

When no Slide L Definite Zone is possible and the more normal condition of τ_{egd} less than τ_2 , prevails, the solution can only have two slides at most. A Slide G or L could result from the flight, and only one ride could be present. Thus, the two most complex solutions would be RGFG and RGFL.

Finally, when the L Definite Zone is absent, and τ_{egd} is greater than τ_2 , there is the added possibility that the Flight terminates in a Slide L, and this Slide L terminates within the G Definite Zone. Thus, the most complicated solution for this case would be RGFLG.

There is always one flight, and at most two Rides. The solution could be as simple as FL or FG. FL is quite common at high amplitudes. The limiting "once-per-rev" solution would be F alone; it would occur with A at its periodic limit, $\sqrt{\pi^2 + 1}$.

2.9.2 The Two Avenues of Approach Toward Finding the Solutions

The equations of motion of the particle for each possible subinterval of the cycle are completely determined now; the conditions that determine which form of motion is occurring, the time of

termination of any of the motion forms and that form which will initiate at any termination, are all completely derived. For any given set of operating conditions, if the velocity were known at any time within the cycle, one could compute the transition velocities and times around the cycle from the equations and conditions. Having the velocities and the times, the displacement could be taken zero at any convenient point, and then the displacement per cycle could be computed by calculating from transition point to transition point around the cycle. In general, however, the velocity is not known at even one point in the cycle.

One approach would certainly be, to set the velocity at any arbitrary value, at any time, say zero, and begin computing from transition point to transition point, letting the conditions and equations determine the transition points as they happen to come. This calculation would continue until the motion became periodic, and that periodic set of transition times and velocities would indeed be the true stable solution, at least for that starting condition. This approach was certainly considered and tried. In fact, it gave the first hints of the character of the final solutions. As might be expected though, the computations are long and cumbersome; there are many transcendental equations that must be solved by numerical methods. This total general mathematical analog seemed at best a long computer program with huge amounts of unimportant results to analyze. The author was on the verge of beginning it, when another avenue of approach became apparent.

The other approach, and the one used in this study, is to anticipate the form of the solution, require periodicity, and then develop formulae for appropriate transition times. With this method, providing the correct form of the solution can be anticipated, one is led directly to the steady state solution and the calculation and checking of only one cycle is required. Obviously, the difficulty lies in predicting the appropriate solution form. As a practical matter, this has not proved troublesome. The solution routines were programmed for computation on a 1620 IBM Digital Computer. Nine different solution forms were programmed for this study, seven of which turned out

appropriate to produce solutions for the operating conditions of interest. These routines and procedures will be presented in the next section.

The above two alternatives blend, to a degree, when the solution contains at least one Ride. Recall that a Ride can only be occurring in between the Slide Definite Zones, and that it must terminate at the beginning of the next Slide Definite Zone. Thus, if either of the two Rides can be anticipated, one definitely knows that the particle must have the velocity of the plane at the beginning of the next Slide Definite Zone. In the first method described above, as soon as the transient solution produced a Ride in the proper place, the very next velocity calculation around the cycle would yield the final solution. In the second method, one need not completely anticipate the form of the solution, but merely the position for a Ride. For example, in this study a Ride was assumed terminating τ_{bgd} ; one calculation around the loop, making the appropriate transitions, proved whether or not a Ride at this position, for these operating conditions, was a possibility.

Thus, the solutions can be logically divided into two main categories; solutions with a Ride, and solutions without a Ride. The next section presents several detailed solutions from each category.

2.10 Solutions Without a Ride

2.10.1 The GFGL Solution

The most complicated solution considered in this category is the GFGL, or the solution in which the impact results in a Slide G, which terminates in the L Definite Zone, causing a Slide L, which in turn persists into the G Definite Zone, bringing about a Slide G, which persists until the time of flight. A more complicated no-ride solution can take place when the amplitudes are very low and the G Definite Zone persists beyond the time of impact; in this case one has to admit the possibility of a Slide L terminating within the G Definite Zone following the impact. However, the present study did not require this solution. Thus, the solution is restricted to the more normal operating amplitudes for which τ_{egd} is less than τ_2 . Hence, we require

$$\tau_{egd} < \tau_2. \tag{43a}$$

In order that the impact result in a Glide G, the velocity of the particle following impact must meet condition (42a)

$$\dot{X}(\tau_2) > \dot{X}'(\tau_2) + \epsilon \Delta \dot{X} \quad (42a)$$

This implies that the velocity following the impact is given by expression (42b). The Slide G following the impact must terminate in the L Definite Zone, hence

$$\tau_{\text{bld}} \leq \tau_{\text{tg}} < \tau_{\text{eld}} \quad (43b)$$

The Slide L must terminate in the G Definite Zone prior to Flight, hence,

$$\tau_{\text{bgd}} \leq \tau_{\text{tl}} < \tau_1 \quad (43c)$$

Further,

$$\tau_2 < \tau_{\text{tg}} \quad (43d)$$

Thus, the above inequalities constitute tests that every GFGL Solution must pass.

Since there are four forms of motion in this solution, there will be four transition times to determine. τ_1 and τ_2 being definitely known, the two remaining transition times are τ_{tg} , when the Slide G following the flight terminates, and τ_{tl} , when the Slide L terminates. These can be determined by requiring periodicity as follows.

τ_{tl} is a Decision Time, and hence, the particle velocity is equal to that of the plane at that time; thus by (29b) the velocity at τ_{tl} is expressed in terms of τ_{tl} . From τ_{tl} to τ_1 , the particle undergoes a Slide G, hence, we may write the velocity at τ_1 in terms of τ_{tl} by utilizing the Slide G velocity Eq. (27c). The velocity at τ_2 is obtained by using the Flight velocity Eq. (31c); hence we obtain $X(\tau_2)$ in terms of τ_{tl} . The velocity following the impact is obtained from (42b) in terms of τ_{tl} . Now a Slide G initiates and continues until τ_{tg} . By substituting the velocity following impact into the Slide G termination Eq. (39a), the first equation relating τ_{tl} and τ_{tg} is obtained. A second equation is obtained by noting that the particle velocity equals the plane velocity at τ_{tg} , and that a Slide L ensues from τ_{tg} to τ_{tl} . Thus, the particle velocity at τ_{tg} is expressed in terms of τ_{tg} by using the velocity of the plane at that time, from Eq. (29b). Using this initial velocity in the Slide L termination equation, we obtain a second expression relating τ_{tl} and τ_{tg} .

Finally by manipulating these two transcendental equations one obtains the following relations:

$$\tau_{tg} = \frac{1}{2} (\gamma + \delta), \quad (44a)$$

$$\tau_{tl} = \tau_{tg} - \gamma \quad (44b)$$

where

$$\gamma = \frac{\pi \phi}{\zeta} \left[\frac{2\zeta - 1}{\phi - 1} \right] + (1 - \epsilon) \frac{A}{2\zeta} \frac{(\phi - 2\zeta)}{(\phi - 1)} \frac{\Delta \dot{X}}{\psi}, \quad (44c)$$

$$\delta = 2 \left\{ \pi - \text{Sin}^{-1} \left[\frac{1}{2\phi \sin \frac{\gamma}{2}} \left(\frac{\delta}{A} - (1 - \epsilon) \frac{\Delta \dot{X}}{\psi} \right) \right] \right\}. \quad (44d)$$

The actual derivation of the above is carried out in Appendix A. 1. 8.

Now since the two transition times, τ_{tl} and τ_{tg} are Decision Times, when the particle velocity equals the plane velocity at these times, we know the velocity at two times in the solution. By utilizing the appropriate velocity equations all other transition velocities may be computed. Knowing the transition velocities the displacement is set equal to zero at any convenient point and subsequently calculated around the cycle, which completes the solution.

In summary then, (44) are used to compute the transition times. Presuming they yield reasonable values, we subject them to the tests (43). Fulfilling these requirements, the transition velocities are computed. We then make the test indicated in (42a). Fulfilling this requirement the displacements are computed and the solution is complete. Failing any of the above tests means that the operating conditions are not satisfied by a GFGL Solution.

The routine to make these computations is presented in Appendix A. 2. written in Fortran computer language for use on an IBM 1620 Digital Computer. Experimental Case 10 on page 100 shows a typical solution for a set of operating conditions that require a GFGL Solution.

2.10.2 The FGL Solution

Another solution that has been of great value in this study is the FGL Solution. The transition between the GFGL and the FGL Solutions occurs as friction is reduced and becomes no longer sufficient to terminate the Slide L prior to the Flight in the GFGL Solution. Thus the Slide L persists up to τ_1 , and hence a necessary check on every FGL Solution is

$$\dot{X}(\tau_1) < \dot{X}'(\tau_1). \quad (45a)$$

The velocity at τ_2 must be such that a Slide G results from the impact hence condition (42a) must be met by any valid FGL Solution. Repeating it

$$\dot{X}(\tau_2) > \dot{X}'(\tau_2) + \epsilon \Delta \dot{X}. \quad (42a)$$

Further, for a Slide G to terminate in a Slide L, an L Definite Zone must be present, hence by condition (38a)

$$\frac{1 - 2\zeta}{A} - (2\zeta - \phi) > 0. \quad (38a)$$

The Slide G must terminate within the Slide L Definite Zone, and so the final check on any solution is

$$\tau_{\text{bld}} \leq \tau_{\text{tg}} < \tau_{\text{eld}}. \quad (45b)$$

There are three transition times in this solution; τ_1 and τ_2 being known, the remaining τ_{tg} can be determined by requiring periodicity as follows. τ_{tg} is a Decision Time, hence at that time the particle has the velocity of the plane. Thus by using the plane velocity Eq. (29b) we obtain $\dot{X}(\tau_{\text{tg}}) = f(\tau_{\text{tg}})$. With this as the initial velocity the particle undergoes a Slide L from τ_{tg} to $\tau_1 + 2\pi$, hence the Slide L velocity Eq. (28c) yields $\dot{X}(\tau_1) = f(\tau_{\text{tg}})$. With this as the initial velocity the particle undergoes a Flight from τ_1 to τ_2 ; thus by means of the Flight velocity Eq. (31c) we obtain $\dot{X}(\tau_2) = f(\tau_{\text{tg}})$. Now by the impact velocity change indicated in (42b), we obtain the velocity just after impact to be $\dot{X}(\tau_2^*) = f(\tau_{\text{tg}})$. Finally, a Slide G ensues back to τ_{tg} , so with $X(\tau_2^*)$ and the initial velocity and τ_2 as the initial velocity and τ_2 as the initial time, we require that the Slide G terminate back at τ_{tg} by use of the Slide G Termination Eq. (39a). The execution of the above yields the following transcendental equation for τ_{tg} .

$$0 = \cos \tau_{tg} + \frac{1}{A} \tau_{tg} - \left(\frac{1-\epsilon}{2}\right) \left(\frac{\tau_2}{A} + \cos \tau_2\right) - \left(\frac{1+\epsilon}{2}\right) \left(\frac{\tau_1}{A} + \cos \tau_1\right) \frac{\pi}{A} \left(\frac{2\xi-1}{\xi}\right) \quad (46)$$

In summary, if a set of operating conditions, that satisfy (38a), yields a solution of (46), that satisfies (45b), and yields a set of velocities that satisfy (45a) and (42a), FGL is the correct solution form, and that set of velocities and transition times is the correct solution for those operating conditions. The displacements are obtained by starting at any convenient point and computing around the cycle. Appendix A. 2. 4 presents the complete Fortran Program to accomplish these calculations on the computer and Experimental Case 8 on page 96 presents a typical example of an FGL solution.

2.10.3 The FL Solution

This solution can come about in two ways. The more normal type of FL Solution, and the one found useful in this study, comes about as the amplitude is increased and the time of impact τ_2 , occurs within the L Definite Zone. This increased amplitude causes an increase in the available x impulse during impact and often causes the impact to result in a Decision Time, thereby causing the particle to initiate a Slide L following the impact. A second type of FL Solution is mentioned here for completeness. This solution might occur if the x velocity prior to impact met condition (42e),

$$\dot{X}(\tau_2) < \dot{X}'(\tau_2) - \epsilon \Delta \dot{X}. \quad (42e)$$

In this case a Slide L would result from impact even if no Slide L Definite Zone existed. The solution would probably become apparent with increasing β , and high amplitudes for when τ_2 is of the order of 2π , the plane is at its maximum x velocity. The solution of this case would pose no difficulty; it is only omitted because it was not needed, and is thought to be obscure.

The first type of FL Solution will now be considered in detail. Certainly a requisite of this solution is that of Slide L Definite Zone exists (38a). Further τ_2 must lie in the L Definite Zone, hence

$$\tau_{\text{bld}} \leq \tau_2 < \tau_{\text{eld}} \quad (47)$$

The impact results in a Decision Time, i. e. the particle has the velocity of the plane after impact, hence from (29b)

$$\frac{\dot{X}(\tau_2^*)}{\psi} = (\phi - \zeta) \cos \tau_2 \quad (48)$$

The particle now undergoes a Slide L from τ_2 to $\tau_1 + 2\pi$. Using (48) as the initial velocity in the Slide L velocity Eq. (27c), we find the velocity at τ_1 to be

$$\frac{\dot{X}(\tau_1)}{\psi} = \frac{(2\zeta - 1)}{A} (2\pi + \tau_1 - \tau_2) + \zeta \cos \tau_1 + (\phi - 2\zeta) \cos \tau_2. \quad (49)$$

To find the velocity just prior to impact, we use the Flight velocity Eq. (31c) from τ_1 to τ_2 with (49) as the initial velocity. This yields

$$\frac{\dot{X}(\tau_2)}{\psi} = \frac{1}{A} \left[2\pi(2\zeta - 1) + \zeta\tau_1 - \zeta\tau_2 \right] + \zeta \cos \tau_1 (\phi - 2\zeta) \cos \tau_2. \quad (50)$$

Finally two tests must be satisfied by the above velocities. First the particle velocity must remain less than the plane velocity throughout the Slide L and at least up until the time of impact, hence from (29c)

$$\frac{\dot{X}(\tau_1)}{\psi} \leq (\phi - \xi) \cos \tau_1. \quad (51)$$

And secondly, the difference between the plane velocity and the particle velocity, prior to impact, must be small enough so that the impact results in a Decision Time. This condition was expressed as (42c)

$$\dot{X}'(\tau_2) - \epsilon \Delta \dot{X} \leq \dot{X}(\tau_2) \leq \dot{X}'(\tau_2) + \epsilon \Delta \dot{X}. \quad (42c)$$

In summary then, if τ_2 satisfies (47), the velocities at τ_1 (49), and τ_2 (50) are computed. If these velocities meet conditions (51) and (42c), an FL Solution of this type is assured.

Appendix A. 2.5 presents the Fortran Program to accomplish these computations on the computer, and Experimental Case 9 on page 98 presents an example of an FL Solution.

2.10.4 Concluding Remarks on the No Ride Solutions

It certainly appears safe to say that other no-ride solutions exist. One would certainly anticipate an FLG and an FG as well as the second kind of FL, at least. Further, if one considers the very low amplitudes for which the G Definite Zone exists beyond the time of impact, more solutions become possible. No attempt is intended at being comprehensive and including all possible solutions. The general procedure used in seeking the above solutions, would serve to solve any other no-ride solutions for which a need arose. The next section will take up a number of the solutions containing a ride.

2.11 Solutions with a Ride

As was stated previously, the solutions containing a Ride are somewhat easier to confirm, but since a Ride adds more possible transitions there are many more possible solutions with Rides than without. The convenient feature of these solutions is that the Ride must definitely be occurring between the Definite Slide Zones and it must terminate, with the velocity of the plane at the beginning of the next definite slide zone. Because of this feature, once the position of the Ride has been assumed, the calculations are quite straightforward following the equations and conditions previously derived. All one need do is proceed from the assumed Ride termination point (either τ_{bgd} or τ_{bld}), calculating transition times and termination velocities around one cycle; if the calculation returns to a Ride in the assumed Ride zone, prior to or even at the assumed Ride termination, the solution is confirmed.

Because of this straightforwardness, it is possible to write two computer programs capable of testing for a solution, one for each possible Ride position. This would solve all possible solutions containing a Ride. Again, however, this becomes a very lengthly complicated program. It is entirely probable that many of the possible solutions are obscure and of little practical value. In this study a much simpler program was written that was capable of checking for six such solutions, and in all cases computed only four of the solutions were needed.

It has been shown that a Slide G Definite Zone always exists. For the case when a Slide L Definite Zone exists (satisfaction of condition (38a)), there will be two positions where a Ride may exist. It is argued that it is probable that a Ride will occur prior to τ_{bgd} , whenever a Ride exists prior to τ_{bld} . This argument proceeds as follows. Consider Eq. (10), the equation for the normal force. Utilizing the definition of A (Eq. (11b)) this may be written

$$\frac{N}{m g \cos \beta} = - A \sin \tau + 1. \quad (52)$$

The possible Ride Zones are near π and 2π or 0. The normal force will be zero or small for a good part of the time prior to $\tau = \pi$, while the normal force will be at its maximum, thereby affording large friction force, in the third and fourth quadrants prior to the ride zone near zero. It is likely that a Ride near zero is the more probable of the two, and hence many more of the practical solutions will be covered by considering this Ridezone as opposed to the second zone. For this reason, and certainly because it satisfied all of the needs of the study, Ride solutions were only considered for cases in which the Ride was occurring prior to or terminating at τ_{bgd} .

Further, it was not found necessary to consider the cases of extremely low amplitude when the Slide G Definite Zone extends beyond the time of impact, $\tau_{egd} > \tau_2$. The same restriction imposed on the FL Solution about the type of Slide L initiation following impact was also included. This is that the only type of Slide L initiation following impact that the calculation routine permits is when the impact occurs in the L Definite Zone and the Slide L results from a Decision Time. It must be restated that these restrictions still left the routine sufficiently general so that a solution was obtained for all operating conditions of interest.

A solution routine was developed and programmed for computation on the digital computer. The routine assumes a Ride terminating at τ_{bgd} in a Slide G which continues to τ_1 , the time of flight. It then calculates the velocity at the end of the Flight, τ_2 , and then goes through the set of impact relations (42) and makes the proper decision. It continues calculating and testing velocities from transition point to transition point along one of six different paths. If the assumed solution passes all of the tests along any one of the paths and terminates in a Ride prior to the beginning of the next G Definite Zone, a station has been found. The routine then computes the remaining velocities and displacements and prints them out. In this way the solution routine tests the operating conditions to determine if a solution exists with any of the following six combinations of motion

forms; RGFGR, RGFGL, RGFG, RGFL, RGFRL, and RGF. A listing of the Fortran program used for these computations together with a brief description of the various steps is contained in Appendix A2.6. Experimental Case 6 on page 92 shows a typical print out from this program together with the solution.

2.12 Further Comments on the Computations

2.12.1 The Effect of ϵ

In order to demonstrate the fact that the impact friction multiplier, ϵ , is a significant factor of the utmost importance, some computer results which demonstrate this fact must be included. Clearly, ϵ only affects one point on the cycle; it controls the amount of x impulse received at impact. However, when friction is small and ϕ is large, the no-ride solutions prevail and these, except for the FL solution are significantly influenced by ϵ . Figure 6 presents the displacements as a function of time, as computed for a case in which the effect of ϵ is large.

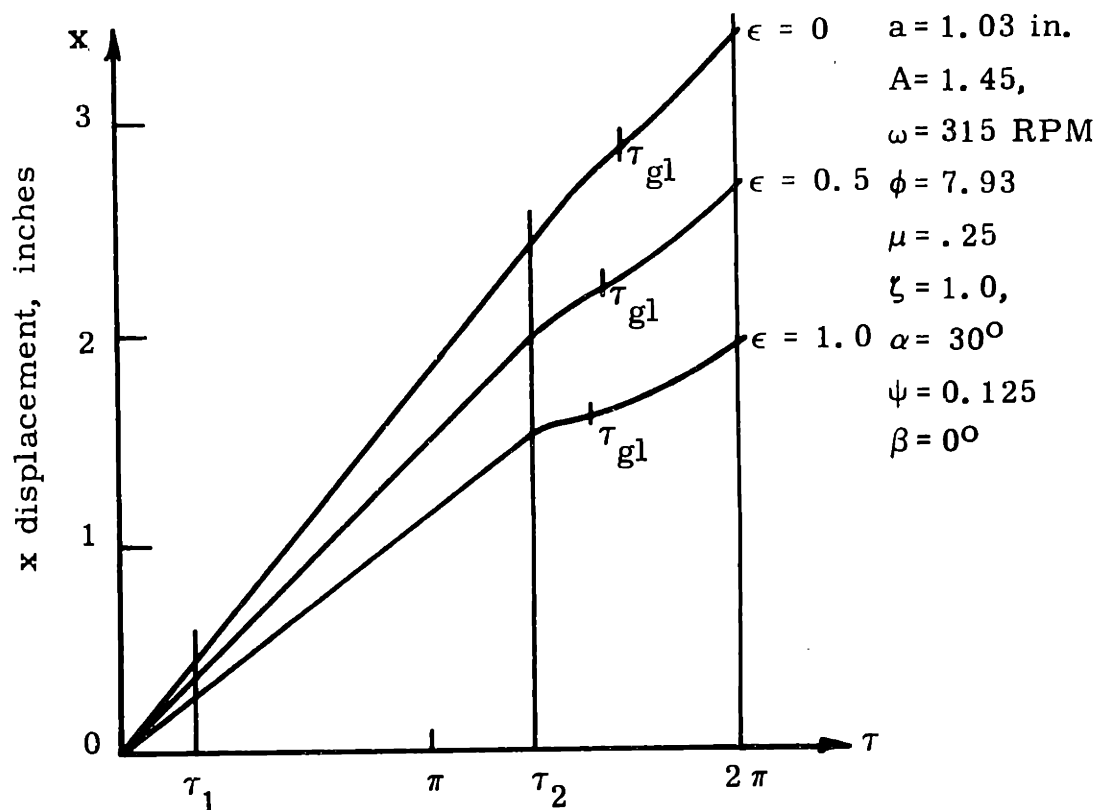


Figure 6

Displacement as a Function of Time for Various Values of ϵ

2.12.2 The Distribution of the Solution Forms

The solution form, i. e., FGL, FL, RFG, etc., is a function of the four variables, A , ϕ , ζ , and ϵ . In order to facilitate the testing of operating conditions for solutions, a set of maps of the distribution of the solution forms for a particular ϵ and ζ can be made. These show the change of solution form as A and ϕ are varied. Since many cases were computed in testing the programs and the experimental data, a collection of this information has been plotted and is shown in Figs. 7 and 8, for $\zeta = 1.0$ (i. e., the plane horizontal), and $\epsilon = 1.0$ and $\epsilon = 0.5$. The boundaries are estimated from the points shown; no attempt has been made to derive their actual mathematical shape.

2.12.3 A Comment on the Solution of Transcendental Equations

Since many transcendental equations arise in the actual computation of the solutions, mention might be made of the way in which they were solved. The Newton-Raphson Method as given in Pipes (Ref. 17) among others was found to be quite quick and convenient. The rules for convergence of the method are given in the reference and will not be repeated, but one must be reasonably close to the desired root to obtain a solution. Further, the answer must be checked to be sure it yields meaningful value. Briefly, if we desire the solution of

$$F(x) = 0, \quad (53a)$$

then we may set up the sequence

$$x_{\text{new}} = x - F(x) / F'(x) \quad (53b)$$

and by starting with a "reasonably" good guess for x , quite quickly converge to an accurate value.

For example, in every computation for a solution, the value of τ_2 had to be computed from Eqs. (16). A crude approximation expression of the τ_2 curve on Fig. 4, was developed and used for

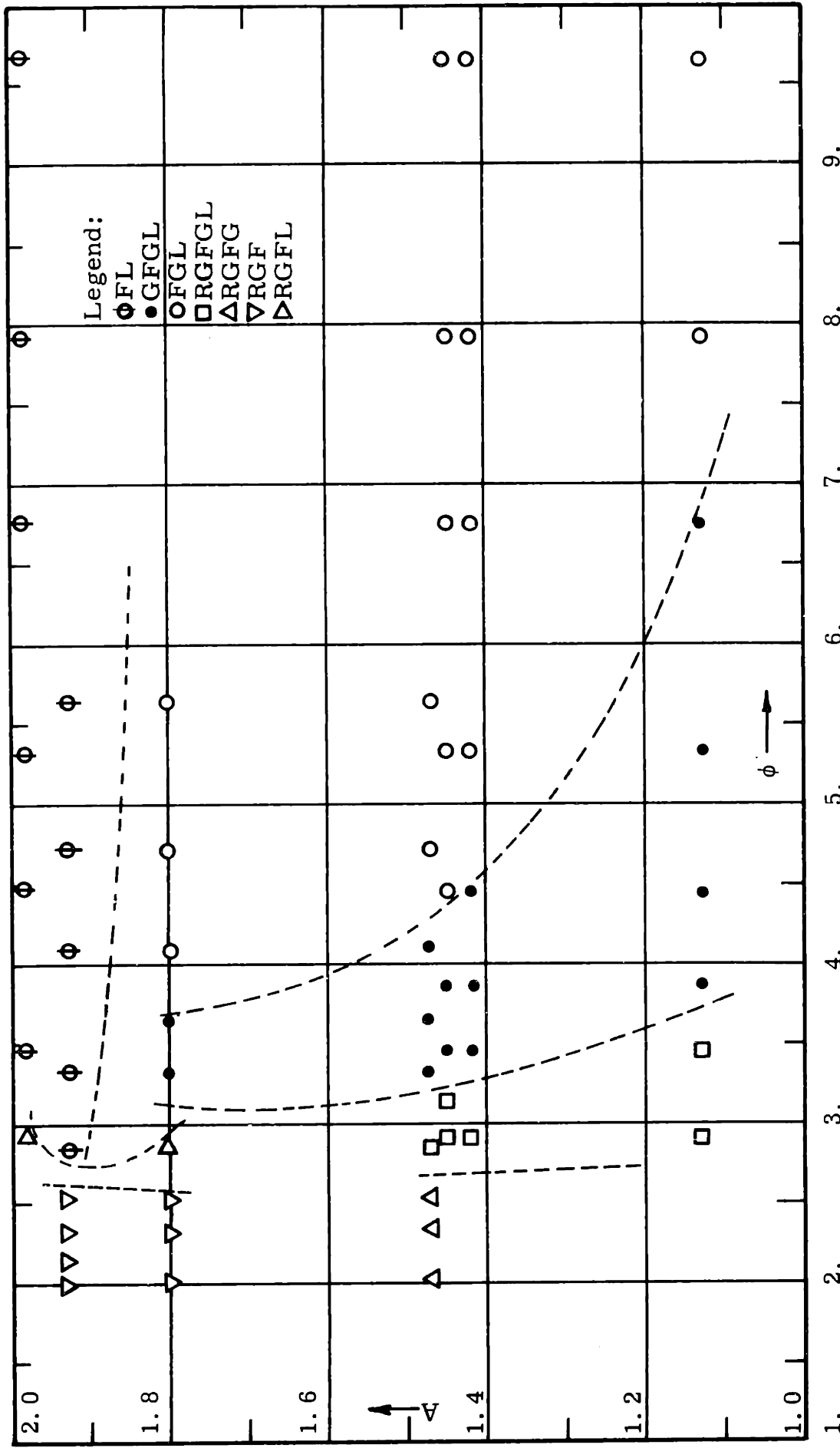


Figure 7
 Distribution of Solution Forms with A and ϕ for $\zeta = 1.0$, $\epsilon = 1.0$

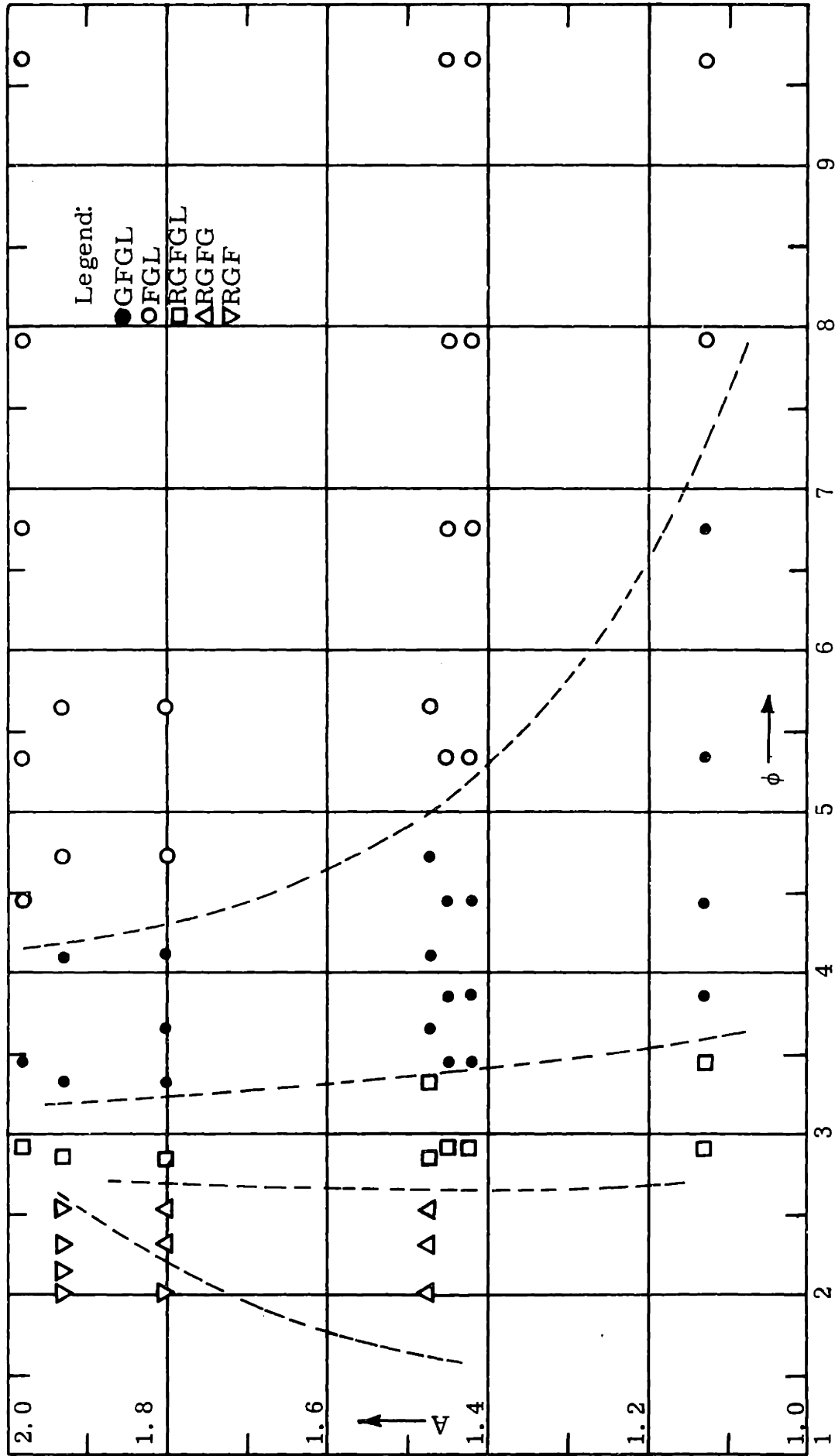


Figure 8
 Distribution of Solution Forms with A and ϕ for $\zeta = 1.0$, $\epsilon = 0.5$

this initial guess. Note the Fortran step just prior to number 10, in all of the computer programs in Appendix 2, in which this approximation is being made. The approximations for the roots of the Slide Termination equations were more difficult, especially in the Ride Program; oftentimes the approximation value had to be changed in order to obtain a solution.

2.13 The Application of the Single Particle Theory to Granular Solids in Troughs

The transportation of granular solids is a very important application of the oscillating conveyor; hence, it is necessary to discuss the applicability of single particle theory to a trough filled with a granular solid.

A granular solid can be thought of as a continuum with a density and bulk modulus. It has absolutely no strength in tension, great strength in compression, and a frictional strength in shear, i. e., the greater the compressive stress, the greater the shear strength. The shearing strength is related to an internal friction coefficient and the compressive principal stresses, see, for example, the explanation of yielding given by Jenike (Ref. 19). For these purposes, a sufficient indication of internal friction is the tangent of the maximum angle of a small hill of the granular solid. There is also another coefficient of friction of interest; this is an external coefficient of friction between the granular bed and the walls of the trough. One would expect the granular solid to move as a slug if the external friction were less than the internal friction. The experiments conducted in this study indicate that the granular materials do move as a slug; see the data photographs in Fig. 14 and note the negligible shift of the marking grains.

Given the empirical knowledge that the bed moves as a slug, it is possible to make some observations about the nature of the external friction between the bed and the trough. Consider a layer of a long rectangular bed of granular material, parallel to the bottom of the trough, up from the bottom a distance η , and of thickness $d\eta$, as shown in Fig. 8.

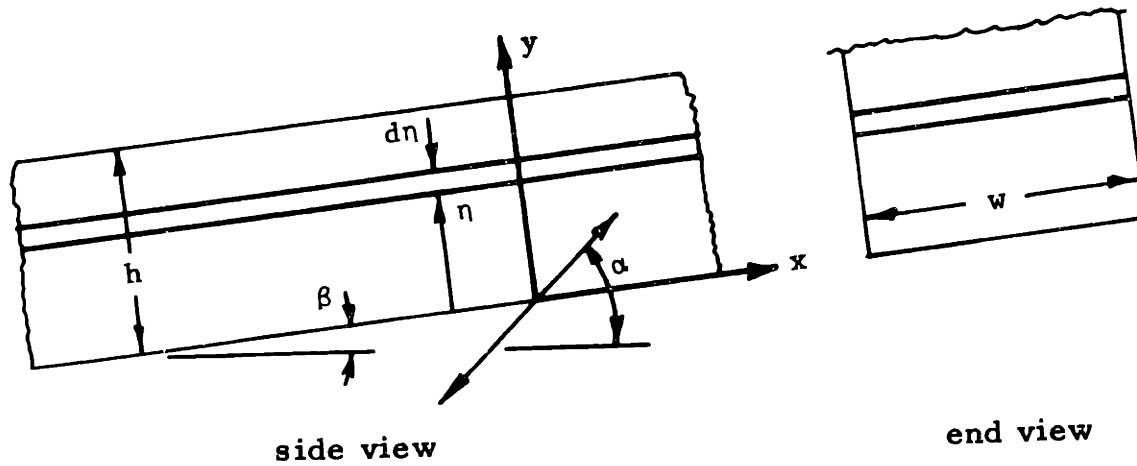


Figure 9 - Diagram of Coordinates and Dimensions of a Bed of Granular Material

The trough is considered to oscillate in a direction α , and is inclined to the horizontal with angle β , as in the case of the single particle analysis. Dynamic equilibrium in the y direction for the layer yields

$$\frac{dp}{d\eta} = -\rho g \cos \beta - \rho \ddot{y} \quad (55a)$$

Note that when the bed is sliding, friction from the walls has no vertical component. When the bed is in the trough, it has the y motion of the trough, hence from (1f), (55a) becomes:

$$\frac{dp}{d\eta} = (-\rho g \cos \beta + \rho a \omega^2 \sin(\alpha - \beta) \sin \tau). \quad (55b)$$

Equation (55b) is integrated with the boundary condition that $p = 0$, when $\eta = h$, to yield

$$p = (h - \eta) (\rho g \cos \beta - \rho a \omega^2 \sin (\alpha - \beta) \sin \tau). \quad (56)$$

Now a very approximate assumption is made temporarily. We assume, as in fluid mechanics, that the pressure is the same in all directions. Hence, while sliding, the frictional force on the bed is given by the product of the coefficient of external friction, μ_e , and the pressure integrated over the area of contact between the bed and the trough. This yields

$$F = \mu_e whl \left(1 + \frac{h}{w}\right) (\rho g \cos \beta - \rho a \omega^2 \sin (\alpha - \beta) \sin \tau). \quad (57)$$

The force analogous to the normal force of Eq. (10) in the single particle theory is the product of the pressure at $\eta = 0$ and the area of the trough bottom, wl . An effective coefficient of sliding friction of a bed of granular material can be taken to be the friction force from (57) divided by this analogous normal force. Thus, we find

$$\mu_{\text{eff}} = \left(1 + \frac{h}{w}\right) \mu_e. \quad (58a)$$

Now to compensate for the assumption of equal pressure in all directions, we state that the full pressure given by (56) is not attained between the walls of the trough and the sides of the bed, that friction provides a percentage of the support of the sides of the bed. Thus, we introduce some factor k (less than unity) on the h/w term in (58a) and obtain

$$\mu_{\text{eff}} = \left(1 + k \frac{h}{w}\right) \mu_e. \quad (58b)$$

While the above is admittedly oversimplified, it does lead us to expect

that deeper beds will have greater friction than the shallower beds, and that they may be related by an expression of the form of (58b).

A further important conclusion can also be drawn from the above. Note that in (55b), (56), and (57), that if ω or a is zero, Eqs. (58) also apply to the non-oscillating tilting of the platform if the particles are sliding. Thus, no matter how complicated the k of (58b) actually is, we may measure the effective coefficient of sliding friction by noting the minimum angle of tilt of the channel for which a constant velocity slug slide of the bed can be maintained. As will be described later, this was the method used experimentally.

Finally, let us consider the possibility that the sides of the bed of particles may suffer some frictional restraint from the walls of the trough during flight. For any frictional force to be present between the walls and the bed, there will have to be a pressure within a bed. However, during flight, if the walls of the trough are such that they do not cause the bed to change shape, i. e., are not leaning inward, the pressure will be zero within the bed, hence, the frictional force between the walls and the bed will be negligible.

Thus, given the experimental observation that a bed of free-flowing granular material moves as a slug in these conveyors, we are led to expect that single particle theory will predict the motion of granular solids providing that the effective coefficient of friction is measured by tilting the channel and noting the minimum angle for which a constant velocity slug slide can be maintained.

CHAPTER III

EXPERIMENTAL ANALYSIS

3.1 Description of the Apparatus

A conveyor motion simulator was built to test the theory. The machine provides an oscillating plane which accurately executes the motion specified by Eq. (1). The plane can be fitted with a channel for the study of granular material and is shown with the channel in place in Figs. 10 and 11. Wood was used as the main construction material principally because of the need for quickly fabricating a large stiff structure. Steel was used in the regions where high stresses demanded it. Both α and β could be varied as shown in the figures, as well as the amplitude and frequency. The machine had a "direct drive" reciprocating motion so that the amplitude, "a" could be held constant during a test. The amplitude could be set between tests by bolting the connecting rod bearing to any one of a series of holes with varying offsets in a crank plane, which in turn was mounted on an idler shaft. This idler shaft was driven through a V-belt by a large variable speed motor which permitted adjustment of the frequency. The plane, itself, was of sandwich construction for weight and stiffness reasons. It was surfaced with a hard epoxy resin and was four feet long and one foot wide. A variable width, transparent-fronted channel (1 1/2 inches deep by a maximum of 2 inches wide) was fitted to the plane for the study of granular materials: see Figs. 12 and 13. The construction details are more fully explained in Appendix 3.1.

For the single particle study, two different particles were used. Early in the experimental study, it was realized that a single particle with a large contact area, (e. g., a 3/4 inch board, 3 inches wide by 6 inches long) was significantly lubricated during impact by

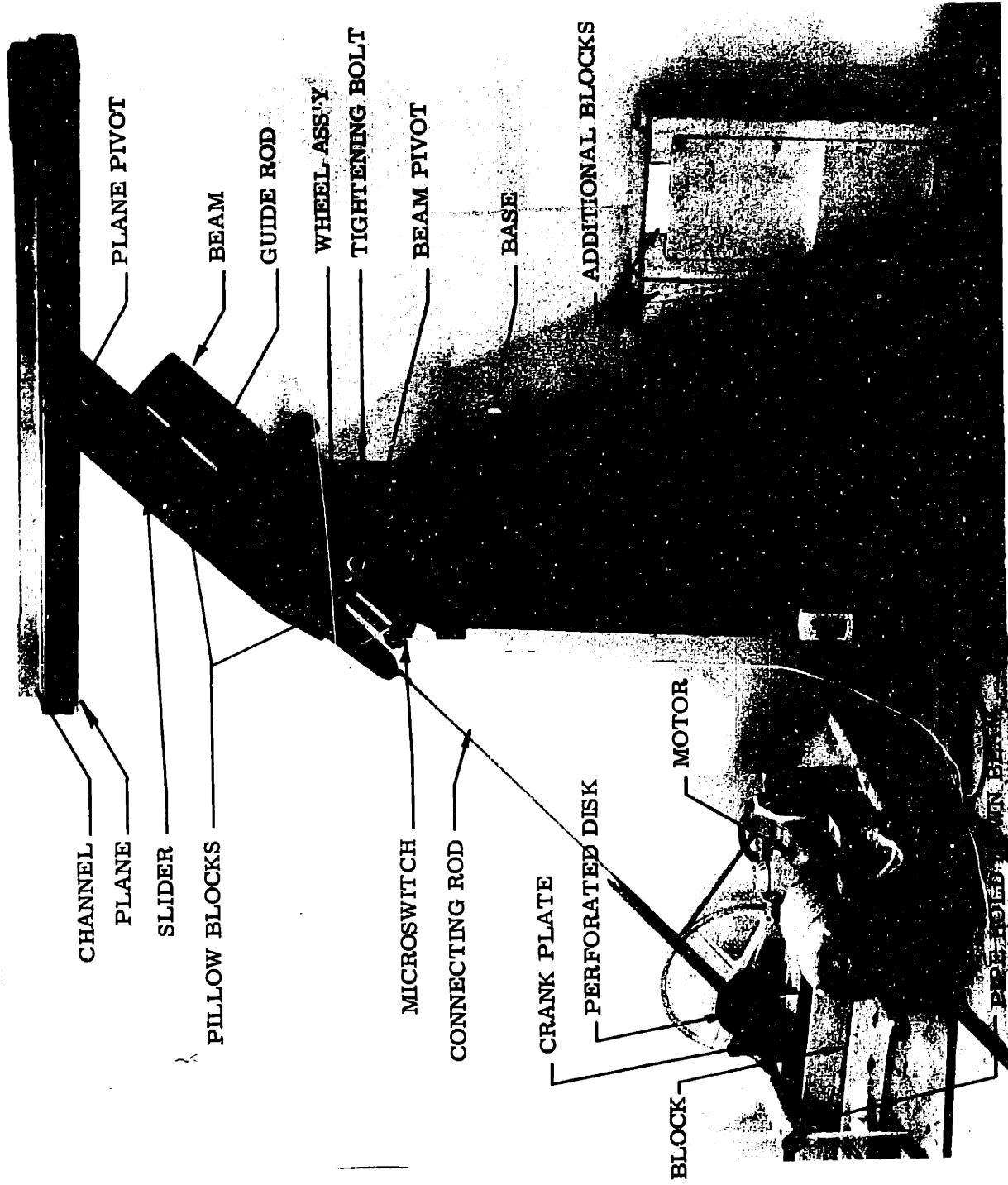


Figure 10 - Conveyor Motion Simulator

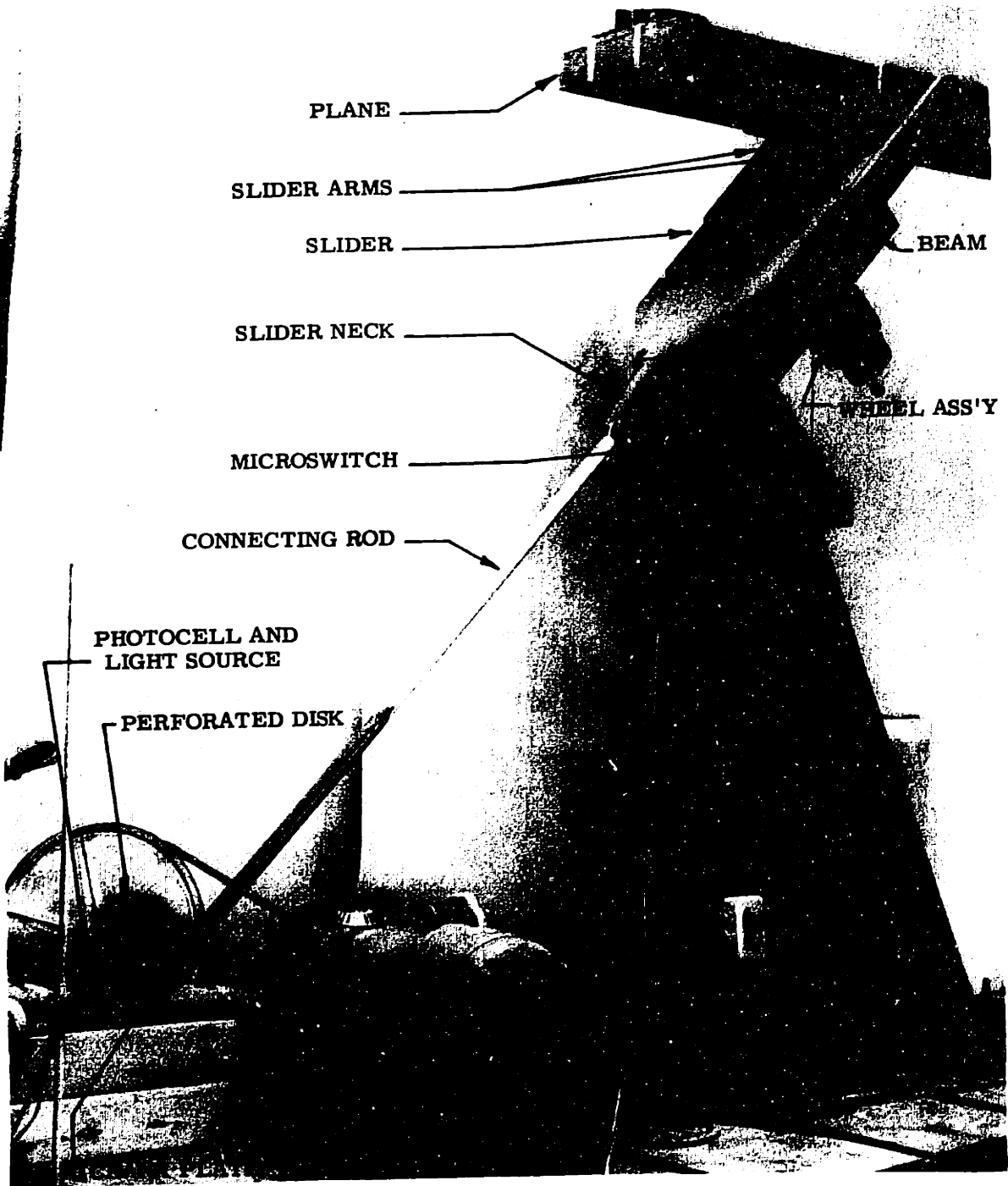


Figure 11 - Oblique View of Conveyor Motion Simulator

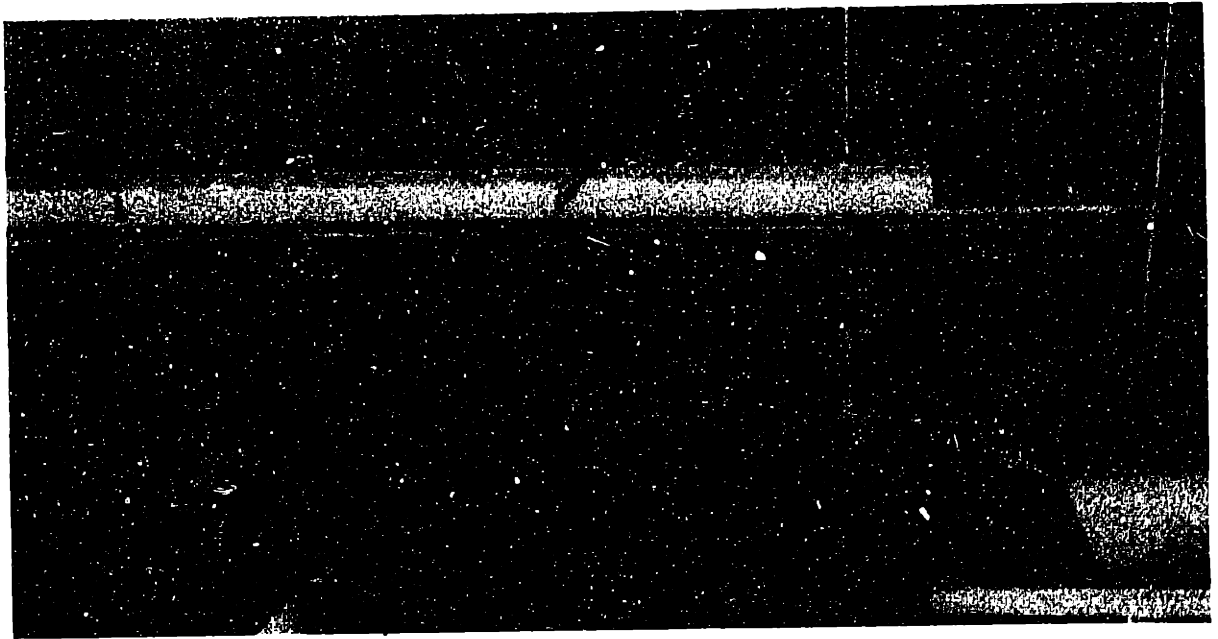


Figure 12 - The Transparent-Fronted Channel Filled with Rice, showing the Dyed Marking Grains

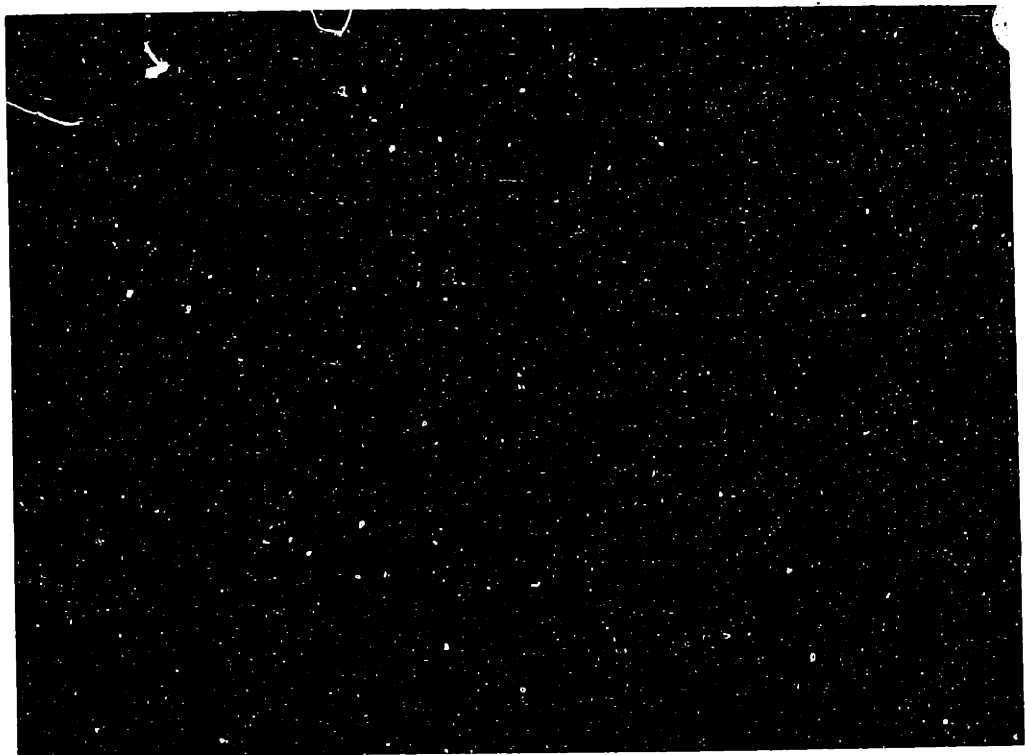


Figure 13 - Looking Down on the Transparent-Fronted Channel

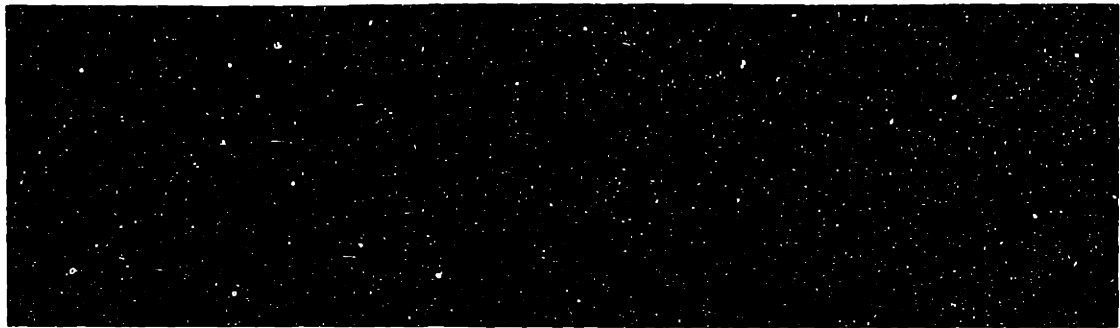
the squeezing out of the air between the board and the plane; thus no x impulse occurred during impact in these first experiments. This is unrealistic to actual practice, hence, the particles used in the study rested on four small pads in the corners. Particle 1 was a wooden board, 2 inches wide by 6 inches long, and $1/2$ inch thick. In its bottom four corners were attached four, $1/4$ inch thick, $1/2$ inch square wood pads; four steel thumb tacks were attached to these pads. The particle was painted black so that it would not be seen by the camera, and on the top of the particle, two pins with $1/8$ inch spherical white heads were attached a known distance apart, fore and aft of the center. Particle 2, was made of $1/4$ inch thick cloth reinforced rubber, two inches wide and three inches long. Four wood pads (without tacks) were attached to its bottom corners. Again, two white headed pins were placed on the top, a known distance apart.

The data was taken photographically by means of a stroboscopic light, triggered by equally spaced holes on a disk mounted on the idler shaft. The details of this disk and the triggering are given in Appendix A3.2. The camera was mounted on a tripod with the lens open as the particle traveled by. The photograph, therefore, contained a sequence of white dots, which were images of the white-headed pins, giving the particle position as a function of time. The known distance between the pins provided a scaling factor. Two of these white pins were also affixed to the plane to give a trace of its motion, thereby affording a check on direction and straightness. (See Figs. 14a and b.)

The particles used in the study of granular materials were small white dried beans or rice. Grains of these particles were dyed black for marking purposes. The procedure for taking granular materials data had to be altered because the white bed of particles would cancel the image of the black marking grains. To obtain the data in these cases, the camera was rotated at 4 RPM by a synchronous motor about a horizontal axis. Thus, the information was spread out across the entire film plane. Data photographs taken in this way are shown in Figs. 14c, d, and e. In these cases the white pins on the plane provided the scaling factor.



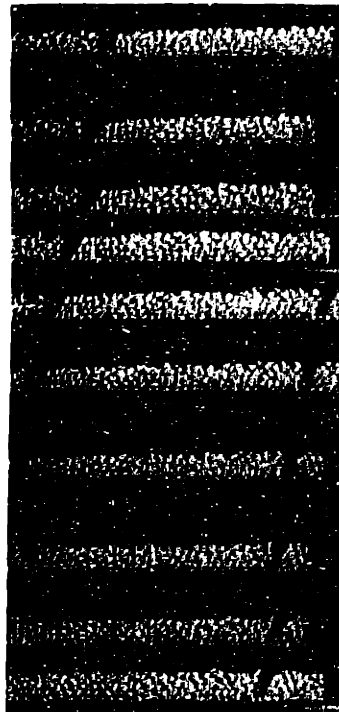
(a) Experimental Case 1
29 points per cycle



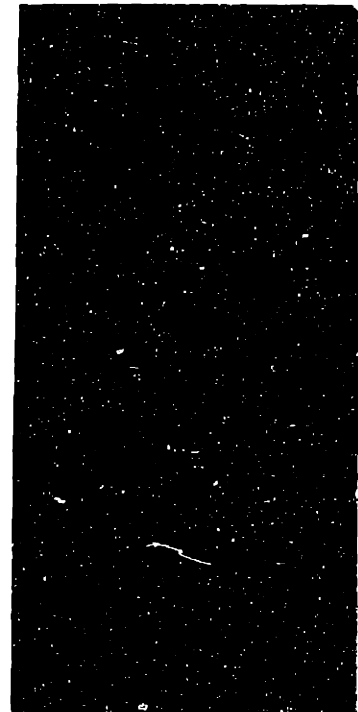
(b) Experimental Case 5
14 points per cycle



(c) Exp. Case 8
6 per cycle



(d) Exp. Case 6
6 per cycle



(e) Exp. Case 9
6 per cycle

Figure 14 - Typical Data Photographs

Table 2 lists the particles used in the experimental cases presented.

| Table 2 Summary of Particles | |
|------------------------------|---|
| Particle 1 | 2 x 6 x 1/2 inches, wood; steel tacks in contact with plane; pin separation = <u>6.45</u> ". |
| Particle 2 | 2 x 3 x 1/4 inches, cloth reinforced rubber; wood pads in contact with plane; pin separation = <u>2.43</u> ". |
| Particle 3 | narrow beans; channel height = 1"; channel width = 1/2". |
| Particle 4 | narrow rice; channel height = 1"; channel width = 1/2". |
| Particle 5 | wide rice; channel height = 1/2"; channel width = 1 1/2". |

3.2 Experimental Procedure

The general procedures are presented as they occurred in a typical single particle test, with digressions where necessary. Then the procedures peculiar to the test of granular materials are presented.

3.2.1 Single Particle Procedure

The plane and the pads on the particle were cleaned by a light sanding and careful dusting. The particle was then placed on the plane and the plane was tilted. The particle was then given a little initial motion downhill. If the particle continued to slide, the angle of tilt was decreased. If the particle came to a stop, the angle of tilt was increased. The final angle of friction was taken to be the minimum angle for which a constant velocity slide of the particle could be maintained. The plane was then locked at this angle and the angles measured with a machinist's protractor that was fitted with a level that could be read to $1/2^{\circ}$.

Next, the angles α and β were set to the desired values with this same protractor.

The frequency was then set at first by a hand tachometer on the idler shaft. The final frequency check and adjustment was made by counting the number of oscillations of the slider occurring in one minute. This was accomplished by causing the slider to trip a micro-switch which, in turn, actuated an electric counter that was energized for precisely one minute by an accurate electric timer.

The perforated disk on the idler shaft that triggered the stroboscopic lamp, contained 29 holes spaced at 12° intervals; this left one blank position to indicate phase. Further, in many of the tests it was unnecessary to record so many points. Unwanted holes could be "blacked out" on the disk with black plastic electrical insulating tape. The majority of the tests were run with fourteen holes spaced at 24° intervals. In both cases the phase was checked by photographing the crank plate on the idler shaft. The crank plate and the connecting rod bearing were painted flat black and marked with reflective tape. (See Fig. 11). Both the camera and the lamp were then focused on the crank plate, the machine started, and the shutter opened for $1/2$ second. This yielded a photograph showing the exact angular position of the blank hole, thereby establishing the phase of that position in the data photographs.

The camera was positioned with its film surface parallel to the x-y coordinate system of the machine, slightly above the mean position of the plane, and $3\ 1/2$ feet back. It was then focused on the anticipated particle path.

The particle was positioned at the far end of the plane, the room darkened, and the stroboscopic lamp energized and aimed at the region of interest. The lamp to path distance was about 2 feet. The machine was then started with a foot switch. When the particle arrived about $3/4$ of the way down the plane, the camera shutter was opened for one second, thus taking the photograph. If the particle had come down the plane with no rotation or other obvious irregularities, the data was presumed good. A second check on the angular velocity was then made.

3. 2. 2 Procedure Peculiar to Granular Materials

The channel was fixed to the plane with fiberglass pressure sensitive tape. The width was adjusted by tightening the movable channel wall against a block of the desired thickness.

To make the friction measurement the channel was filled to the desired level with the granular material. A box was attached to one end of the channel to catch the spilling particles. Then the plane, channel and box were carefully tipped, during which time the channel was tapped. As the tip angle increased the particles would begin to shift some at each tap, while at the lower end, end particles would be spilling into the box haphazardly. Finally, when the angle was just great enough, the whole remaining mass of particles would begin a constant velocity slide with no relative velocity between them. This angle was taken to be the angle of sliding friction for the particles. As can be imagined, this is a time consuming measurement; repeated tests gave values that varied to the extent that it seemed unrealistic to presume knowledge of the friction coefficient any more accurately than ± 0.05 .

Since the camera was to be rotated and since each image was to cover the full width of the film it was necessary to reduce the number of flashes per cycle to six. No phasing by missing images was attempted for the tests of granular materials; the discontinuities in the displacement time curve were considered sufficient to identify the phase, as well as the fact that points of flight could be visually observed. (See Figs. 14c, d, and e).

After having set α , β , and the frequency, the channel was again filled to the desired level. Then, two pieces of thick celluloid, the width of the channel, were used to spread a vertical column of the grains apart. Grains dyed with black ink were then dropped in this slot and the celluloid removed. The top surface was smoothed out and the bed was ready for test. Figure 12 shows a bed of rice ready for test.

The camera was set at a distance of 8 feet from the channel and aimed such that the channel was at the bottom of the film plane. With the room darkened and the stroboscopic light energized, the machine was started. When the marking grains came into view of the camera, the rotator was started and the shutter opened for one second, thus taking the photograph.

3.3 Processing The Data

3.3.1 Data Photographs

The film used throughout was Kodak Tri-X Roll Film, Size 120. It was processed in a tank using Acufine Film Developer (Baumann Photo-Chemical Corporation; Chicago, Illinois). This developer increases the film speed from 700 to about 1200. No other special film techniques were involved. Adequate negatives were always obtained with the camera lens opening at f3.5, the stroboscopic light set on low intensity, and located no further than 2 feet from the particles.

The printing was performed on an Omega Type D II Enlarger. The enlarger was mounted horizontally on a dolly, the image being projected vertically on a panel to which the enlarging paper was pinned. Many of the prints were exposed with the lens as far as 8 feet from the panel, especially during the single particle work, where the prints were enlarged back to original size. Special care had to be exercised to keep the film plane and the vertical panel parallel and in line, to avoid distortion. No other special chemicals or techniques were involved.

3.3.2 Analyzing the Single Particle Photographs

These photographs were enlarged to actual scale so that displacements could be directly traced onto vellum graph paper. Consider Fig. (14a), the data photograph for Experimental Case 1. The phase photograph fortuitously demonstrated that the $\tau = 0$ point was the first dot after the gap. (When this was not the case, interpolation had to be used). The trace of the most forward pin gave two such dots;

thus a horizontal line through these two points locates the $y = 0$ line. A coordinate system with its abscissa divided into thirty equal parts was drawn on tracing paper and placed over the photograph with the origin on the first $\tau = 0$ point (near center of photograph), and the abscissa over the $y = 0$ line on the print. Then, a horizontal line from the next point on the print was drawn to intersect a vertical line from the next division on the abscissa and this was continued for the whole cycle. Following this, a line perpendicular to the $y = 0$ line and through the $\tau = 0$ point was drawn on the point. This was the $x = 0$ line. A new coordinate system, again with thirty equal divisions on the abscissa, was then placed over the print with its origin at the $\tau = 0$ point and its abscissa over the $x = 0$ line. Finally, a vertical line from the next division was drawn up to a horizontal line from the next pin image, and so on throughout the cycle. Thus, with a minimum of effort the full scale displacement graphs were produced. Since the points were already on tracing paper they could be conveniently placed over the plotted computer solution for comparison.

3. 3. 3 Analyzing the Photographs of Granular Materials

In these cases, since only six images were recorded per cycle, it was only necessary that the prints be enlarged to about half of the original size. A scale factor was established by noting the distance between the white-headed pins attached to the plane (Note the pins on Fig. 10). Notice in Figs. 14 c, d, and e, that the pins can be clearly seen for over half of the images; a reference line for measuring x displacement of the marking grains was established by vertically connecting images of the same pin, one cycle apart. Thus, from this reference line the displacements were measured and recorded.

Two minor complications arise with this procedure. As the camera is rotating, the lens to subject distance is changing; the magnification on the negative varies with the reciprocal of the cosine of the angle between the camera axis and the image. To compensate for this effect an individual scale factor was measured or interpolated for each image. The errors at the extreme end of the negatives would have been as great as 5% without this correction. The other complication was that minor local random convection of the grains takes place.

Thus, at the boundary of the marking grains, where it was desired to follow an individual prominent grain or notch in the grains, often 6 or 7 cycles later the particular observation point would disappear. While this only causes an error on the order of the size of the grains, no greater than 5%, when the marking point disappears the displacement curve is apt to contain an erratic error of this magnitude; this should be born in mind while examining the data.

3.4 Final Comments on the Experimental Analysis

A list of the specific pieces of equipment used in the experiments is contained in Appendix A3.3.

The experiments were successful. The actual plots of the data from the 10 cases presented are given in the next section in comparison with the theory, Figs. (15-24). A quick glance at Fig. 15, with 29 images per cycle indicates a dramatic fit of data to experimental results.

CHAPTER IV

A COMPARISON OF THE THEORETICAL AND EXPERIMENTAL ANALYSES

4.1 Introductory Comments

Some comment is in order on the actual mechanics of preparing the comparison of the theoretical and experimental results. In the single particle case, phase was definitely known and both curves could be plotted on the same sheet starting from zero time. The computer was used to calculate the solution with the measured coefficient of friction for $\epsilon = 0$, and $\epsilon = 1$. These plots were then superposed on the experimental solution; the data would invariably lie within the two curves. A linear interpolation of the last point of the experimental curve between the two theoretical curves would yield an intermediate value of ϵ . This value of ϵ was then fed to the computer and that resulting solution is presented here.

The impact friction multiplier, ϵ , has its greatest effect when friction is comparatively low, as has been mentioned. When friction is increased, as is the case with granular materials, ϵ has a comparatively small effect. Thus for granular materials the value of ϵ was not as critical as for single particles. For these cases only two computer solutions were calculated for each experiment, $\epsilon = 0.5$, and 1.0, the best fit being presented.

Further, in the case of granular materials, phase was only very approximately known by noting those data points for which the bed was definitely in flight. (See Figures 14c, d, e.) The two curves, originally plotted on different sheets of vellum, were shifted along each other (with the axes parallel) to obtain the best fit. Most data (except the high

amplitude FL solutions) contain a distinct notch following the impact which is helpful here. For this reason the data in the case of granular materials does not necessarily start at zero, nor end at the end of a cycle.

On the following pages the results of 10 experimental cases are compared with their theoretical solutions. Table 3 summarizes the pertinent values and characteristics; the particles have been described in Table 2. The bulk of the experiments were conducted with $\alpha = 30^\circ$, the typical value used by conveyor manufacturers. X displacements are the output used to compare the theory with the data; measured y displacements are presented for four of the single particle cases as well as the y displacement of the plane to indicate the Flight. The x velocities for four of the solution forms (GFGL, FGL, FL, RGFGL) are plotted along with the x velocity of the plane to illustrate the various motion forms.

Note in observing the curves that the particle decelerates during a Slide G and accelerates during a Slide L; during a Flight the particle has constant velocity except when β is not zero.

Following each Figure the actual listing of the computer solution is presented. A Fortran symbols table is included in Appendix A2. Some brief running comments are added in the lower portions of each list.

4.2 The Comparison

TABLE 3 DATA SUMMARY

| Experimental Case No. | Plotted on Figure No. | Data Photo No. | Velocity Diagram | Y-Displacement | a (in.) | ω (RPM) | α (Degrees) | β (Degrees) | μ (Measured) | ϵ (Estimated) | A | ϕ | S | Solution Form | Particle Type (see table 2) | Δx (inches) | x_{avg} (in./sec.) |
|-----------------------|-----------------------|----------------|------------------|----------------|---------|----------------|--------------------|-------------------|------------------|------------------------|------|--------|------|---------------|-----------------------------|---------------------|----------------------|
| SINGLE PARTICLES | | | | | | | | | | | | | | | | | |
| 1 | 15 | 14a | no | yes | 2.01 | 220 | 30 | 0 | 0.33 | .85 | 1.38 | 6.25 | 1.0 | FGL | 1 | 4.95 | 18.16 |
| 2 | 16 | — | no | no | 1.03 | 261 | 47 | 0 | 0.33 | .80 | 1.46 | 3.82 | 1.0 | GFGL | 2 | 3.22 | 14.03 |
| 3 | 17 | — | no | yes | 1.03 | 318 | 30 | -4 | 0.33 | .65 | 1.66 | 6.97 | 1.27 | GFGL | 2 | 4.57 | 29.23 |
| 4 | 18 | — | no | yes | 1.03 | 318 | 30 | +4 | 0.28 | .7 | 1.30 | 6.66 | .800 | FGL | 1 | 0.13 | 0.67 |
| 5 | 19 | 14b | no | yes | 1.03 | 318 | 30 | +4 | 0.33 | 0.4 | 1.30 | 5.95 | .825 | FGL | 2 | 0.98 | 5.22 |
| GRANULAR MATERIALS | | | | | | | | | | | | | | | | | |
| 6 | 20 | 14d | yes | no | 0.76 | 305 | 47 | 0 | 0.5 | 1.0 | 1.47 | 2.86 | 1.0 | RGFGL | 3 | 2.53 | 12.88 |
| 7 | 21 | — | no | no | 1.03 | 315 | 30 | 0 | 0.6 | 1.0 | 1.45 | 3.89 | 1.0 | GFGL | 4 | 3.87 | 20.33 |
| 8 | 22 | 14c | yes | no | 1.03 | 312 | 30 | 0 | 0.4 | 1.0 | 1.42 | 5.33 | 1.0 | FGL | 5 | 2.79 | 14.48 |
| 9 | 23 | 14e | yes | no | 1.03 | 368 | 30 | 0 | 0.4 | 1.0 | 1.98 | 5.33 | 1.0 | FL | 5 | 3.90 | 23.92 |
| 10 | 24 | — | yes | no | 1.03 | 278 | 30 | 0 | 0.5 | 1.0 | 1.13 | 4.46 | 1.0 | GFGL | 3 | 3.21 | 14.87 |

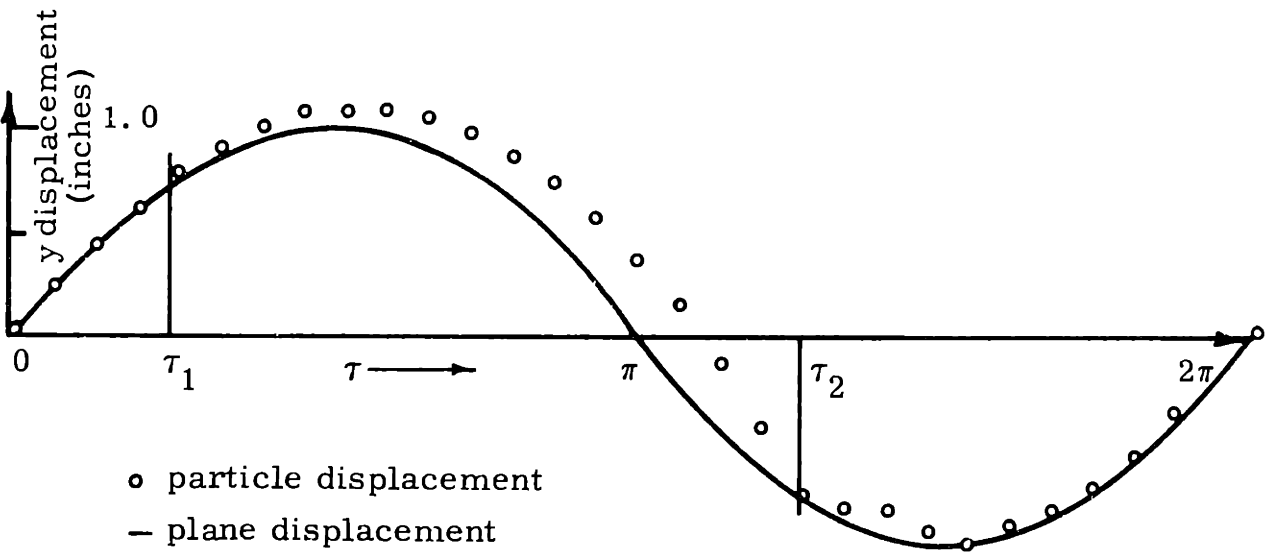
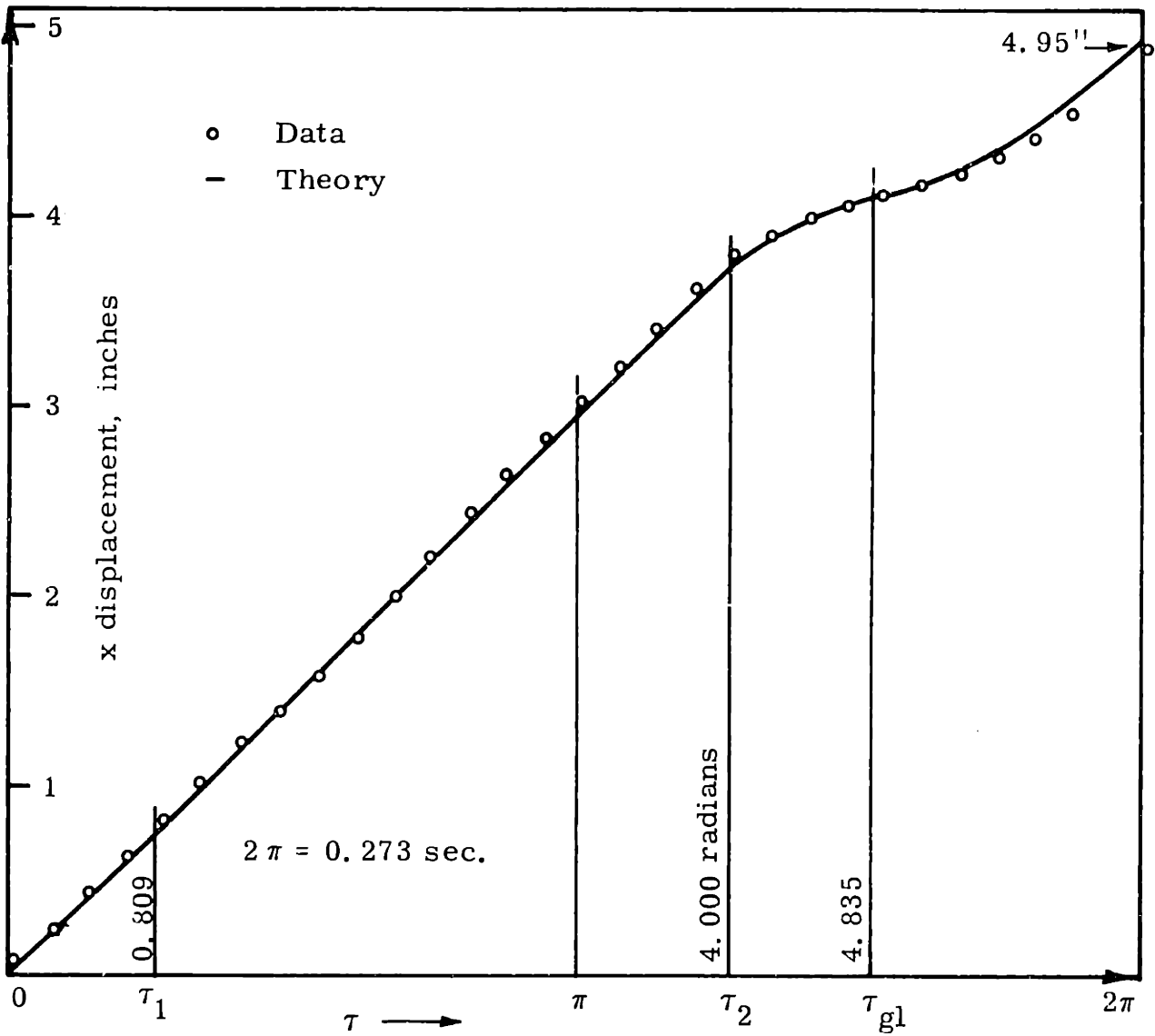


Figure 15
 Experimental Case 1

Calculated Results for Experimental Case I

2.01000 220.00000 .33000 30.00000 0.00000 .85000
 GABE6 - 55 SOLNS WITH L BUT NO R, FL,FGL,GFGL
 AO = 2.01000 INCHES, OMEGA = 220.00000 RPM, MU = .33000
 ALPHA = 30.00000 DEGREES, BETA = 0.00000 DEGRS
 IMPACT LUBRICATION FACTOR = .85000
 A = 1.38158 PHI = 6.24862 ZETA = 1.00000 PSI = .16500
 PLANE MAX X VEL= 4.01031E+01 MAX X DISPL= 1.74070E-00
 FINAL VALUES TFL = .80930 TI = 3.99773
 TEGD,TEGD,IBLD,TELD
 1.16095E-01 3.02549E-00 3.31278E-00 6.11199E-00

THIS IS A FGL SOLN
 FINAL VALUE OF TGL = 4.83498
 NO VELOCITIES XDSTGL = .64182 XDSTFL = 2.84355 XDSTI = 2.84355
 XDSTIS = 2.02546 XDS2GL = .64182
 XSTFL = 0.00000 XSTI = 9.06648 XSTGL = 10.19709
 XS2TFL = 14.93009
 AVERAGE VELOCITIES, XDSAV = 2.37628 XDAV = .39208
 XLDAV = 18.15650 INCHES PER SECOND
 REL DISPL PER CYCL = 2.46356ABS DISPL PER CYC = 4.95177

VELOCITIES IN IPS FOR INCRS OF 2PI/20
 1.96195E+01 2.09830E+01 2.16352E+01 2.17267E+01 2.17267E+01 2.17267E+01
 2.17267E+01 2.17267E+01 2.17267E+01 2.17267E+01 2.17267E+01 2.17267E+01
 2.17267E+01 1.44821E+01 1.06147E+01 6.51618E-00 7.39036E-00 1.12577E+01
 1.46855E+01 1.75082E+01 1.96195E+01

DISPLS IN INCHES FOR SAME INCRS
 0.00000E-99 2.77680E-01 5.69021E-01 8.65059E-01 1.16133E-00 1.45760E-00
 1.75388E-00 2.05015E-00 2.34643E-00 2.64270E-00 2.93897E-00 3.23525E-00
 3.53152E-00 3.80252E-00 3.97402E-00 4.09096E-00 4.17250E-00 4.30003E-00
 4.47752E-00 4.69779E-00 4.95177E-00

TRANS VELS 2.17267E+01 2.17267E+01 1.54760E+01 4.90400E-00
 TRANS DISPLS 7.39466E-01 3.74637E-00 4.12134E-00 5.69124E-00

EXPERIMENTAL CASE 1

This is a low frequency, high displacement amplitude, low friction, moderate "generalized amplitude" case. Twenty nine measured points provide a detailed picture of the particle motion. Note the definite bounce in the Y displacement curve, which can be seen in Figure 14a. The x motion seems unaffected by it. This is an FGL solution; note that the transition times predicted by the theory are corroborated by the data.

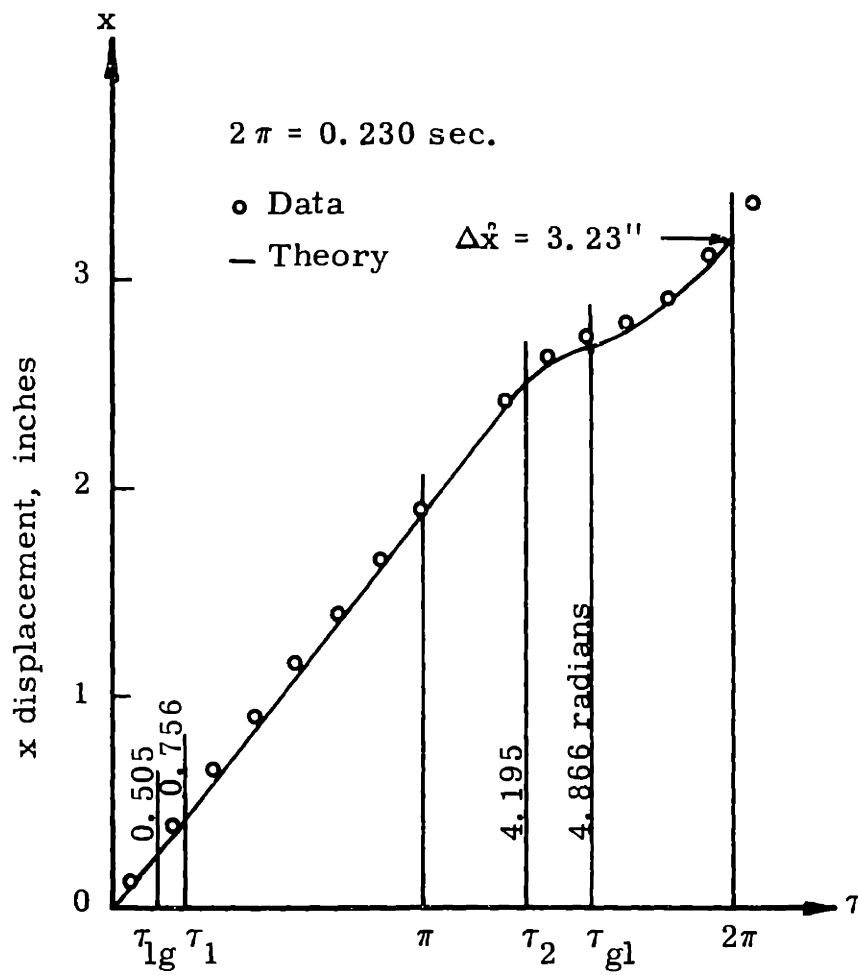


Figure 16
Experimental Case 2

Calculated Results for Experimental Case 2

```

1.03000 261.00000 .33000 47.00000 0.00000 .80000
GABE6 - SS SOLNS WITH L BUT NO R, FL,FGL,GFGL
AO = 1.03000 INCHES, OMEGA = 261.00000 RPM, MU = .33000
ALPHA = 47.00000 DEGREES, BETA = 0.00000 DEGRS
IMPACT LUBRICATION FACTOR = .80000

A = 1.45750 PHI = 3.82579 ZETA = 1.00000 PSI = .24134
PLANE MAX X VEL= 1.91994E+01 MAX X DISPL= 7.02456E-01
FINAL VALUES TFL = .75611 TI = 4.19510
TBGD,TEGD,TBLD,TELD
1.80311E-01 2.96127E-00 3.52683E-00 5.89794E-00

THIS IS A GFGL SOLUTION
TGL = 4.86559 TLG = .50511
XDSTLG = 2.47290 XDSTFL = 2.44830 XDSTI = 2.44830
XDSTIS = 1.53832 XDSTGL = .43118 XDS2LG = 2.47280
XSTLG = 0.00000 XSTFL = .61656 XSTI = 9.03626
XSTGL = 9.70101 XS2LG = 12.97705
XDSAV = 2.06535 XDAV = .49846 XDLAV = 14.03281 INCHES PER SECOND
X2LG = 3.13197 XLCYCL = 3.22593 DISPLACEMENT PER CYCLE IN INCHES

VELOCITIES IN IPS FOR INCRS OF 2PI/20
1.52955E+01 1.64274E+01 1.66766E+01 1.66347E+01 1.66347E+01 1.66347E+01
1.66347E+01 1.66347E+01 1.66347E+01 1.66347E+01 1.66347E+01 1.66347E+01
1.65347E+01 1.66347E+01 8.24458E-00 4.68050E-00 4.74281E-00 8.10136E-00
1.10689E+01 1.34985E+01 1.52955E+01

DISPLS IN INCHES FOR SAME INCRS
0.00000E-99 1.82949E-01 3.74583E-01 5.65851E-01 7.57054E-01 9.48258E-01
1.13946E-00 1.33066E-00 1.52186E-00 1.71307E-00 1.90427E-00 2.09548E-00
2.28668E-00 2.47788E-00 2.61500E-00 2.68939E-00 2.73332E-00 2.80743E-00
2.91805E-00 3.05984E-00 3.22593E-00

TRANS VELS 1.68018E+01 1.66347E+01 1.66347E+01 1.04519E+01 2.92961E-00
TRANS DISPLS 2.99158E-01 4.52428E-01 2.54546E-00 2.71071E-00 3.52509E-00

```

EXPERIMENTAL CASE 2

Here the frequency is increased but roughly the same generalized amplitude is maintained. Here and in the next three cases 14 points were measured per cycle. The oscillation angle is increased from 30° to 47° . Although the friction is the same, note the drastic decrease in ϕ due to the oscillation angle change; thus an increase in oscillation angle is similar to an increase in friction.

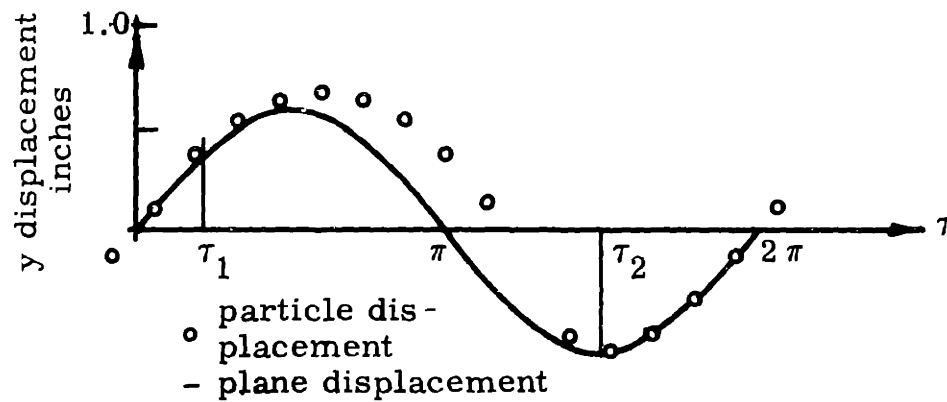
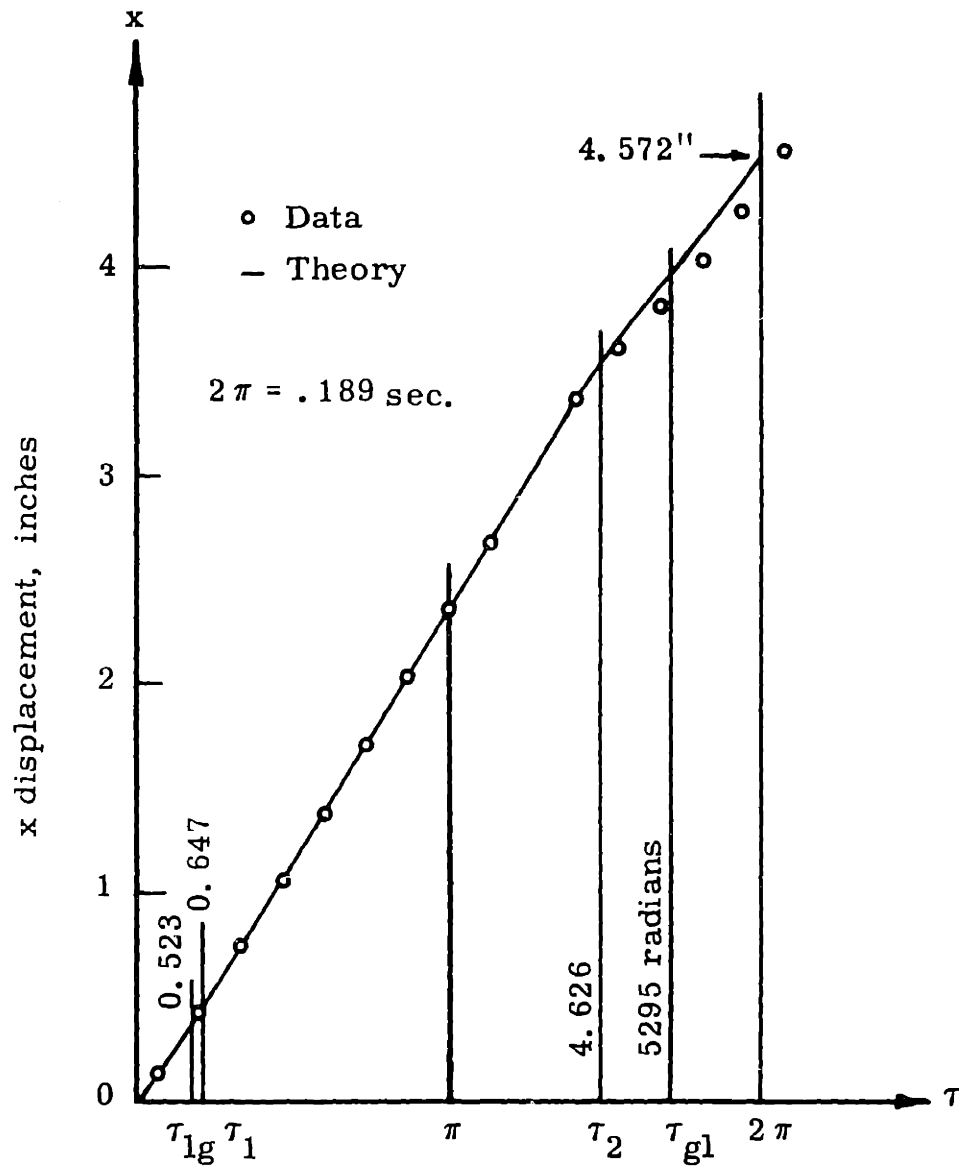


Figure 17
Experimental Case 3

Calculated Results for Experimental Case 3

1.03000 318.00000 .33000 30.00000 -4.00000 .65000
GABE6 - 55 SOLNS WITH L BUT NO R, FL,FGL,GFGL
AO = 1.03000 INCHES, OMEGA = 318.00000 RPM, MU = .33000
ALPHA = 30.00000 DEGREES, BETA = -4.00000 DEGRS
IMPACT LUBRICATION FACTOR = .65000

A = 1.65835 PHI = 6.96941 ZETA = 1.26887 PSI = .14543
PLANE MAX X VEL= 2.84359E+01 MAX X DISPL= 8.53907E-01
FINAL VALUES TFL = .64726 TI = 4.62623
TBGD,TEGD,TBLD,TELD
3.66302E-02 3.05495E-00 3.35238E-00 6.07239E-00

THIS IS A GFGL SOLUTION

TGL = 5.29475 TLG = .52311
XDSTLG = 4.93818 XDSTFL = 4.95028 XDSTI = 5.59540
XDSTIS = 4.34541 XDSTGL = 3.13523 XDS2LG = 4.93816
XSTLG = 0.00000 XSTFL = .61365 XSTI = 21.59414
XSTGL = 24.08694 XS2LG = 30.52410
XDSAV = 4.85805 XDAV = .70651 XDLAV = 24.23337 INCHES PER SECOND
X2LG = 4.43915 XLCYCL = 4.57233 DISPLACEMENT PER CYCLE IN INCHES

VELOCITIES IN IPS FOR INCRS OF 2PI/20

2.30597E+01 2.42031E+01 2.46790E+01 2.49322E+01 2.51862E+01 2.54403E+01
2.56944E+01 2.59485E+01 2.62026E+01 2.64567E+01 2.67107E+01 2.69648E+01
2.72189E+01 2.74730E+01 2.77271E+01 2.08723E+01 1.79713E+01 1.60912E+01
1.89447E+01 2.12968E+01 2.30597E+01

DISPLS IN INCHES FOR SAME INCRS

0.00000E-99 2.23422E-01 4.54649E-01 6.88661E-01 9.25069E-01 1.16387E-00
1.40507E-00 1.64867E-00 1.89467E-00 2.14306E-00 2.39385E-00 2.64704E-00
2.90262E-00 3.16060E-00 3.42098E-00 3.66649E-00 3.84964E-00 4.00675E-00
4.17236E-00 4.36262E-00 4.57233E-00

TRANS VELs 2.46331E+01 2.46934E+01 2.79115E+01 2.16762E+01 1.56394E+01
TRANS DISPLS 3.76771E-01 4.68694E-01 3.61144E-00 3.98485E-00 4.94910E-00

EXPERIMENTAL CASE 3

This is an illustration of a case in which the plane is tipped downward. This is again a moderate amplitude, low friction case. Naturally the velocity increases.

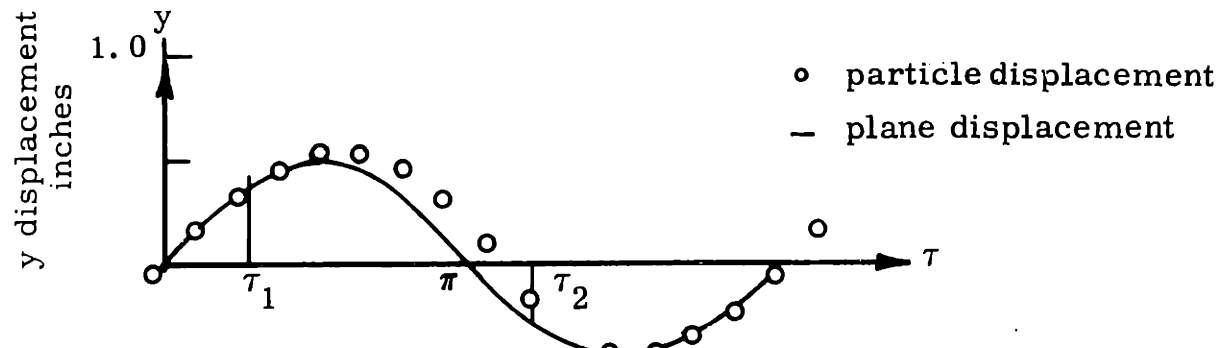
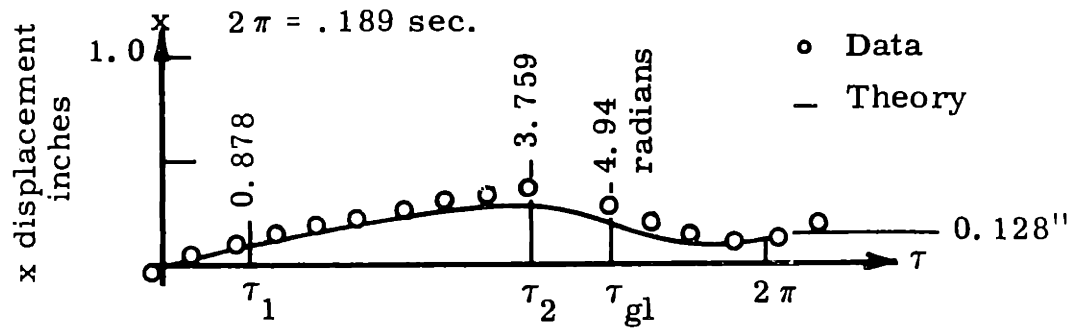


Figure 18 Experimental Case 4

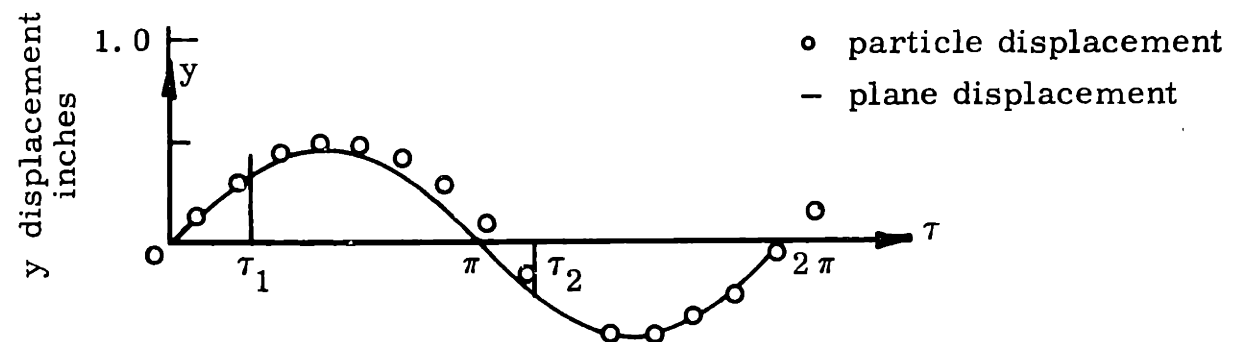
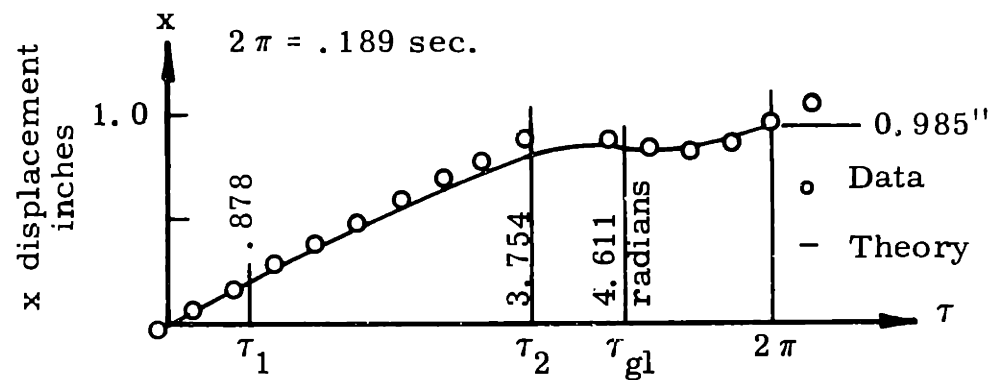


Figure 19 Experimental Case 5

Calculated Results for Experimental Case 4

1.03000 318.00000 .28000 30.00000 4.00000 .70000
GABE6 - 55 SOLNS WITH L BUT NO R, FL,FGL,GFGL
AO = 1.03000 INCHES, OMEGA = 318.00000 RPM, MU = .28000
ALPHA = 30.00000 DEGREES, BETA = 4.00000 DEGRS
IMPACT LUBRICATION FACTOR = .70000

A = 1.30004 PHI = 6.65938 ZETA = .80016 PSI = .15339
PLANE MAX X VEL= 3.08286E+01 MAX X DISPL= 9.25757E-01
FINAL VALUES TFL = .87759 TI = 3.75398
TRGD,TFGD,TBLD,TELD
1.15765E-01 3.02582E-00 3.23299E-00 6.19178E-00

THIS IS A FGL SOLN

FINAL VALUE OF TGL = 4.49412
ND VELOCITIES XDSTGL = -1.26871 XDSTFL = .64727 XDSTI = .20513
XDSTIS = -.21789 XDS2GL = -1.26871
XSTFL = 0.00000 XSTI = 1.22591 XSTGL = .69056
XS2TFL = .80791
AVERAGE VELOCITIES, XDSAV = .12858 XDAV = .01972
XLDAV = .67655 INCHES PER SECOND

REL DISPL PER CYCL = .12393ABS DISPL PER CYC = .12765

VELOCITIES IN IPS FOR INCKS OF 2PI/20

2.79321E-00 3.35046E-00 3.51576E-00 3.35317E-00 3.09908E-00 2.84500E-00
2.59092E-00 2.33684E-00 2.08275E-00 1.82867E-00 1.57459E-00 1.32051E-00
-1.24998E-00 -3.45288E-00 -5.89801E-00 -5.23340E-00 -3.16909E-00 -1.23214E-00
4.62567E-01 1.82386E-00 2.79321E-00

DISPLS IN INCHES FOR SAME INCRS

0.00000E-99 2.93014E-02 6.19796E-02 9.45883E-02 1.25023E-01 1.53061E-01
1.78702E-01 2.01947E-01 2.22794E-01 2.41244E-01 2.57297E-01 2.70953E-01
2.81126E-01 2.59173E-01 2.15212E-01 1.58072E-01 1.18489E-01 9.78768E-02
9.44771E-02 1.05552E-01 1.27653E-01

TRANS VELs 3.40564E-00 1.07932E-00 -1.14647E-00 -6.67541E-00
TRANS DISPLS 8.80039E-02 2.81699E-01 1.97113E-01 2.15655E-01

EXPERIMENTAL CASES 4 and 5

These are grouped together because they are almost identical except for a change of 0.05 in μ . These are moderate amplitude, low friction cases that illustrate the motion of a single particle going uphill. Notice the extreme effect of friction in this "uphill" case. Certainly case 4 would be useless in any practical conveying situation. The data photograph for case 4 looks very much like the familiar "ovals" that many students make in penmanship class. Figure 14b is the actual full size data print for Case 5.

Calculated Results for Experimental Case 5

1.03000 318.00000 .33000 30.00000 4.00000 .40000
 GABE6 - SS SOLNS WITH L BUT NO R, FL,FGL,GFGL
 AO = 1.03000 INCHES, OMEGA = 318.00000 RPM, MU = .33000
 ALPHA = 30.00000 DEGREES, BETA = 4.00000 DEGRS
 IMPACT LUBRICATION FACTOR = .40000

A = 1.30004 PHI = 5.95183 ZETA = .82515 PSI = .17531
 PLANE MAX X VEL= 3.08286E+01 MAX X DISPL= 9.25757E-01
 FINAL VALUES TFL = .87759 TI = 3.75398
 TBGD,TEGD,TBLD,TELD
 1.29600E-01 3.01198E-00 3.25814E-00 6.16663E-00

THIS IS A FGL SOLN
 FINAL VALUE OF TGL = 4.61072
 ND VELOCITIES XDSTGL = -.52031 XDSTFL = 1.36628 XDSTI = .97943
 XDSTIS = .73015 XDS2GL = -.52031
 XSTFL = 0.00000 XSTI = 3.37359 XSTGL = 3.48494
 XS2TFL = 5.45368
 AVERAGE VELOCITIES, XDSAV = .86797 XDAV = .15217
 XLDAV = 5.21947 INCHES PER SECOND

REL DISPL PER CYCL = .95612 ABS DISPL PER CYC = .98480

VELOCITIES IN IPS FOR INCRS OF 2PI/20
 7.36745E-00 8.06958E-00 8.30977E-00 8.16352E-00 7.90943E-00 7.65535E-00
 7.40127E-00 7.14719E-00 6.89310E-00 6.63902E-00 6.38494E-00 6.13086E-00
 4.27096E-00 1.72006E-00 -1.11632E-00 -2.31935E-00 1.58957E-01 2.48716E-00
 4.52987E-00 6.17963E-00 7.36745E-00

DISPLS IN INCHES FOR SAME INCRS
 0.00000E-99 7.31955E-02 1.50798E-01 2.28748E-01 3.04564E-01 3.77983E-01
 4.49004E-01 5.17629E-01 5.83857E-01 6.47688E-01 7.09122E-01 7.68158E-01
 8.24055E-01 8.52586E-01 8.55609E-01 8.33772E-01 8.23641E-01 8.36297E-01
 8.69668E-01 9.20527E-01 9.84808E-01

TRANS VELs 8.21599E-00 5.88966E-00 4.39066E-00 -3.12884E-00
 TRANS DISPLS 2.12791E-01 8.21982E-01 8.42090E-01 1.19759E-00

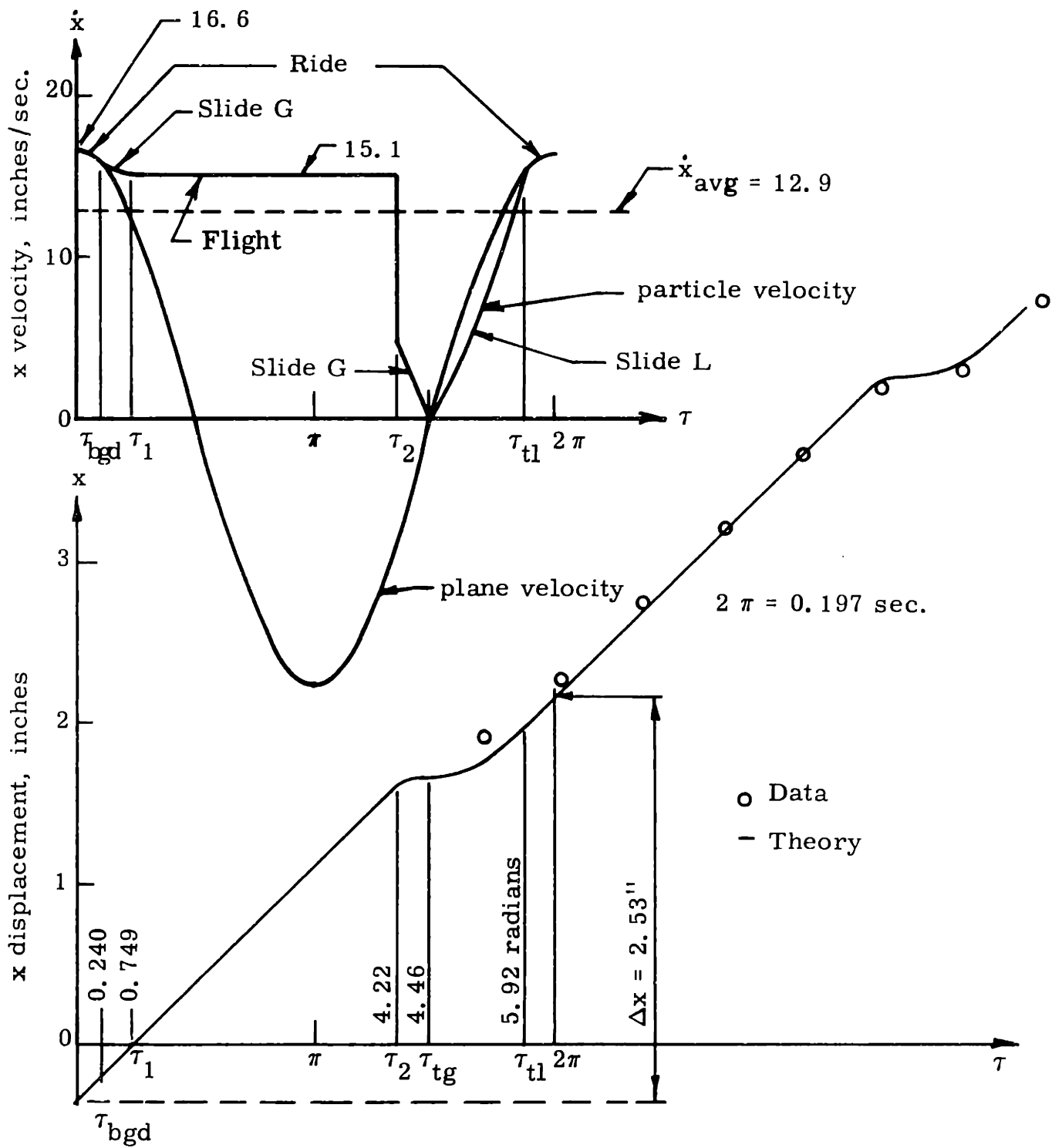


Figure 20

Experimental Case 6

Calculated Results for Experimental Case 6

.76000 305.00000 .50000 47.00000 0.00000 1.00000
RESULTS OF ABBREVIATED SOLUTION - THOSE WITH RGF-
AO = .76000 INCHES, OMEGA = 305.00000 RPM, MU = .50000
ALPHA = 47.00000 DEGREES, BETA = 0.00000 DEGRS
IMPACT LUBRICATION FACTOR = 1.00000

A = 1.46860 PHI = 2.06502 ZETA = 1.00000 PSI = .36567
PLANE MAX X VEL= 1.65548E+01 MAX X DISPL= 5.18317E-01
FINAL VALUES TFL = .749C1 TI = 4.22205

THIS IS AN RGFGL SOLN
TBGD,TEGD,TBLD,TELD,TTG,TTL
2.39961E-01 2.90162E-00 4.04779E-00 5.37698E-00 4.63632E-00 5.91970E-00
XDBGD,XDTFL,XDTI,XDTIS,XDTIG,XDTTL
1.60805E+01 1.51250E+01 1.51250E+01 4.81146E-00-1.22494E-00 1.54732E+01
XTFL,XTI,XTTG,XTTL,XBGD,X2TFL
0.00000E-99 1.84466E-00 1.86852E-00 1.97943E-00 2.28689E-00 2.53289E-00
AVERAGE VELOCITY (IPS)= 1.28755E+01

EXPERIMENTAL CASE 6

The remainder of the cases are for granular materials.

The particles in this case are "narrow beans" (height greater than the depth in the channel). The shake angle is also increased, hence this is a very high friction case; note that ϕ is at its lowest value in Table 3. The solution is RGFGL and quite complicated; note the velocity diagram. This is the only case presented that contains a Ride. The data photograph is Figure 14d.

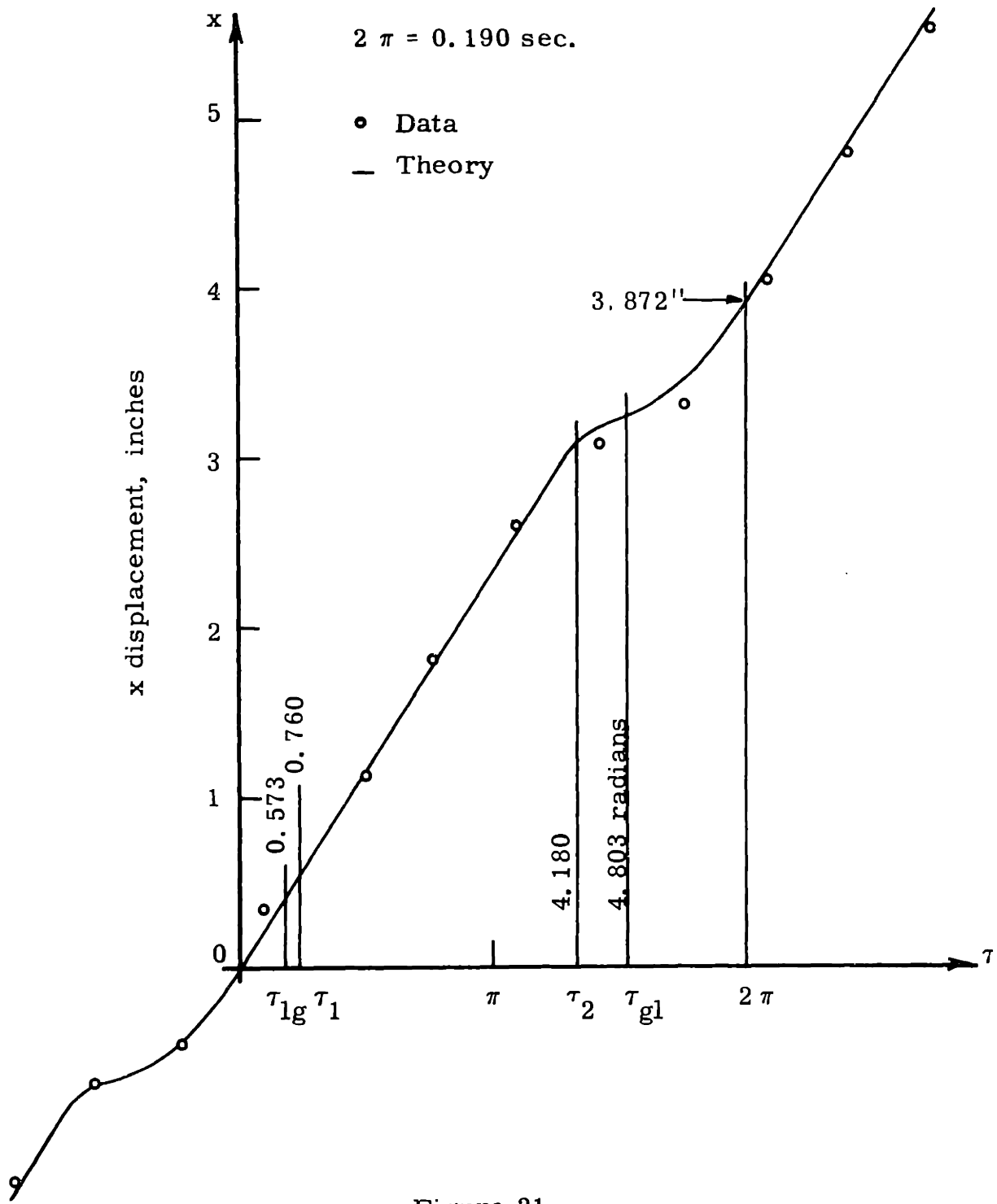


Figure 21
Experimental Case 7

Calculated Results for Experimental Case 7

1.03000 315.00000 .60000 30.00000 0.00000 1.00000
 GABE6 - SS SOLNS WITH L BUT NO R, FL,FGL,GFGL
 AO = 1.03000 INCHES, OMEGA = 315.00000 RPM, MU = .60000
 ALPHA = 30.00000 DEGREES, BETA = 0.00000 DEGRS
 IMPACT LUBRICATION FACTOR = 1.00000

A = 1.45142 PII = 3.88674 ZETA = 1.00000 PSI = .30000
 PLANE MAX X VEL = 2.94244E+01 MAX X DISPL = 8.97005E-01
 FINAL VALUES TFL = .76008 TI = 4.18014
 TBGD,TEGD,TBLD,TELD
 1.78205E-01 2.96338E-00 3.51540E-00 5.90937E-00

THIS IS A GFGL SOLUTION

TGL = 4.80295 TLG = .57307
 XDSTLG = 2.42555 XDSTFL = 2.41216 XDSTI = 2.41216
 XDSTIS = 1.28805 XDSTGL = .26104 XDS2LG = 2.42553
 XSTLG = 0.00000 XSTFL = .45192 XSTI = 8.70169
 XSTGL = 9.18846 XS2LG = 12.52928
 XDSAV = 1.99409 XDAV = .59822 XDLAV = 20.32567 INCHES PER SECOND
 X2LG = 3.75879 XLCYCL = 3.87155 DISPLACEMENT PER CYCLE IN INCHES

VELOCITIES IN IPS FOR INCRS OF 2PI/20

2.23272E+01 2.40345E+01 2.46538E+01 2.45870E+01 2.45870E+01 2.45870E+01
 2.45870E+01 2.45870E+01 2.45870E+01 2.45870E+01 2.45870E+01 2.45870E+01
 2.45870E+01 2.45870E+01 9.57461E-00 4.21854E-00 6.45913E-00 1.15068E+01
 1.59680E+01 1.96221E+01 2.23272E+01

DISPLS IN INCHES FOR SAME INCRS

0.00000E-99 2.21557E-01 4.54655E-01 6.88906E-01 9.23069E-01 1.15723E-00
 1.39139E-00 1.62555E-00 1.85972E-00 2.09388E-00 2.32804E-00 2.56220E-00
 2.79637E-00 3.03053E-00 3.17730E-00 3.24310E-00 3.28351E-00 3.36943E-00
 3.50082E-00 3.67101E-00 3.87156E-00

TRANS VELs 2.47235E+01 2.45870E+01 2.45870E+01 1.31291E+01 2.66081E-00
 TRANS DISPLs 4.13309E-01 5.52953E-01 3.10213E-00 3.25255E-00 4.28486E-00

EXPERIMENTAL CASE 7

In this case α has been dropped back to the more normal 30°, and the particles are "narrow rice," the highest friction particles used. Still the decrease in shake angle causes an increase in ϕ , the nondimensional variable indicating friction. The solution is GFGL.

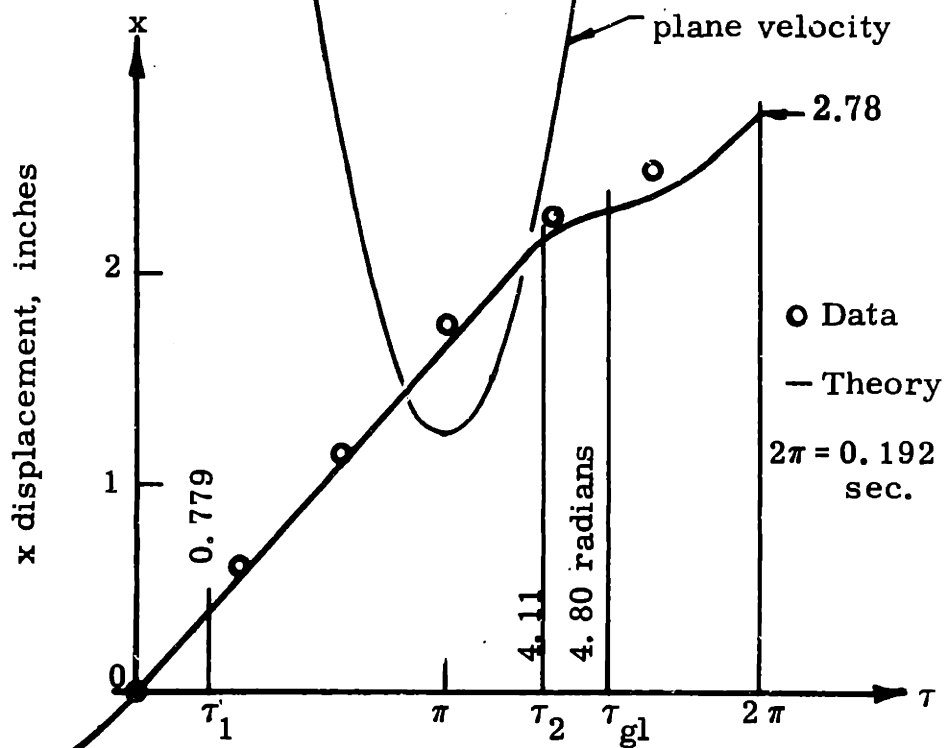
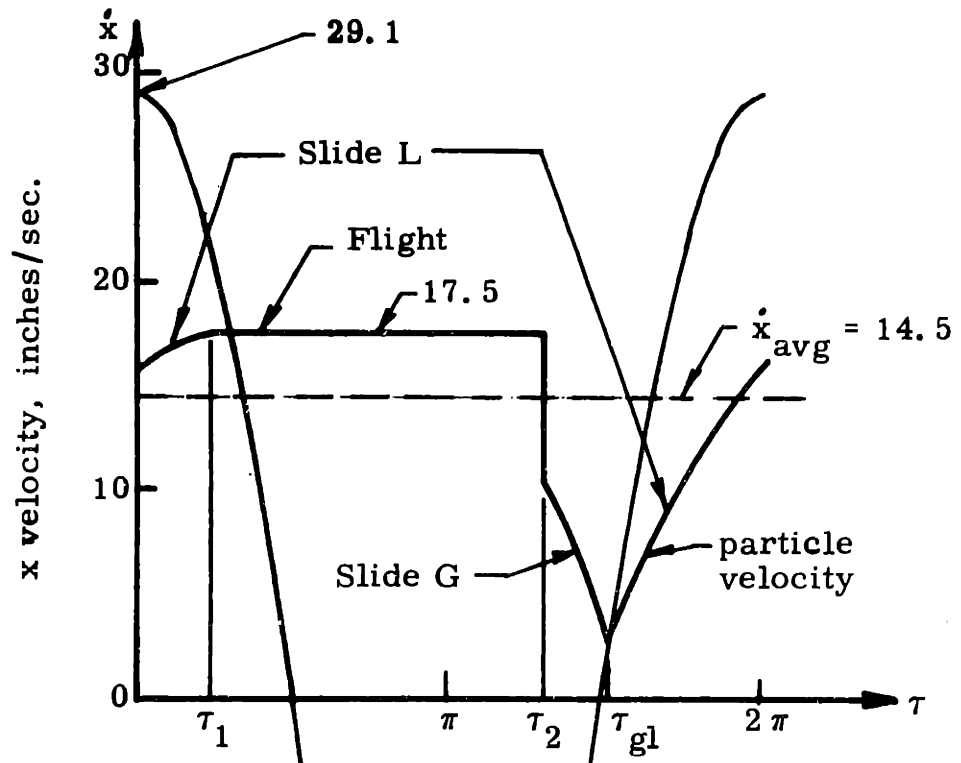


Figure 22
Experimental Case 8

Calculated Results for Experimental Case 8

1.03000 312.00000 .40000 30.00000 0.00000 1.00000
GABE6 - SS SOLNS WITH L BUT NO R, FL,FGL,GFGL
AO = 1.03000 INCHES, OMEGA = 312.00000 RPM, MU = .40000
ALPHA = 30.00000 DEGREES, BETA = 0.00000 DEGRS
IMPACT LUBRICATION FACTOR = 1.00000

A = 1.42390 PHI = 5.33011 ZETA = 1.00000 PSI = .20000
PLANE MAX X VEL= 2.91441E+01 MAX X DISPL= 8.92005E-01
FINAL VALJES TFL = .77861 TI = 4.11073
TBGD,TEGD,TBLD,TELD
1.32143E-01 3.00944E-00 3.35407E-00 6.07070E-00

THIS IS A FGL SOLN

FINAL VALUE OF TGL = 4.80383
ND VELOCITIES XDSTGL = .39543 XDSTFL = 2.60176 XDSTI = 2.60176
XDSTIS = 1.53953 XDS2GL = .39544
XSTFL = 0.00000 XSTI = 8.66938 XSTGL = 9.34687
XS2TFL = 13.52178
AVERAGE VELOCITIES, XDSAV = 2.15208 XDAV = .43041
XLDVAV = 14.48477 INCHES PER SECOND

REL DISPL PER CYCL = 2.70440ABS DISPL PER CYC = 2.78553

VELOCITIES IN IPS FOR INCRS OF 2PI/20

1.57701E+01 1.69257E+01 1.74546E+01 1.75113E+01 1.75113E+01 1.75113E+01
1.75113E+01 1.75113E+01 1.75113E+01 1.75113E+01 1.75113E+01 1.75113E+01
1.75113E+01 1.75113E+01 7.27319E-00 3.70834E-00 5.17958E-00 8.54083E-00
1.15148E+01 1.39557E+01 1.57701E+01

DISPLS IN INCHES FOR SAME INCRS

0.00000E-99 1.57716E-01 3.23479E-01 4.91772E-01 6.60151E-01 8.28529E-01
9.96908E-01 1.16528E-00 1.33366E-00 1.50204E-00 1.67042E-00 1.83880E-00
2.00718E-00 2.17555E-00 2.26761E-00 2.32049E-00 2.35617E-00 2.42237E-00
2.51917E-00 2.64209E-00 2.78553E-00

TRANS VELS 1.75113E+01 1.75113E+01 1.03619E+01 2.66153E-00
TRANS DISPLS 4.03945E-01 2.18984E-00 2.32940E-00 3.18948E-00

EXPERIMENTAL CASE 8

The channel width is increased using the same particles and friction considerably reduced. This would be a low friction, moderate amplitude case. Note the drop in conveying velocity in the table. The solution is FGL and the data photograph is Figure 14c.

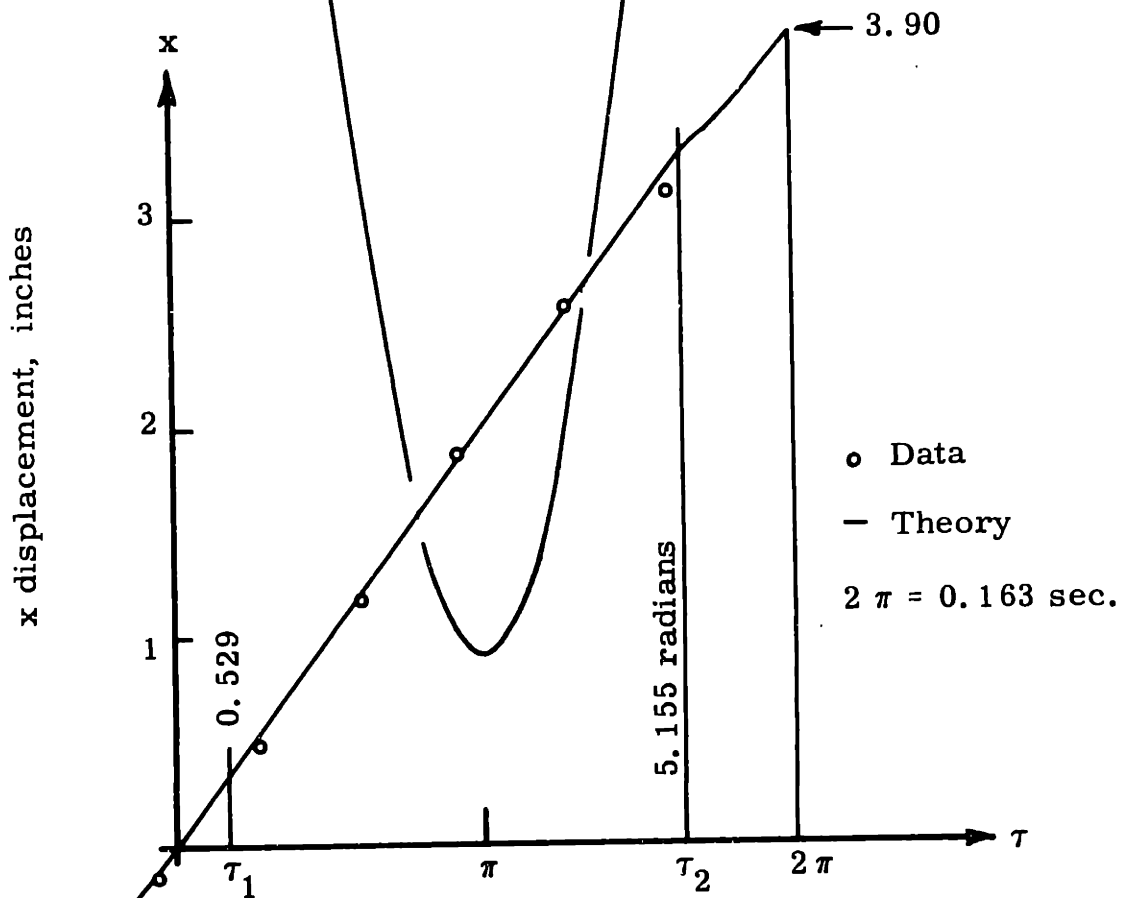
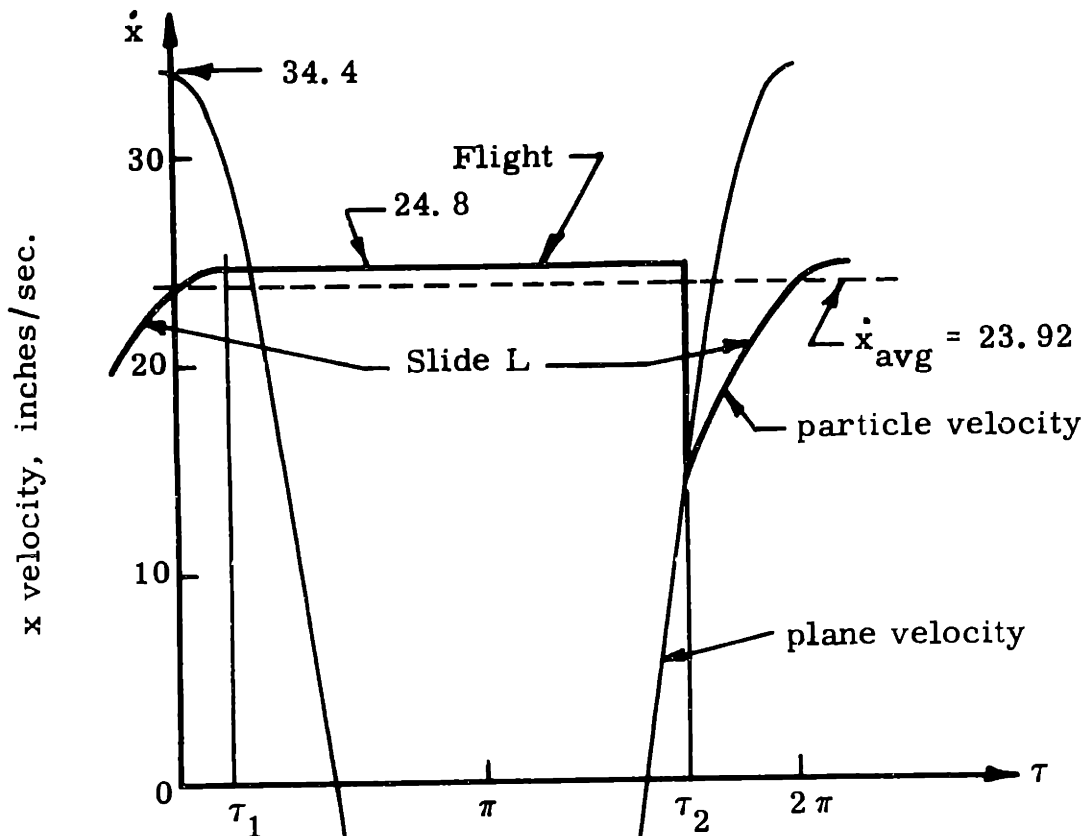


Figure 23
Experimental Case 9

Calculated Results for Experimental Case 9

1.03000 368.00000 .40000 30.00000 0.00000 1.00000
GABE6 - SS SOLNS WITH L BUT NO R, FL,FGL,GFGL
AO = 1.03000 INCHES, OMEGA = 368.00000 RPM, MU = .40000
ALPHA = 30.00000 DEGREES, BETA = 0.00000 DEGRS
IMPACT LUBRICATION FACTOR = 1.00000

A = 1.98092 PHI = 5.33011 ZETA = 1.00000 PSI = .20000
PLANE MAX X VEL= 3.43751E+01 MAX X DISPL= 8.92005E-01
FINAL VALUES TFL = .52916 TI = 5.15526
TBGD,TEGD,TBLD,TELD
9.48520E-02 3.04673E-00 3.29376E-00 6.13101E-00

THIS IS A FL SOLN
XDSTFL = 3.12684E-00XDSTI = 3.12684E-00XDSTIS = 1.85562E-00
XSTFL = 0.00000E-99XSTI = 1.44650E+01XS2FL = 1.89313E+01

XDSAV = 3.01301E-00XDLAV = 2.39191E+01IPS, XLCYCL(IN) = 3.89986E-00

VELOCITIES IN IPS FOR INCRS OF 2PI/20
2.37879E+01 2.46584E+01 2.48228E+01 2.48228E+01 2.48228E+01 2.48228E+01
2.48228E+01 2.48228E+01 2.48228E+01 2.48228E+01 2.48228E+01 2.48228E+01
2.48228E+01 2.48228E+01 2.48228E+01 2.48228E+01 2.48228E+01 2.48228E+01
1.97538E+01 2.21404E+01 2.37879E+01

DISPLS IN INCHES FOR SAME INCRS
0.00000E-99 1.97996E-01 4.00053E-01 6.02413E-01 8.04773E-01 1.00713E-00
1.20949E-00 1.41185E-00 1.61421E-00 1.81657E-00 2.01893E-00 2.22129E-00
2.42365E-00 2.62601E-00 2.82837E-00 3.03073E-00 3.23309E-00 3.39177E-00
3.54089E-00 3.71213E-00 3.89986E-00

TRANS VELs 2.48228E+01 2.48228E+01 1.47311E+01
TRANS DISPLS 3.36185E-01 3.31599E-00 4.23605E-00

EXPERIMENTAL CASE 9

Here we have taken the above case and increased the amplitude. This would be low friction, high amplitude. The particles are again "wide rice." The solution is FL; note the smoothness of the displacement plot. Figure 14e is the data photograph for this case; note the high lift of the bed and the particles bouncing out of the channel.

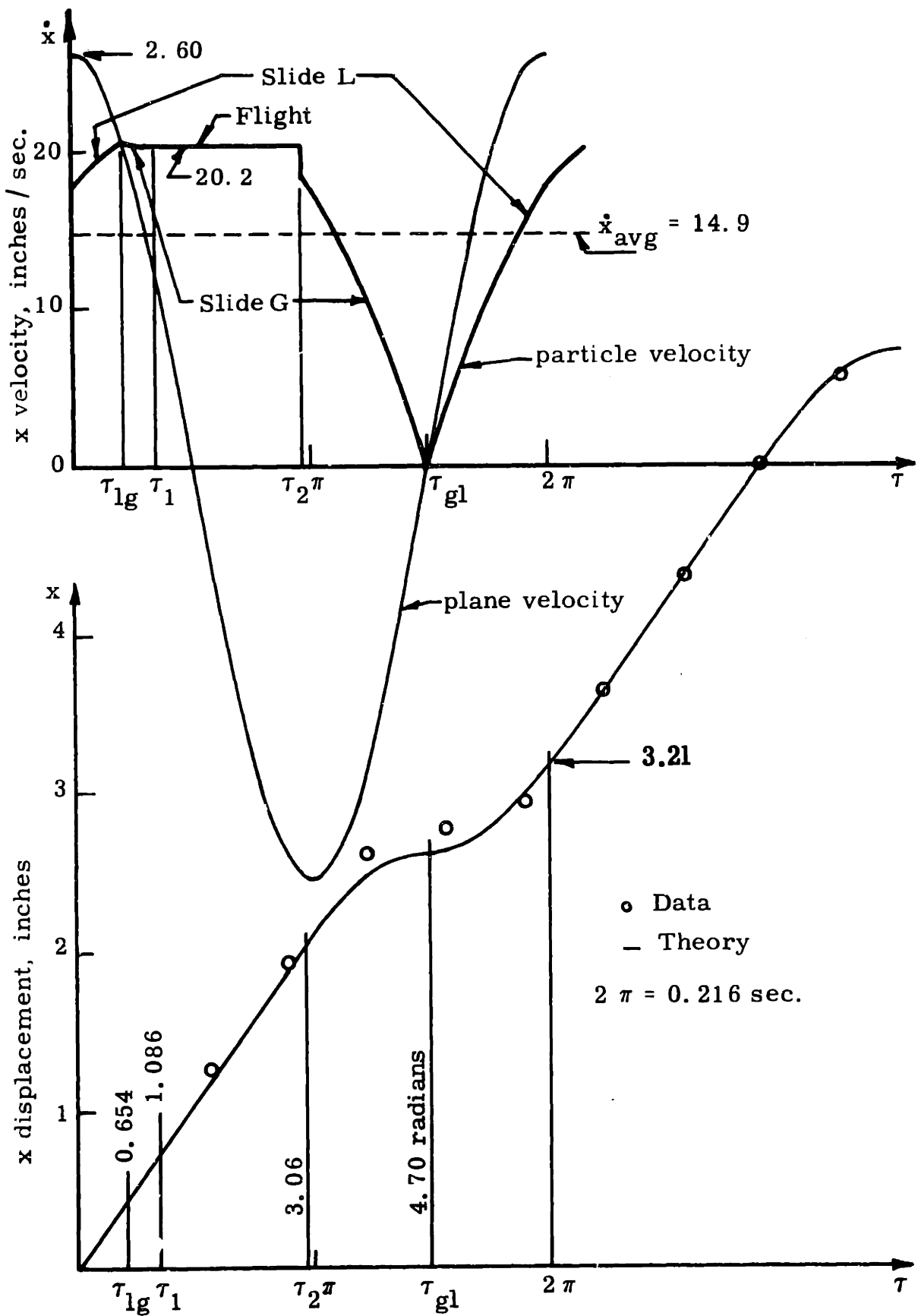


Figure 24
Experimental Case 10

Calculated Results for Experimental Case 10

1.03000 278.00000 .50000 30.00000 0.00000 1.00000
GABE6 - SS SOLNS WITH L BUT NO R, FL, FGL, GFGL
AO = 1.03000 INCHES, OMEGA = 278.00000 RPM, MU = .50000
ALPHA = 30.00000 DEGREES, BETA = 0.00000 DEGRS
IMPACT LUBRICATION FACTOR = 1.00000

A = 1.13047 PHI = 4.46409 ZETA = 1.00000 PSI = .25000
PLANE MAX X VEL= 2.59682E+01 MAX X DISPL= 8.92005E-01
FINAL VALUES TFL = 1.08559 TI = 3.05909
TBGD, TEGD, TBLD, TELD
1.99475E-01 2.94211E-00 3.50877E-00 5.91600E-00

THIS IS A GFGL SOLUTION

TGL = 4.70332 TLG = .65482
XDSTLG = 2.74756 XDSTFL = 2.69328 XDSTI = 2.69328
XDSTIS = 2.41054 XDSTGL = -.03144 XDS2LG = 2.74754
XSTLG = 0.00000 XSTFL = 1.16761 XSTI = 6.48279
XSTGL = 8.69429 XS2LG = 12.46198
XDSAV = 1.98338 XDAV = .49584 XDLAV = 14.86821 INCHES PER SECOND
X2LG = 3.11550 XLCYCL = 3.20896 DISPLACEMENT PER CYCLE IN INCHES

VELOCITIES IN IPS FOR INCRS OF 2PI/20

1.78050E+01 1.95215E+01 2.05398E+01 2.02288E+01 2.01899E+01 2.01899E+01
2.01899E+01 2.01899E+01 2.01899E+01 2.01899E+01 1.75487E+01 1.50986E+01
1.19505E+01 8.20886E-00 4.03583E-00 -1.07546E-01 4.29221E-00 8.46521E-00
1.22068E+01 1.53549E+01 1.78050E+01

DISPLS IN INCHES FOR SAME INCRS

0.00000E-99 2.02056E-01 4.18805E-01 6.38874E-01 8.56814E-01 1.07469E-00
1.29256E-00 1.51044E-00 1.72832E-00 1.94619E-00 2.15734E-00 2.33415E-00
2.48069E-00 2.58993E-00 2.65630E-00 2.67526E-00 2.69894E-00 2.76808E-00
2.88008E-00 3.02939E-00 3.20897E-00

TRANS VELS 2.05968E+01 2.01899E+01 2.01899E+01 1.80704E+01 -2.35740E-01
TRANS DISPLS 4.37530E-01 7.38192E-01 2.10685E-00 2.67631E-00 3.64649E-00

EXPERIMENTAL CASE 10

In this case we have "narrow beans," but at the more normal 30° oscillation angle. The solution is moderate friction, very low amplitude, and the solution is GFGL. Note that at the one transition point the particle velocity drops to slightly negative value. On the data photograph the flight could not be noticed.

4.3 Final Comments on the Comparison

Bearing in mind that ϵ was adjusted for the "best fit," but that it only affected one point of the cycle, the agreement between the theory and the data is excellent. The transitions between the various motion forms occur as predicted which is indicated by the change of curvature of the data curves at the proper transition times calculated from the theory.

One tempting conclusion is that, for granular materials, a value of unity for ϵ provides good results. This apparent agreement is mostly due to the method of data analysis. Certainly further research is needed before this could be taken as a rule.

CONCLUDING REMARKS, COMPARISONS, RECOMMENDATIONS
FOR FUTURE RESEARCH5. 1 A Comparison of this Study with Previous Investigations

As far as the literature is concerned, this is the only study that presents data concerning the detailed motion of the particles during the cycle. Reference (8) does present some adequately detailed data, but only for oscillating conveyors with very low amplitude in which no flight is occurring. References (2, 3, 5, and 13) only attempt to measure average velocity. This is certainly part of the reason they have not discovered the complexity of the solutions.

Reference (13) suggests that an adequate method of predicting conveying velocities is to take the velocity of the plane at the time of flight as the average velocity. Looking at the four cases in which the velocity diagram is given, Figs., 20, 22, 23, and 24, one can compare the plane velocity at τ_1 with the average velocity (the dotted line) quite easily. The errors are approximately - 8% + 60% + 25% and - 15%, respectively. This is certainly crude, but will in general yield an order of magnitude result.

Reference (2) does find the FGL Solution, but totally neglects the impact and therefore they find very poor agreement with their data. They do mention, however, that their lack of consideration of the impact is a possible flaw in their analysis. Further they had conducted their tests with oscillation angles of 20° or less, which are much less than the oscillation angles of the practical conveyors used in this country. Such low angles lead to very high values of ϕ . From Figs. 7 and 8, note that the FGL Solution does indeed predominate for high ϕ values. Had they tried to extend their analysis to an oscillation angle of 30° , it would have been incorrect, or had they used a light flat particle so that gas lubrication on impact nullified the effect of impact, they would have found

excellent agreement. Also they used a static coefficient of friction, which certainly has not been indicated by this study.

5.2 Effective Friction of Granular L Materials in Channels

It may be noted by reference to Table 3, in that at least the trend indicated by Eq. (58b) is observed in the measured values of the coefficient of friction for the two different channel width to height ratios in the tests with rice. Taking the measured coefficients of friction and the two height-width ratios one can calculate the value of k in (48b) in this particular instance to be $1/3$, which seems entirely reasonable, but also highly uncertain being based on one test. Certainly though, deeper channels will have higher friction and will in general travel at higher velocities.

5.3 The Impact Friction Multiplier, ϵ

This is a very important parameter that must be experimentally determined. ϵ severely affects the results in the low friction cases. It is certainly recommended that future study be given this important parameter.

5.4 The Practical use of the Theory

It has been demonstrated that the solutions, while complicated, are obtainable, especially by the use of the digital computer. Any desired output can be arranged in a nondimensional form and will be expressible as a function of A , ϕ , ζ , ϵ , all multiplied by ψ . Thus, if interested in the required power, one would prepare a computer routine that would integrate the product of the appropriate components of N as well as F and the velocity of the plane, around one cycle.

Another example of the use of the theory would be optimizing. When the conveyors are horizontal, ζ is always 1.0. If for a class of particles, ϵ or A is not to be varied a great deal, average velocity, for instance, could be plotted against ϕ . Knowing this optimum value of ϕ , one could then insert the proper friction coefficient in the definition of ϕ , from Table 1, and obtain an optimum value of the oscillation angle α .

5. 5 The Final Conclusion

Finally, a theory has been developed and proved that does predict and explain material transport on sinusoidally oscillating conveyors in which the oscillation is in a straight line, inclined to the trough and of a magnitude great enough to cause small flights of the particles.

For single particles on planes, the coefficient of friction, μ , is measured by noting the minimum static angle of the plane for which a constant velocity slide of the particle can be maintained. The value of the impact friction multiplier, ϵ , must be determined experimentally.

Granular materials do move as a slug. Again the coefficient of friction must be measured by noting the minimum static angle of friction for which a constant velocity slug slide of the bed of particles can be maintained. Using this value of μ and an experimentally determined impact friction multiplier, ϵ , the single particle theory is applicable directly.

THEORETICAL DETAILS

APPENDIX A 1. 1

τ_2 ALWAYS LIES OUTSIDE THE DEFINITE FLY ZONE

Table A1

| A | τ_1 | τ_1' | τ_2 |
|--------|----------|-----------|----------|
| 1.1000 | 1.1411 | 2.0005 | 2.8823 |
| 1.1305 | 1.0856 | 2.0560 | 3.0591 |
| 1.1722 | 1.0218 | 2.1198 | 3.2660 |
| 1.2674 | 0.9092 | 2.2324 | 3.6642 |
| 1.3000 | 0.8776 | 2.2640 | 3.7540 |
| 1.3195 | 0.8600 | 2.2816 | 3.8159 |
| 1.3396 | 0.8428 | 2.2988 | 3.8771 |
| 1.3816 | 0.8093 | 2.3323 | 3.9977 |
| 1.4025 | 0.7938 | 2.3478 | 4.0545 |
| 1.4239 | 0.7786 | 2.3630 | 4.1107 |
| 1.4514 | 0.7601 | 2.3815 | 4.1801 |
| 1.4686 | 0.7490 | 2.3926 | 4.2221 |
| 1.5510 | 0.7007 | 2.4409 | 4.4095 |
| 1.5831 | 0.6837 | 2.4579 | 4.4772 |
| 1.5909 | 0.6797 | 2.4619 | 4.4933 |
| 1.6120 | 0.6692 | 2.4724 | 4.5359 |
| 1.6583 | 0.6473 | 2.4943 | 4.6262 |
| 1.8036 | 0.5877 | 2.5539 | 4.8829 |
| 1.8316 | 0.5775 | 2.5641 | 4.9286 |
| 1.9250 | 0.5463 | 2.5953 | 5.0733 |
| 1.9339 | 0.5434 | 2.5982 | 5.0867 |
| 1.9809 | 0.5292 | 2.6124 | 5.1553 |
| 2.0790 | 0.5018 | 2.6398 | 5.2914 |
| 2.1902 | 0.4741 | 2.6675 | 5.4360 |
| 2.50 | 0.4115 | 2.7301 | 5.794 |
| 3.00 | 0.3398 | 2.8018 | 6.307 |
| 3.50 | 0.2897 | 2.8519 | 6.7863 |
| 4.00 | 0.2527 | 2.8889 | 7.3117 |

Table A1, clearly shows that for all values of A greater than 1.10, τ_2 is always greater than τ_1' , the end of the fly definite zone. In the following paragraph, it is proved that this is also the case for values of A between 1.0 and 1.1.

As A approaches unity, both τ_1, τ_2 , approach $\pi/2$. By expressing τ_1 and τ_2 in terms of the variables T_1 and T_2 , having origin at $\pi/2$, one can replace the sine and cosine terms in Eqs. (14) and (16), with adequate series approximations and complete the required proof. Hence define:

$$T_1 \equiv \tau_1 - \pi/2 \quad (\text{A1.1a})$$

$$T_2 \equiv \tau_2 - \pi/2 \quad (\text{A1.1b})$$

$$T_1' \equiv \tau_1' - \pi/2 \quad (\text{A1.1c})$$

These definitions yield:

$$\tau_1 = T_1 + \pi/2 \quad (\text{A1.2a})$$

$$\tau_2 = T_2 + \pi/2 \quad (\text{A1.2b})$$

$$T_1' = -T_1 \quad (\text{A1.2c})$$

$$\sin \tau_1 = \cos T_1 \quad (\text{A1.2d})$$

$$\sin \tau_2 = \cos T_2 \quad (\text{A1.2e})$$

$$\cos \tau_1 = -\sin T_1 \quad (\text{A1.2f})$$

$$\cos \tau_2 = -\sin T_2 \quad (\text{A1.2g})$$

Substitution of Eqs. (A1.2) into (16), yields:

$$\cos T_2 - \cos T_1 = -\frac{1}{2} \cos T_1 (T_2 - T_1)^2 - (T_2 - T_1) \sin T_1. \quad (\text{A1.3a})$$

Since it is desired to compare T_1' with T_2 , Eq. (A1.2c) is substituted into (A1.3a) which yields:

$$\cos T_2 - \cos T_1' = -\frac{1}{2} \cos T_1' (T_2 + T_1')^2 + (T_2 + T_1') \sin T_1'.$$

(A1.3b)

This expression can be examined for sufficiently small T's by substituting a truncated series expansion for the sine and cosine terms. Retaining terms with a power of 4 and less, these substitutions are (Ref. 15):

$$\sin x = x - x^3/6, \quad (\text{A1.4a})$$

$$\cos x = 1 - x^2/2 + x^4/24. \quad (\text{A1.4b})$$

The substitution of (A1.4) into (A1.3b), together with the dropping of terms whose order is greater than four, yields the following:

$$T_2^4 - 6T_1'^2 T_2^2 - 8T_1'^3 T_2 + 3T_1'^4 = 0 \quad (\text{A1.5})$$

Consider the substitution

$$R = T_2/T_1'. \quad (\text{A1.6})$$

If R can be shown greater than unity, the required proof is complete. Equation (A1.5) is divided by T_1' , and then Eq. (A1.6) is substituted in that result; this yields:

$$R^4 - 6R^2 - 8R - 3 = 0. \quad (\text{A1.7})$$

Since this polynomial has only one sign change, by Descartes' Rule (Ref. 15), it may only have one positive real root. This root is easily verified to be 3, and hence for T's such that Eqs. (A1.4) are valid

$$T_2 = 3T_1'. \quad (\text{A1.8})$$

Agreeing that Eqs. (A1.4), are not valid all the way out to $A = 1.1$, the application of Eq. (A1.8), at $A = 1.1$, only results in an error of about 10%. Thus T_2 always exceeds T_1' , τ_2 always exceeds τ_1' , and the impact always occurs after the limiting value of the fly definite zone.

APPENDIX A1.2

THE NONDIMENSIONAL OPERATING CONDITIONS ϕ, ζ, ψ .

These quantities are:

$$\phi \equiv \frac{\mu + \cot(\alpha - \beta)}{\mu + \tan \beta} \quad (\text{A1.9})$$

$$\zeta \equiv \frac{\mu}{\mu + \tan \beta} \quad (\text{A1.10})$$

$$\psi \equiv (\mu + \tan \beta) \sin(\alpha - \beta) \quad (\text{A1.11})$$

Consider the quantity ϕ . From Eq. (9)

$$|\tan \beta| < \mu. \quad (\text{A1.12})$$

Thus the denominator of Eq. A1.9, is always positive and lies in the range

$$0 < \mu + \tan \beta < 2\mu. \quad (\text{A1.13})$$

Consider the numerator of Eq. (A1.9). As α approaches β , the numerator goes to a large positive number. From Eq. (4)

$$\beta < \alpha \leq \pi/2.$$

Thus $(\alpha - \beta)$ is always positive. The $\cot(\alpha - \beta)$, continuously decreases with increasing $(\alpha - \beta)$. Thus for any specific value of the denominator, ϕ can be made smaller by increasing α . Now to find the minimum value of ϕ , merely put α , at its maximum value $\pi/2$, and the following results.

$$\phi_{\min} = \frac{\mu + \cot(\pi/2 - \beta)}{\mu + \tan \beta} = \frac{\mu + \tan \beta}{\mu + \tan \beta} = 1 \quad (\text{A1.14})$$

Thus ϕ , definitely lies in the range

$$1 \leq \phi < \infty. \quad (\text{A1.15})$$

It is of value to also show that the almost trivial case of $\alpha = \pi/2$, is the only condition under which ϕ can equal unity. Set the left hand side of Eq. (A 1.9) equal to unity and obtain

$$\mu + \cot(\alpha - \beta) = \mu + \tan \beta, \quad (\text{A1.16})$$

or

$$\frac{1}{\tan(\alpha - \beta)} = \tan \beta. \quad (\text{A1.17})$$

The trigonometric identity concerning the tangent of the difference of two angles yields:

$$\frac{1 + \tan \alpha \tan \beta}{\tan \alpha - \tan \beta} = \tan \beta \quad (\text{A1.18})$$

Multiplication of the numerator and the denominator of the right hand side of Eq. (A1.18), by the denominator of the left hand side yields:

$$\frac{1 + \tan \alpha \tan \beta}{\tan \alpha - \tan \beta} = \frac{\tan \alpha \tan \beta - \tan^2 \beta}{\tan \alpha - \tan \beta} \quad (\text{A1.19})$$

Cancellation yields:

$$\frac{1}{\tan \alpha - \tan \beta} = \frac{-\tan^2 \beta}{\tan \alpha - \tan \beta} \quad (\text{A1.20})$$

Since one cannot admit imaginary values of the tangent of β , and since $\alpha > \beta$, the only way in which Eq. (A1.20) can be satisfied is by having $\alpha = \pi/2$, thereby causing the denominators of both sides to go to infinity.

Thus, it has been shown that ϕ , lies in the range one to infinity, and that the only condition for which ϕ , can equal unity is the almost trivial case for which $\alpha = \pi/2$.

Consider Eq. (A1.10) defining ζ . By Eq. (A1.12), the denominator is always positive, as is the numerator. By inserting the two extreme values of β , the range of ζ , can be seen to be:

$$0.5 < \zeta < \infty \quad (\text{A1.21})$$

Finally, consider Eq. (A1.11) defining ψ .

$$\psi = (\mu + \tan \beta) \sin (\alpha - \beta). \quad (\text{A1.22})$$

In Eq. (A1. 13) the range of $(\mu + \tan \beta)$ has been given, and by recalling Eq. (4), it is clear that the $\sin (\alpha - \beta)$ lies between zero and positive one. Inserting the extreme values in the definition leads to the following range.

$$0 < \psi < 2\mu. \quad (\text{A1. 23})$$

The fact that ψ always remains positive is a great saving in presentation and manipulation. ψ is used as a multiplier on all of the results, which enables the elimination of one variable. The fact that it is always positive and finite assures that no maxima or inequalities are upset by its inclusion.

A RIDE TERMINATING IN A SLIDE G

For a Slide G to be impending, the Required Force must be negative, and at the instant of transition from the Ride to the Slide G, the Required Force will just equal the Force Available for a Slide G; subsequent to this transition the Required Force will become more negative than the Available Force for a Slide G. To find this instant of transition τ_{bgd} , equate F_r from Eq. (32b), with F_{ag} from (33b). This yields:

$$\sin \tau_{bgd} = \frac{1}{A\phi} \quad (A1. 24)$$

hence the definition of the quantity ϕ . It is well to recall Eq. (A1. 15) which demonstrated that the range of limits of ϕ were from unity to positive infinity, with the value of unity only occurring for the special case of $\alpha = \pi/2$. Since both A and ϕ are positive, Eq. (A1. 24) apparently yields two values of τ_{bgd} , one in the first and one in the second quadrant. It will now be shown that only the first quadrant value is correct.

When a Ride is terminating in a Slide G, the Required Force is becoming more negative than the Force Available for a Slide G, or

$$\frac{\partial}{\partial \tau} (\bar{F}_r - \bar{F}_{ag}) < 0. \quad (A1. 25)$$

Subtraction of Eq. (33b) from (32b), yields:

$$\frac{\bar{F}_r - \bar{F}_{ag}}{\psi} = \frac{1}{A} - \phi \sin \tau. \quad (\text{A1. 26})$$

Taking the derivative indicated in (A1. 25), yields:

$$\frac{\partial}{\partial \tau} \left(\frac{\bar{F}_r - \bar{F}_{ag}}{\psi} \right) = -\phi \cos \tau \quad (\text{A1. 27})$$

From Eq. (A 1. 25), it can be seen that the right hand side of Eq. (78) must be negative for a valid transition from a Ride to a Slide G. Since ϕ , is positive, the $\cos \tau_{bgd}$, must also be positive. Thus, only the first quadrant solution of Eq. (A1. 24) is valid. By using the notation of principal values of inverse trigonometric functions, the transition time τ_{bgd} , may be precisely specified as follows:

$$\tau_{bgd} = \text{Sin}^{-1} \frac{1}{A \phi}. \quad (\text{A1. 28})$$

One further important point can be deduced from the above. Since $\phi > 1$, (except for $\alpha = \pi/2$) the $\sin \tau_{bgd}$, will always be less than the $\sin \tau_1$, and since both angles are definitely in the first quadrant

$$\tau_{bgd} \leq \tau_1. \quad (\text{A1. 29})$$

Thus, if a Ride is occurring in the first quadrant, it will always make a transition to a Slide G prior to the flight. Only in the special case of $\alpha = \pi/2$, can a ride persist in the first quadrant up to the time of flight.

A RIDE TERMINATING IN A SLIDE L

The conditions and time at which a Ride may terminate in a Slide L are investigated in much the same way. For a ride to be occurring, the Required Force must be less positive than the Force Available for a Slide L; for a Slide L to be impending, the Required Force must be positive, and at the instant of transition, must become equal to the Force Available for a Slide L. Following the transition the Required Force must be greater than the Available Force. The termination time τ_{bld} is determined when $F_r = F_{\text{al}}$. By equating (32b) and (34a) we obtain:

$$\sin \tau_{\text{bld}} = \frac{2\zeta - 1}{2\zeta - \phi} \cdot \frac{1}{A}. \quad (\text{A1. 30})$$

At first sight it appears that Eq. (A1. 30) may offer four possible values; it will be shown that only one is valid.

Since A is definitely positive, concern is focused on the coefficient of $1/A$. Recall from Eq. (A1. 21), that the minimum value of ζ is 0.5; thus the numerator of the right hand side of Eq. (A1. 30) is never negative. Consider the ramifications of the fact that F_r must definitely be positive for a Slide L to develop. By substituting Eq. (A1. 30), into the equation for F_r , (32b), and requiring this positiveness at that time, the following is obtained:

$$0 < \frac{\zeta(1 - \phi)}{2\zeta - \phi}. \quad (\text{A1. 31})$$

ζ is definitely positive. From Eq. (A1. 15), it is seen that $(1 - \phi) \leq 0$, and only equal to zero for the special case where $\alpha = \pi/2$. Thus, $(2\zeta - \phi)$, the denominator of Eq. (A1. 30) must definitely be negative. Since the denominator of Eq. (A1. 30) is negative and the numerator is positive, the right hand side is negative, and the $\sin \tau_{\text{bld}}$ is negative. Thus, τ_{bld} is in the third or fourth quadrant.

By employing the fact that F_r must be becoming more positive than F_{al} , the argument is completed. In symbols this requires:

$$\frac{\partial}{\partial \tau} \left(\frac{\bar{F}_r - \bar{F}_{\text{al}}}{\psi} \right) > 0. \quad (\text{A1. 31a})$$

Subtracting Eq. (34a), from (32b) yields:

$$\frac{\bar{F}_r - \bar{F}_{\text{al}}}{\psi} = \frac{1 - 2\zeta}{A} + (2\zeta - \phi) \sin \tau. \quad (\text{A1. 32})$$

Taking the derivative indicated in (A1. 31a) yields:

$$\frac{\partial}{\partial \tau} \left(\frac{\bar{F}_r - \bar{F}_{\text{al}}}{\psi} \right) = (2\zeta - \phi) \cos \tau. \quad (\text{A1. 33})$$

From Relation (A1. 31) it can be seen that the right hand side of (A1. 33) must be negative. The factor $(2\zeta - \phi)$ was just shown to be negative; hence, the $\cos \tau_{\text{bld}}$ must definitely be negative. Since both the sine and the cosine of τ_{bld} have been shown to be negative, τ_{bld} has only one value in a cycle and this value lies in the third quadrant. Again, using the notation of the principal values of inverse trigonometric functions, this may be precisely specified as follows:

$$\tau_{\text{bld}} = \pi - \text{Sin}^{-1} \left(\frac{2 \zeta - 1}{2 \zeta - \phi} \right), \quad (\text{A1. 34})$$

where for any valid transition to occur

$$2 \zeta - \phi < 0. \quad (\text{A1. 35})$$

Briefly summarizing, there are two times in each cycle where a Ride may terminate in a Slide. Excepting the exceptional case of $\alpha = \pi/2$, a Ride, if occurring in the first quadrant will terminate in a Slide G at τ_{bgd} , as specified in Eq. (A1. 28); if occurring in the third quadrant and $(2 \zeta - \phi) < 0$, a Ride will terminate in a Slide L at τ_{bld} , as specified in Eq. (A1. 34).

APPENDIX A1. 5

THE G DEFINITE ZONE

When a Slide G is occurring, the friction force on the particle is negative. For a Slide G to initiate, the Required Force must be negative and more negative than that available from friction. The limits of the G Definite zone are the two times for which F_r equals F_{ag} ; these are the two solutions of Eq. (A1. 24). To determine which of them is the beginning of the zone, note that at the beginning of the zone, F_r will be becoming more negative than F_{ag} ; thus the time at the beginning of G Definite will be that solution of Eq. (A1. 24) for which the derivative of $(F_r - F_{ag})$ is negative. This was shown to be the first quadrant value, or τ_{bgd} , as specified in Eq. (A1. 28). Thus, times at the beginning and end of the G Definite Zone will be called respectively τ_{bgd} , (time at the beginning of G Definite), and τ_{egd} , (the time at the end of G Definite). Using principal value notation once again these may be precisely specified as follows:

$$\tau_{bgd} = \text{Sin}^{-1} \left(\frac{1}{A\phi} \right), \quad (37a)$$

$$\tau_{egd} = \pi - \text{Sin}^{-1} \left(\frac{1}{A\phi} \right). \quad (37b)$$

Since both the G Definite Zone and the Fly Definite Zone are in the first and second quadrants, the consequences of this overlapping must be considered. The Fly Definite Zone takes precedence, for to have any slide at all, the particle must be on the plane. Except when $\phi = 1$, (the special case of $\alpha = \pi/2$), some portion of the G Definite Zone always exists prior to the flight. Hence, virtually all

situations will contain this portion of the G Definite Zone. For extremely low amplitudes, (A), however, τ_2 , the impact time can occur prior to τ_{egd} , and a second portion of the G Definite Zone will then exist following the impact. This is definitely a complicating factor in the analysis and leads to several different, although uncommon solutions. Fortunately, the amplitude for which τ_2 , the impact time equals π , is approximately 1.15, a value far below that normally used in applications. Since τ_{egd} is always less than π , one need not be concerned with this possibility when the amplitude (A), exceeds 1.15. Any analysis however, of cases with very low amplitudes would definitely have to admit this possibility. No such cases were computed in this study.

APPENDIX A1. 6

L DEFINITE ZONE

The logic here proceeds as in the previous section. When a Slide L is occurring, the friction force must be positive. Further, for a Slide L to initiate, the Required Force must be positive, and more positive than that available from friction. The limits of the L Definite Zone are those two times when F_r equals F_{al} , when F_r is positive. The logic following Eq. (A1. 31), in the Ride Termination Section, demonstrated that, for F_r to be positive, $(2 \zeta - \phi)$ had to be negative, which in turn led to the conclusion that the two solutions of the equation resulting from the equating of F_r and F_{al} , (Eq. (A1. 30)) had to be in the third and fourth quadrants. To establish which of the two solutions is the beginning of the L Definite Zone, recall that F_r must be becoming more positive than F_{al} at the beginning of the zone. Thus, the derivative of $F_r - F_{al}$ must be positive at the beginning of the zone. The reasoning following Eq. (A1. 33) in the Ride termination section proved that this was the third quadrant value. Now the limits of the L Definite Zone may be written, again using the notation of principal values, as follows:

$$\tau_{\text{bld}} = \pi - \text{Sin}^{-1} \left[\frac{2 \zeta - 1}{2 \zeta - \phi} \cdot \frac{1}{A} \right], \quad (38b)$$

$$\tau_{\text{eld}} = 2 \pi + \text{Sin}^{-1} \left[\frac{2 \zeta - 1}{2 \zeta - \phi} \cdot \frac{1}{A} \right]. \quad (38c)$$

It was earlier remarked that it was to be shown that for certain values of operating conditions a Slide L Definite Zone is impossible. This can be seen as follows. Recall Eq. (A1. 32) in the Ride termination

section, the equation for the difference between F_r and F_{al} . Clearly, this quantity must be positive in any valid L Definite Zone. The factor on $\sin \tau$, was shown to be negative. Thus, that relation is most positive when the $\sin \tau$, is most negative, or when $\tau = 3\pi/2$. For the limiting case, beyond which it is impossible to make this difference positive, set the $\sin \tau = -1$, and require the result to be positive. This yields:

$$\frac{1 - 2 \zeta}{A} - (2 \zeta - \phi) > 0. \quad (38a)$$

Thus, summarizing, an L Definite Zone exists if (38a), and it begins at (38b) and ends at (38c).

APPENDIX A1.7

NEITHER SLIDE CAN TERMINATE IN ITS CORRESPONDING DEFINITE ZONE

Assume a Slide G in the G Definite Zone. This means that the particle velocity is greater than the plane velocity. Hence $(\dot{X} - \dot{X}')$ is positive. Slide termination will occur when the relative velocity becomes zero. For a positive quantity to become zero, its derivative must become negative, or the relative acceleration of the particle with respect to the plane must become negative prior to the termination. Subtraction of Eq. (29c) from (29b), yields this relative acceleration to be

$$\left(\frac{\ddot{X} - \ddot{X}'}{\psi} \right)_G = \frac{1}{-A} + \phi \sin \tau. \quad (\text{A1.36})$$

The substitution of the limits of the G Definite Zone, $\tau_{bgd'}$ and $\tau_{egd'}$ (Eqs. (37a), (37b)) into the above, shows the relative acceleration to be zero at these limits. Since these limits are symmetrical about $\pi/2$, the positive sine term becomes more positive between the limits. Thus, the relative acceleration of the particle with respect to the plane is positive throughout the G Definite Zone, and no termination can occur within that zone.

Thus, if a Slide G is occurring within the G Definite Zone, prior to the time of flight, τ_1 , it must persist until τ_1 . Further, if the limit of the G Definite Zone extends beyond the time of impact, $(\tau_{egd'} > \tau_2)$, and if a Slide G is occurring after the time of impact and prior to $\tau_{egd'}$ the slide must persist until after $\tau_{egd'}$.

To make the same proof for the Slide L, assume that a Slide L is occurring within the L Definite Zone. Here the particle velocity

is less than the plane velocity; the relative velocity of the particle with respect to the plane, $(\dot{X} - \dot{X}')$, is negative. Slide termination will occur when the relative velocity becomes equal to zero. Clearly, for the relative velocity to become zero, its rate of change or the relative velocity to become zero, its rate of change or the relative acceleration of the particle with respect to the plane must become positive prior to any slide termination. The subtraction of Eq. (29c), from (28b), yields this acceleration to be

$$\left(\frac{\ddot{X} - \ddot{X}'}{\psi} \right)_L = \frac{1}{A} (2 \zeta - 1) - (2 \zeta - \phi) \sin \tau. \quad (\text{A1.37})$$

It may be quickly verified that the relative acceleration is zero at the limits of the Slide L Definite Zone by the substitution of these limits, τ_{bld} (Eq. (38b)), and τ_{eld} (Eq. (38c)), into Eq. (A1.37). In the first paragraph of the section defining the L Definite Zone, it was proved that the quantity $(2 \zeta - \phi)$ had to be negative in order that any L Definite Zone exist, hence the coefficient of the sine term in Eq. (A1.37) is positive. The L Definite Zone being in the third and fourth quadrants, the $\sin \tau$ is always negative, and more negative within the zone than at its extremities. Thus, the relative acceleration of the particle with respect to the plane is negative throughout the L Definite Zone when a Slide L is occurring, and hence no Slide L Termination can occur within that zone. In summary, if a Slide L is occurring within the Slide L Definite Zone, it must persist until after τ_{eld} .

APPENDIX A1. 8

THE DERIVATION OF THE GFGL EQUATIONS

The x velocity of the particle at τ_{t1} , must equal the velocity of the plane. Hence, from Eq. (29b)

$$\frac{\dot{X}(\tau_{t1})}{\psi} = (\phi - \zeta) \cos \tau_{t1}. \quad (29b)$$

With this value of initial velocity, the particle undergoes a Slide G from τ_{t1} to the time of flight, τ_1 . The substitution of Eq. (29b) into Eq. (27c) yields:

$$\frac{\dot{X}(\tau_1)}{\psi} = \frac{1}{-A} (\tau_1 - \tau_{t1}) - \zeta \cos \tau_1 + \phi \cos \tau_{t1}. \quad (A1. 38)$$

The particle now flies from τ_1 to τ_2 . Using Eq. (A1. 38) as the initial velocity in the velocity equation for a Flight, Eq. (31c), the velocity at τ_2 , just prior to impact may be expressed as

$$\frac{\dot{X}(\tau_2)}{\psi} = \frac{1}{A} \left[-\zeta \tau_1 + \tau_2 (\zeta - 1) + \tau_{t1} \right] - \zeta \cos \tau_1 + \phi \cos \tau_{t1}. \quad (A1. 39)$$

The velocity immediately after the impact, $\dot{X}(\tau_2^*)$, is obtained by substituting Eq. (A1. 39) and (41), into (42b): This yields

$$\frac{X(\tau_2^*)}{\psi} = \frac{1}{A} \left[\zeta \tau_1 (\epsilon - 1) + \tau_2 (\zeta - \epsilon \zeta - 1) + \tau_{t1} \right] + \zeta (\epsilon - 1) \cos \tau_1 + \phi \cos \tau_{t1} - \zeta \epsilon \cos \tau_2. \quad (\text{A1. 40})$$

A Slide G begins following the impact and continues until τ_{tg} . The time τ_{tg} would normally be determined by the Slide G Termination Equation, (39a). The substitution of Eq. (A1. 40) into (39a), yields the following

$$\left(\cos \tau_{tg} - \cos \tau_{t1} \right) + \frac{1}{A\phi} (\tau_{tg} - \tau_{t1}) - \frac{(1 - \epsilon) \zeta}{\phi} \left[\frac{1}{A} (\tau_2 - \tau_1) + \cos \tau_2 - \cos \tau_1 \right] = 0. \quad (\text{A1. 41})$$

By use of the definition of $\Delta \dot{X}$, Eq. (A1. 41), this may be more simply written as

$$\left(\cos \tau_{tg} - \cos \tau_{t1} \right) + \frac{1}{A\phi} (\tau_{tg} - \tau_{t1}) - \frac{(1 - \epsilon) \Delta \dot{X}}{\phi \psi} = 0. \quad (\text{A1. 42})$$

Equation (A1. 42) is the first equation in the two unknowns, τ_{tg} , and τ_{t1} . The other equation is obtained by requiring that the particle initiate a Slide L at τ_{tg} , with the velocity of the plane at that time, and that this Slide L terminate at $\tau_{t1} + 2\pi$, thereby assuring periodicity. The velocity of the particle is equal to the velocity of the plane at τ_{tg} , hence from Eq. (29b)

$$\frac{\dot{X}(\tau_{tg})}{\psi} = (\phi - \zeta) \cos \tau_{tg}. \quad (\text{A1. 43})$$

Now by substituting τ_{tg} for τ_i , and $(\tau_{tl} + 2\pi)$, for τ_{tl} , in Eq. (39b), the Slide L termination equation, the required equation becomes

$$\frac{2\pi}{A} (2\zeta - 1) - \frac{(2\zeta - 1)}{A} (\tau_{tg} - \tau_{tl}) - (2\zeta - \phi) (\cos \tau_{tg} - \cos \tau_{tl}) = 0. \quad (A1.44)$$

It is convenient to define two new angles, γ , and δ , as follows

$$\gamma = \tau_{tg} - \tau_{tl}, \quad (A1.45)$$

$$\delta = \tau_{tg} + \tau_{tl}. \quad (A1.46)$$

From Eq. (A1.42)

$$\cos \tau_{tg} - \cos \tau_{tl} = \frac{(1 - \epsilon)}{\phi} \frac{\Delta \dot{X}}{\psi} - \frac{\gamma}{A\phi}. \quad (A1.47)$$

The substitution of Eq. (A1.47) into (A1.44) yields the angle γ , to be

$$\gamma = \frac{\pi\phi}{\zeta} \left[\frac{2\zeta - 1}{\phi - 1} \right] + (1 - \epsilon) \frac{A}{2\zeta} \frac{(\phi - 2\zeta)}{(\phi - 1)} \frac{\Delta \dot{X}}{\psi}. \quad (44c)$$

From the familiar trigonometric identity about the difference between the cosine of two angles, one may write

$$\cos \tau_{tg} - \cos \tau_{tl} = -2 \sin \frac{\delta}{2} \sin \frac{\gamma}{2}. \quad (A1.48)$$

The substitution of Eq. (A1. 48), into (A1. 47), permits the value of δ , to be obtained from

$$\sin \frac{\delta}{2} = \frac{1}{2 \phi \sin \frac{\gamma}{2}} \left[\frac{\gamma}{A} - (1 - \epsilon) \frac{\Delta \dot{X}}{\Psi} \right]. \quad (\text{A1. 49})$$

Equation (44c) yields γ , directly with no ambiguity. Equation (A1. 49) however, involves inverse trigonometric functions and hence is multi-valued. Consideration must be given to obtaining the correct solution of (A1. 49). τ_{t1} must be an acute positive angle; further, τ_{tg} must lie in the L Definite Zone and will be therefore of the order of $3\pi/2$. Thus, from Eq. (A1. 45), γ will be of the order of π , while δ will be of the order of 2π . Necessarily then, $\delta/2$ is of the order of π . This being the case, the desired solution of Eq. (A1. 49) can be written without ambiguity by utilizing the notation of principal values of inverse trigonometric functions as follows

$$\delta = 2 \left[\pi - \text{Sin}^{-1} \left\{ \frac{1}{2 \phi \sin \frac{\gamma}{2}} \left(\frac{\gamma}{A} - (1 - \epsilon) \frac{\Delta \dot{X}}{\Psi} \right) \right\} \right]. \quad (44d)$$

Finally, from Eqs. (A1. 44) and (A1. 45), one obtains

$$\tau_{tg} = (\gamma + \delta)/2 \quad (44a)$$

$$\tau_{t1} = \tau_{tg} - \gamma. \quad (44b)$$

APPENDIX A2

THE FORTRAN PROGRAMS OF THE SOLUTION ROUTINES

A2.1 Solutions Without Rides

This Appendix contains the actual Fortran Programs of the solution routine. The programs for the solutions without Rides each consist of a general introductory program which computes the parameters common to all routines, together with a subroutine for the particular solution form. If the capacity of the IBM 1620 Computer had been greater, all three of the subroutines could have been assembled into one program. Thus, the complete FGL solution routine consists of this general program plus the FGL subroutine, the GFGL Routine consists of the general program plus the GFGL Subroutine, and so on. The general program is shown only once and is not repeated with each subroutine.

APPENDIX A2.2

INTRODUCTORY NO-RIDE PROGRAM

```

C   AO IN INCHES, WOMEGA IN RPM, ALPHA AND BETA IN DEGREES
1  READ 4, AO, WOMEGA, WMU, ALPHAM, BETAM, EPS
   DIMENSION X(21), XD(21)
2  FORMAT(50H GABE6 - 5S SOLNS WITH L BUT NO R, FL, FGL, GFGL      )
   PUNCH 9, AO, WOMEGA, WMU, ALPHAM, BETAM, EPS
   PUNCH 2
3  FORMAT(1H 6H AO = F10.5, 17H INCHES, OMEGA = F10.5, 11H RPM, MU = F1
10.5/11H   ALPHA = F10.5, 17H DEGREES, BETA = F10.5, 6H DEGRS      )
   PUNCH 3, AO, WOMEGA, WMU, ALPHAM, BETAM
4  FORMAT(   6F10.5)
   PUNCH 7, EPS
5  ALPHA = ALPHAM*3.1416/180.0
   BETA = BETAM*3.1416/180.0
   A=AO*WOMEGA**2*0.000028403*SINF(ALPHA-BETA)/COSF(BETA)
   IF(A-1.)27,27,6
6  PHI=(WMU+1.0/TANF(ALPHA-BETA))/(WMU+TANF(BETA))
   ZETA=WMU/(WMU+TANF(BETA))
   PSI=(WMU+TANF(BETA))*SINF(ALPHA-BETA)
   PUNCH 40, A, PHI, ZETA, PSI
7  FORMAT(1X, 29H IMPACT LUBRICATION FACTOR = F10.5)
   TFL = ASINF(1.0/A)
   DISFAK=AO*PSI
   VELFAK=DISFAK*.10472*WOMEGA
   PLAVEL=VELFAK*(PHI-ZETA)
   PLADIS=DISFAK*(PHI-ZETA)
   PUNCH 8, PLAVEL, PLADIS
8  FORMAT(17H PLANE MAX X VEL= E12.5, 13H MAX X DISPL= E12.5      )
9  FORMAT(///6F10.5)
   BE = -1.0/(2.0*A)
   CE = TFL/A+COSF(TFL)
   DE = -TFL**2/(2.0*A)-TFL*COSF(TFL)+1.0/A
   TI=1.57+SQRTF(11.0*(A-1.0))
10 TINEW=TI-((-SINF(TI)+BE*TI**2+CE*TI+DE)/(-COSF(TI)+2.0*BE*TI+CE)
   TEST=ABSF(TI-TINEW)
   IF(TEST-.00005)12,11,11
11 TI=TINEW
   GO TO 10
12 PUNCH 13, TFL, TiNEW
   TI=TINEW
13 FORMAT(   21H FINAL VALUES  TFL = F10.5, 9H   TI = F10.5)
   DXDS=ZETA*((TI-TFL)/A+COSF(TI)-COSF(TFL))
   AIPH=1.0/(A*PHI)
   TBGD=ASINF(AIPH)
   TEGD=3.14159-TBGD
20 IF((1.-2.*ZETA)/A+PHI-2.*ZETA)25,25,22
22 AIPHP=(2.*ZETA-1.0)/(A*(2.*ZETA-PHI))
   TBLD=3.14159-ASINF(AIPHP)
   TELD=6.28319+ASINF(AIPHP)
   GO TO 30
25 PUNCH 26

```

INTRODUCTORY NO-RIDE PROGRAM

```
26 FORMAT(/26HNO SLIDE L DEFINITE ZONE      )
   GO TO 1
27 PUNCH 28,A
28 FORMAT(25HFAILD- A UNDER   1,A =      E12.5)
   GO TO 1
30 R=1.
   PUNCH 31,TBGD,TEGD,TBLD,TELD
31 FORMAT(20HTBGD,TEGD,TBLD,TELD   /4E12.5)
32 CALL FGL1 (A,PHI,ZETA,EPS,DXDS,TFL,TI,PSI,WOMEGA,AO,R,TBGD,TEGD,
  1TBLD,TELD,DISFAK,VELFAK)
40 FORMAT(/ 5H A = F10.5, 7H PHI = F10.5, 8H ZETA = F10.5, 7H PSI =
  1 F10.5)
   GO TO 1
   END
```

```
CALL GFGL1(A,PHI,ZETA,EPS,DXDS,TFL,TI,PSI,WOMEGA,AO,R,TBGD,TEGD,
  1TELD,TELD,DISFAK,VELFAK)
```

```
33 CALL FL1 (A,PHI,ZETA,EPS,DXDS,TFL,TI,PSI,WOMEGA,AO,R,TBGD,TEGD,
  1TBLD,TELD,DISFAK,VELFAK)
```

APPENDIX A2.3

THE GFGL SUBROUTINE

```

SUBROUTINE GFGL(A,PHI,ZETA,EPS,DXDS,TFL,TI,PSI,WOMEGA,AO,R,TBGD,
1TEGD,TBLD,TELD,DISFAK,VELFAK)
C USING GFGL SOLN TO GET TGL AND TLG AND TEST
  DIMENSION X(21),XD(21)
  GAMMA=3.1416*PHI/ZETA*(2.*ZETA-1.)/(PHI-1.)+A/2.*DXDS*(1.-EPS)/
1ZETA*(PHI-2.*ZETA)/(PHI-1.)
  DIN=(GAMMA/A-(1.-EPS)*DXDS)*1./(2.*PHI*SIN2(GAMMA/2.))
  IF(DIN-1.)2,1,1
1 PUNCH 90,DIN
90 FORMAT(38HFAILED IN GFGL,DIN EXCEEDS 1,DIN =      E12.5)
  RETURN
2 DELTA = 2.0*(3.1416-ASINF(DIN))
  TGL =(GAMMA+DELTA)/2.0
  TLG = TGL-GAMMA
  IF(TFL-TLG)3,3,4
3 PUNCH 91,TLG,TGL
91 FORMAT(42HFAILED IN GFGL,TFL UNDER TLG, TLG,TGL =      2E12.5)
  RETURN
4 IF(TLG-TBGD)5,6,6
5 PUNCH 92,TLG,TBGD
92 FORMAT(41HFAILED IN GFGL,TLG UNDER TBGD,TLG,TBGD =      2E12.5)
  RETURN
6 IF(TGL-TBLD)7,8,8
7 PUNCH 93,TGL,TBLD
93 FORMAT(40HFAILED IN GFGL,TGL UNDER TBLD,TGL,TBLD =      2E12.5)
  RETURN
8 IF(TGL-TELD)10,9,9
9 PUNCH 94,TGL,TELD
94 FORMAT(41HFAILED IN GFGL,TGL EXCEEDS TELD,TGL,TELD =      2E12.5)
  RETURN
10 IF(TGL-TI)11,11,12
11 PUNCH 95,TGL
95 FORMAT(33HFAILED IN GFGL,TGL UNDER TI,TGL =      E12.5)
  RETURN
12 XDSTLG=(PHI-ZETA)*COSF(TLG)
  XDSTFL=- (TFL-TLG)/A-ZETA*(COSF(TFL)-COSF(TLG))+XDSTLG
  XDSTI=(ZETA-1.0)*(TI-TFL)/A+XDSTFL
  XDSTIS=XDSTI-EPS*DXDS
  XDSTGL=- (TGL-TI)/A-ZETA*(COSF(TGL)-COSF(TI))+XDSTIS
  XDSPTI=(PHI-ZETA)*COSF(TI)
  IF(XDSTIS-XDSPTI)13,13,14
13 PUNCH 96
96 FORMAT(36HFAILED IN GFGL, XDSTIS UNDER XDSPTI      )
  RETURN
14 XDS2LG=(2.0*ZETA-1.0)*(6.2832+TLG-TGL)/A+ZETA*(COSF(TLG)-COSF(TGL)
1)+XDSTGL
  PUNCH 16
16 FORMAT(/ 24H THIS IS A GFGL SOLUTION      )
  PUNCH 17,TGL,TLG
17 FORMAT(1H 7H TGL = F10.5,11H      TLG = F10.5)

```

```

PUNCH 18, XDSTLG, XDSTFL, XDSTI, XDSTIS, XDSTGL, XDS2LG
18 FORMAT(1H 10H XDSTLG = F10.5, 12H XDSTFL = F10.5, 11H XDSTI = F1
10.5/12H XDSTIS = F10.5, 12H XDSTGL = F10.5, 10H XDS2LG = F10
1.5)
C JUST DID VELOCITIES, NOW DO XS
XSTLG=0.0
XSTFL=-(TFL-TLG)**2/(2.0*A)-ZETA*(1.0/A-SINF(TLG))+(XDSTLG+ZETA*CO
1SF(TLG))*(TFL-TLG)+XSTLG
XSTI=(ZETA-1.0)*(TI-TFL)**2/(2.0*A)+XDSTFL*(TI-TFL)+XSTFL
XSTGL=-(TGL-TI)**2/(2.0*A)-ZETA*(SINF(TGL)-SINF(TI))+(ZETA*COSF(TI
1)+XDSTIS)*(TGL-TI)+XSTI
XS2LG=(2.0*ZETA-1.0)*(TLG+6.2832-TGL)**2/(2.0*A)+ZETA*(SINF(TLG)-S
1INF(TGL))+(XDSTGL-ZETA*COSF(TGL))*(TLG+6.2832-TGL)+XSTGL
XDSAV=XS2LG/6.2832
XDAV=PSI*XDSAV
XLDAV=WOMEGA*6.2832*AU*XDAV/60.
X2LG=PSI*XS2LG
XLCYCL=AO*X2LG
PUNCH 19, XSTLG, XSTFL, XSTI, XSTGL, XS2LG
19 FORMAT(1H 9H XSTLG = F10.5, 11H XSTFL = F10.5, 10H XSTI = F10.5
1/11H XSTGL = F10.5, 11H XS2LG = F10.5)
PUNCH 20, XDSAV, XDAV, XLDAV
20 FORMAT(1H 9H XDSAV = F10.5, 10H XDAV = F10.5, 11H XLDAV = F10.5,
118H INCHES PER SECOND )
PUNCH 21, X2LG, XLCYCL
21 FORMAT(1H 8H X2LG = F10.5, 13H XLCYCL = F10.5, 33H DISPLACEMENT
1PER CYCLE IN INCHES )
XO=.5/A*(6.2832-TGL)**2*(2.*ZETA-1.)-ZETA*SINF(TGL)+(XDSTGL-ZETA*
1COSF(TGL))*(6.2832-TGL)
DELX=XS2LG-XSTGL-XO
DO 70 I=1,21
TINDEX=I
T=(TINDEX-1.)*.31416
IF(T-TLG)60,61,61
60 XD(I)=VELFAK*((2.*ZETA-1.)/A*(T+6.2832-TGL)+ZETA*(COSF(T)-COSF(TGL
1)))+XDSTGL)
X(I)=DISFAK*(.5/A*(2.*ZETA-1.)*(T+6.2832-TGL)**2+ZETA*(SINF(T)-SIN
1F(TGL))+(XDSTGL-ZETA*COSF(TGL))*(T+6.2832-TGL)-XO)
GO TO 70
61 IF(T-TFL)62,63,63
62 XD(I)=VELFAK*((TLG-T)/A-ZETA*(COSF(T)-COSF(TLG)))+XDSTLG)
X(I)=DISFAK*(-.5/A*(T-TLG)**2-ZETA*(SINF(T)-SINF(TLG))+(ZETA*COSF(
1TLG)+XDSTLG)*(T-TLG)+XSTLG+DELX)
GO TO 70
63 IF(T-TI)64,65,65
64 XD(I)=VELFAK*((ZETA-1.)/A*(T-TFL)+XDSTFL)
X(I)=DISFAK*(.5/A*(ZETA-1.)*(T-TFL)**2+XDSTFL*(T-TFL)+XSTFL+DELX)
GO TO 70
65 IF(T-TGL)66,67,67
66 XD(I)=VELFAK*((TI-T)/A-ZETA*(COSF(T)-COSF(TI)))+XDSTIS)

```

```

      X(I)=DISFAK*(-.5/A*(T-TI)**2-ZETA*(SINF(T)-SINF(TI))+(ZETA*COSF(TI
1)+XDSTIS)*(T-TI)+XSTI+DELX)
      GO TO 70
67 XD(I)=VELFAK*((T-TGL)*(2.*ZETA-1.)/A+ZETA*(COSF(T)-COSF(TGL))+XDST
1GL)
      X(I)=DISFAK*(.5/A*(2.*ZETA-1.)*(T-TGL)**2+ZETA*(SINF(T)-SINF(TGL))
1+(XDSTGL-ZETA*COSF(TGL))*(T-TGL)+XSTGL+DELX)
70 CONTINUE
      PUNCH 71
71 FORMAT(// 1X,38H VELOCITIES IN IPS FOR INCRS OF 2PI/20 )
      PUNCH 72,(XD(I),I=1,71)
72 FORMAT(6E12.5)
      PUNCH 73
73 FORMAT(//1X,32H DISPLS IN INCHES FOR SAME INCRS )
      PUNCH 72,(X(I),I=1,21)
C   MUST GET TRANS PTS
      XDLTG=VELFAK*XDSTLG
      XDLTFL=VELFAK*XDSTFL
      XDITI=VELFAK*XDSTI
      XDITIS=VELFAK*XDSTIS
      XDITGL=VELFAK*XDSTGL
      PUNCH 74,XDITLG,XDITFL,XDITI,XDITIS,XDITGL
74 FORMAT(//1X,12HTRANS VEL5 5E12.5)
      XLTLG=DISFAK*(XSTLG+DELX)
      XLTFL=DISFAK*(XSTFL+DELX)
      XLTI=DISFAK*(XSTI+DELX)
      XLTGL=DISFAK*(XSTGL+DELX)
      XL2LG=DISFAK*(XS2LG+DELX)
      PUNCH 75,XLTLG,XLTFL,XLTI,XLTGL,XL2LG
75 FORMAT(1X,12HTRANS DISPLS 5E12.5)
      R=0.
      RETURN
      END

```

APPENDIX A2.4

THE FGL SUBROUTINE

```

C   USING FGL SOLN
      SUBROUTINE FGL1(A,PHI,ZETA,EPS,DXDS,TFL,TI,PSI,WOMEGA,AO,R,TBGD,
1  TEGD,TBLD,TELD,DISFAK,VELFAK)
      DIMENSION X(21),XD(21)
      TGL = 4.712
      EE=.5*(EPS-1.)*(TI/A+COSF(TI))- .5*(1.+EPS)*(TFL/A+COSF(TFL))-3.141
16/A*(2.*ZETA-1.)/ZETA
      DO 2 I=1,10
1  TGLNEW=TGL-(COSF(TGL)+TGL/A+EE)/(-SINF(TGL)+1.0/A)
      TEST=ABSF(TGL-TGLNEW)
      IF(TEST-.00005)4,2,2
2  TGL=TGLNEW
      PUNCH 3
3  FORMAT(29HFAILD- COULDNT CONVG ON TGL      )
      RETURN
4  TGL=TGLNEW
      IF(TGL-TBLD)5,7,7
5  PUNCH 6,TGL
6  FORMAT(34HFAILD IN FGL,TGL UNDER TBLD,TGL =   E12.5)
      RETURN
7  IF(TGL-TELD)7,8,8
8  PUNCH 9,TGL
9  FORMAT(36HFAILD IN FGL,TGL EXCEEDS TELD,TGL =   E12.5)
      RETURN
70 IF(TGL-TI)80,80,81
80 PUNCH 10,TGL
10 FORMAT(25HFAILD IN FGL,TGL UNDER TI   E12.5)
      RETURN
81 PUNCH 82
82 FORMAT(/ 19H THIS IS A FGL SOLN      )
      PUNCH 15,TGL
15 FORMAT(1H 22H FINAL VALUE OF TGL = F10.5)
      XDSTGL=(PHI-ZETA)*COSF(TGL)
      XDS2FL=(2.0*ZETA-1.0)*(TFL+6.2832-TGL)/A+ZETA*(COSF(TFL)-COSF(TGL)
1) +XDSTGL
C   FLY FR TFL TO TI
      XDSPFL=(PHI-ZETA)*COSF(TFL)
      IF(XDSPFL-XDS2FL)83,85,85
83 PUNCH 84,XDSPFL,XDS2FL
84 FORMAT(27HFAILD,XDSPFL UNDER XDS2FL,   2E12.5)
      RETURN
85 XDSTI =(ZETA-1.0)*(TI-TFL)/A+XDS2FL
      XDSTFL=XDS2FL
C   GET IMPACT VELOCITY CHANGE
      XDSTIS=XDSTI-EPS*DXDS
      XDSPTI=(PHI-ZETA)*COSF(TI)
      IF(XDSTIS-XDSPTI)86,86,88
86 PUNCH 87
87 FORMAT(35HFAILD IN FGL, XDSTIS UNDER XDSPTI      )

```



```

RETURN
C   SLI G TO TGL
88  XDS2GL=-(TGL-TI)/A-ZETA*(COSF(TGL)-COSF(TI))+XDSTIS
    PUNCH 50,XDSTGL,XDSTFL,XDSTI,XDSTIS,XDS2GL
50  FORMAT(1H 26H ND VELOCITIES  XDSTGL = F10.5,12H  XDSTFL = F10.5,
111H  XDSTI = F10.5/12H  XDSTIS = F10.5  ,12H  XDS2GL = F10.5)
C   COMPUTE XS
    XSTFL=0.0
    XSTI=(ZETA-1.0)*(TI-TFL)**2/(2.0*A)+XDSTFL*(TI-TFL)+XSTFL
    XSTGL=-(TGL-TI)**2/(2.0*A)-ZETA*(SINF(TGL)-SINF(TI))+(ZETA*COSF(TI
1)  )+XDSTIS)*(TGL-TI)+XSTI
    XS2TFL=(2.0*ZETA-1.0)*(TFL+6.2832-TGL)**2/(2.0*A)+ZETA*(SINF(TFL)-
1  SINF(TGL))+(XDSTGL-ZETA*COSF(TGL))*(TFL+6.2832-TGL)+XSTGL
    XDSAV=XS2TFL/6.2832
    XDAV=PSI*XDSAV
    XLDAV=WOMEGA*6.2832*AO*XDAV/60.
    X2TFL=PSI*XS2TFL
    XLCYCL=AO*X2TFL
    PUNCH 90,XSTFL,XSTI,XSTGL,XS2TFL
90  FORMAT(1H 9H XSTFL = F10.5,10H  XSTI = F10.5,11H  XSTGL = F10.5
1/12H  XS2TFL = F10.5)
    PUNCH 91,XDSAV,XDAV,XLDAV
91  FORMAT(1H 29H AVERAGE VELOCITIES, XDSAV = F10.5,10H  XDAV = F10.5
1/11H  XLDAV = F10.5,18H INCHES PER SECOND )
    PUNCH 92, X2TFL,XLCYCL
92  FORMAT(/1X,21HREL DISPL PER CYCL = F10.5,20HABS DISPL PER CYC = F1
10.5  )
    XO=.5/A*(2.*ZETA-1.)*(6.2832-TGL)**2-ZETA*SINF(TGL)+(XDSTGL-ZETA*
1  COSF(TGL))*(6.2832-TGL)
    DELX=XS2TFL-XSTGL-XO
    DO 105 I=1,21
    TINDEX=I
    T=(TINDEX-1.)*.31416
    IF(T-TFL)94,95,95
94  XD(I)=VELFAK*((2.*ZETA-1.)/A*(T+6.2832-TGL)+ZETA*(COSF(T)-COSF(TGL
1)  )+XDSTGL)
    X(I)=DISFAK*(.5/A*(2.*ZETA-1.)*(T+6.2832-TGL)**2+ZETA*(SINF(T)-SIN
1  F(TGL))+(XDSTGL-ZETA*COSF(TGL))*(T+6.2832-TGL)-XO)
    GO TO 105
95  IF(T-TI)96,97,97
96  XD(I)=VELFAK*((ZETA-1.)/A*(T-TFL)+XDSTFL)
    X(I)=DISFAK*((ZETA-1.)*.5/A*(T-TFL)**2+XDSTFL*(T-TFL)+XSTFL+DELX)
    GO TO 105
97  IF(T-TGL)98,99,99
98  XD(I)=VELFAK*((TI-T)/A-ZETA*(COSF(T)-COSF(TI))+XDSTIS)
    X(I)=DISFAK*(-.5/A*(T-TI)**2-ZETA*(SINF(T)-SINF(TI))+(ZETA*COSF(TI
1)  )+XDSTIS)*(T-TI)+XSTI+DELX)
    GO TO 105
99  XD(I)=VELFAK*((2.*ZETA-1.)/A*(T-TGL)+ZETA*(COSF(T)-COSF(TGL))+XDST
1  GL)

```

```

      X(I)=DISFAK*((2.*ZETA-1.)*.5/A*(T-TGL)**2+ZETA*(SINF(T)-SINF(TGL))
1+(XDSTGL-ZETA*COSF(TGL))*(T-TGL)+XSTGL+DELX)
105 CONTINUE
      PUNCH 109
      PUNCH 106,(XD(I),I=1,21)
106 FORMAT(6E12.5)
      PUNCH 110
      PUNCH 106,(X(I),I=1,21)
C      GET TRANS PTS
      XDLTFL=VELFAK*XDSIFL
      XDLTI=VELFAK*XDSTI
      XDLTIS=VELFAK*XDSTIS
      XDLTGL=VELFAK*XDSTGL
      PUNCH 107,XDLTFL,XDLTI,XDLTIS,XDLTGL
107 FORMAT(//1X,11HTRANS VELS 4E12.5)
      XLTFL=DISFAK*(XSTFL+DELX)
      XLTI=DISFAK*(ASTI+DELX)
      XLTGL=DISFAK*(XSTGL+DELX)
      XL2FL=DISFAK*(XS2TFL+DELX)
      PUNCH 108,XLTFL,XLTI,XLTGL,XL2FL
108 FORMAT(1X,12HIRANS DISPLS 4E12.5)
109 FORMAT(// 1X,38H VELOCITIES IN IPS FOR INCRS OF 2PI/20 )
110 FORMAT(//1X,32H DISPLS IN INCHES FOR SAME INCRS )
      R=0.
      RETURN
      END

```

THE FL SUBROUTINE

APPENDIX A2.5

```

SUBROUTINE FL(A,PHI,ZETA,EPS,DXDS,TFL,TI,PSI,WOMEGA,AO,R,TBGD,
1 TEGD,TBLD,TELD,DISFAK,VELFAK)
DIMENSION X(21),XD(21)
5 IF(TBLD-TI)8,8,6
6 PUNCH 7
7 FORMAT(28HFAILD IN FL,TBLD EXCEEDS TI )
RETURN
8 IF(TELD-TI)9,9,110
9 PUNCH 10
10 FORMAT(26HFAILD IN FL,TELD UNDER TI )
RETURN
110 XDSTIS=(PHI-ZETA)*COSF(TI)
XDSTFL=(2.*ZETA-1.)/A*(TFL+6.2832-TI)+ZETA*(COSF(TFL)-COSF(TI))+
1 XDSTIS
XDSPFL=(PHI-ZETA)*COSF(TFL)
IF(XDSPFL-XDSTFL)111,113,113
111 PUNCH 112
112 FORMAT(46HFL SOLN NG, PART VEL EXCEEDS PLANE VEL AT TFL )
RETURN
113 XDSTI=(ZETA-1.)/A*(TI-TFL)+XDSTFL
XDSPTI=(PHI-ZETA)*COSF(TI)
IF(XDSTI-XDSPTI-EPS*DXDS)123,123,121
121 PUNCH 122
122 FORMAT(52HFL SOLN NG, PART VEL EXCEEDS PLANE VEL PLUS IMPULSE )
RETURN
123 IF(XDSTI-XDSPTI+EPS*DXDS)124,126,126
124 PUNCH 125
125 FORMAT(52HFL SOLN NG, PART VEL UNDER PLANE VEL MINUS IMPULSE )
RETURN
126 PUNCH 127
127 FORMAT(/1X,18H THIS IS A FL SOLN )
XSTFL=0.
XSTI=(ZETA-1.)/A*.5*(TI-TFL)**2+XDSTFL*(TI-TFL)
XS2FL=(2.*ZETA-1.)/A*.5*(TFL+6.2832-TI)**2+ZETA*(SINF(TFL)-SINF(TI
1 ))+(XDSTIS-ZETA*COSF(TI))*(TFL+6.2832-TI)+XSTI
PUNCH 128,XDSIFL,XDSTI,XDSTIS
128 FORMAT(1X,9HXDSTFL = E12.5, 8HXDSTI = E12.5,9HXDSTIS = E12.5 )
PUNCH 129,XSTFL,XSTI,XS2FL
129 FORMAT(1X,8HXSTFL = E12.5,7HXSTI = E12.5,8HXS2FL = E12.5 )
XDSAV=XS2FL/6.2832
XDLAV=XS2FL*AO*PSI*WOMEGA/60.
XLCYCL=XS2FL*PSI*AO
PUNCH 130,XDSAV,XDLAV,XLCYCL
130 FORMAT(/1X,8HXDSAV = E12.5, 8HXDLAV = E12.5, 19HIPS, XLCYCL(IN)
1 = E12.5 )
XO=(2.*ZETA-1.)/A*.5*(6.2832-TI)**2-ZETA*SINF(TI)+(XDSTIS-ZETA*COS
1 F(TI))*(6.2832-TI)
DELX=XS2FL-XO-XSTI
DO 140 I=1,21
TINDEX=I

```

```

      T=(TINDEX-1.)*.31416
      IF(T-TFL)131,132,132
131 XD(I)={(2.*ZETA-1.)/A*(T+6.2832-TI)+ZETA*(COSF(T)-COSF(TI))+XDSTIS
      1)*VELFAK
      X(I)=DISFAK*(.5/A*(2.*ZETA-1.)*(T+6.2832-TI)**2+ZETA*(SINF(T)-SINF
      1(TI)))+(XDSTIS-ZETA*COSF(TI))*(T+6.2832-TI)-XJ)
      GO TO 140
132 IF(T-TI) 133,134,134
133 XD(I)=VELFAK*((ZETA-1.)/A*(T-TFL)+XDSTFL)
      X(I)=DISFAK*((ZETA-1.)*.5/A*(T-TFL)**2+XDSTFL*(T-TFL)+XSTFL+DELX)
      GO TO 140
134 XD(I)=VELFAK*((2.*ZETA-1.)/A*(T-TI)+ZETA*(COSF(T)-COSF(TI))+XDSTIS
      1)
      X(I)=DISFAK*(.5/A*(2.*ZETA-1.)*(T-TI)**2+ZETA*(SINF(T)-SINF(TI)))+(
      1XDSTIS-ZETA*COSF(TI))*(T-TI)+XSTI+DELX)
140 CONTINUE
      PUNCH 144
      PUNCH 141,(XD(I),I=1,21)
141 FORMAT(6E12.5)
      PUNCH 145
      PUNCH 141,(X(I),I=1,21)
      GET TRANS PTS
      XDITFL=VELFAK*XDSTFL
      XDITI=VELFAK*XDSTI
      XDITIS=VELFAK*XDSTIS
      PUNCH 142,XDITFL,XDITI,XDITIS
142 FORMAT(//1X,12HTRANS VELs 3E12.5 )
      XLITFL=DISFAK*(XSTFL+DELX)
      XLITI=DISFAK*(XSTI+DELX)
      XLIT2FL=DISFAK*(XS2FL+DELX)
      PUNCH 143,XLITFL,XLITI,XLIT2FL
143 FORMAT(1X,14H TRANS DISPLS 3E12.5 )
144 FORMAT(// 1X,18H VELOCITIES IN IPS FOR INCRS OF 2PI/20 )
145 FORMAT(//1X,32H DISPLS IN INCHES FOR SAME INCRS )
      RETURN
      END

```

APPENDIX A2. 6

THE PROGRAM FOR SOLUTIONS CONTAINING A RIDE

The solution routine for solutions with Rides is quite long and involved for, as it tests the operating conditions, it may go down any one of six paths. Hence, a briefer, less precise, description of the Fortran instructions is included. The numbers to the left of the description statements refer to the numbering of the Fortran program which follows this list. The numbering symbolism 41 + 1, refers to the first instruction in the Fortran program following statement number 41.

- 1 thru 13+5 The program computes $A, \phi, \zeta, \psi, \tau_1, \tau_2, \frac{\Delta \dot{X}}{\psi}, \tau_{bgd}, \tau_{egd}$
- 13 + 5 The velocity at the beginning of the Slide G Definite Zone is equal to the velocity of the plane.
- 13 + 6 The velocity at the time of flight, τ_1 , is obtained by using the Slide G velocity equation, (27c), between τ_{bgd} and τ_1 , thus, $\dot{X}(\tau_1)$ is obtained.
- 13 + 7 The velocity just prior to impact is obtained by applying the Flight velocity equation (Eq. (31c)) between τ_1 and τ_2 . Hence $\dot{X}(\tau_2)$ is obtained.
- 13 + 8 The velocity of the plane at impact is computed, by using Eq. (29b), at τ_2 . Hence, $\dot{X}'(\tau_2)$ is obtained.
- 14 - 1 A check is now made to assure that the particle velocity is not less than the plane velocity minus the maximum frictional impulse.
- 16 A check is next made to assure that Slide G Definite Zone does not extend beyond the time of impact.
- 20 A check is now made to see if a Slide L Definite Zone is possible (condition (38a)).

22 If an L Definite Zone is possible, τ_{bld} , and τ_{eld} , are computed.

26 If not, τ_{bld} , is set to zero for coding.

30 A check is now made to see if a Slide G or a Decision Time results from the impact, (42).
If a Decision Time results, jump to Step 150, otherwise continue.

31 Compute $\dot{X}(\tau_2^*)$, using (42b). A Slide G ensues.
Compute τ_{tg} , by using (39a).

40 + 1 Check τ_{tg} to see that it exceeds τ_2 .

43 Check τ_{tg} to see that it comes prior to $\tau_{bgd} + 2\pi$. If it does not, the Ride as was assumed is impossible.

45 Compute the velocity at τ_{tg} ; it equals that of the plane.

47 + 3 Check if a Slide L Definite Zone exists. If so, continue; if not, skip to Step 123.

48 Check if τ_{tg} , the slide termination, occurs before or after the beginning of the L Definite Zone, τ_{bld} . If after, skip to 90; if before, continue.
The particle undergoes a ride to τ_{bld} .

50 $\dot{X}(\tau_{bld})$ is computed equal to the plane velocity at that time.
A Slide L begins.

50 + 3 Compute τ_{tl} , using the Slide L Termination Eq. (39b).

60 + 1 Check τ_{tl} , to assure that it exceeds τ_{eld} .

65 Check τ_{tl} , to assure that it occurs prior to $\tau_{bgd} + 2\pi$; if not, the Ride as assumed is impossible.

69 Compute the velocity at τ_{tl} . It will equal the plane velocity at that time.

70 The solution is not complete and this path has led to a RGFGRL Solution.

- 70 thru 81 The program computes the remaining velocities and displacements, the average velocity and then stops.
- 90 Continuing from Step 48. The Slide G following impact had terminated beyond τ_{bld} . Now check to see if it occurs within the L Definite Zone, i.e., before τ_{eld} . If not, go to Step 118; if so, continue.
A Slide L ensues from τ_{tg} .
- 91 Compute τ_{tl} from the Slide L termination Eq. (39b).
- 97 + 1 Check to assure that τ_{tl} occurs past τ_{eld} .
- 102 Check to assure that τ_{tl} occurs prior to $\tau_{bgd} + 2\pi$. If not, the Ride as assumed is impossible.
- 106 Compute velocity at τ_{tl} , equal to plane velocity at that time.
- 107 The solution is now complete and this path has led to RGFGL Solution.
The program computes remaining velocities, displacements, and the average velocity.
- 118 Continuing from Step 90. An L Definite Zone existed, but particle continued in a Slide G Right through it. Go to Step 123.
- 123 Continuing from 47 + 3 and 118. This solution is now complete.
A ride follows τ_{tg} and continues through the end of the cycle. This is an RGFG Solution. The program calculates the remaining velocities, displacements and average velocity and then stops.
- 150 Continuing from Step 30. The impact has resulted in a Decision Time.
Compute $\dot{X}(\tau_2^*)$, equal to plane velocity at impact.
- 150 + 2 Check to see if a Slide L Definite Zone is possible. If not, skip to Step 180; if so, continue.

- 151 Check to see if τ_2 is less than τ_{bld} . If so, skip to 154; if not, continue.
- 152 Check to see if τ_2 is greater than τ_{eld} . If so, skip to 178; if not, continue.
- 153 The impact has resulted in a Decision Time in the L Definite Zone; a Slide L ensues. If the Slide L termination passes the tests, this leg will have resulted in a RGFL Solution.
Skip to 155.
- 154 Continuing from 151. The impact resulted in a Decision Time prior to the L Definite Zone, hence the particle undergoes a Ride to τ_{bld} .
Compute the velocity at τ_{bld} , equal to the plane velocity at that time. If τ_{tl} passes the tests, this path will have led to a RGFL Solution.
- 155 Continuing from 154 and 153. A Slide L ensues. Compute τ_{tl} from Slide L termination Eq. (39b).
- 160 + 1 Check τ_{tl} to assure that it occurs after τ_{eld} .
- 165 Check τ_{tl} to assure that it occurs prior to $\tau_{bgd} = 2\pi$.
If not, the Ride as assumed is impossible.
- 169 Compute velocity at τ_{tl} , equal to plane velocity. The solution is confirmed. The program computes remaining velocities, displacements, and average velocity.
- 178 Continuing from 152. An L Definite Zone exists, but the particle flew through it, thus no Slide L will occur.
- 180 Continuing from 178 and 150 + 2. No Slide L is possible after the Flight and hence a Ride initiates following the impact. This ride will continue until τ_{bgd} , and hence the solution is complete. This path has led to a RFG Solution.
- 182 The program computes the remaining velocities, displacements, and average velocities.

FORTRAN PROGRAM FOR SOLUTIONS WITH RIDES

```

C   GABE4
1  READ 4,AO,WOMEGA,WMU,ALPHAM,BETAM,EPS
2  FORMAT( 50H RESULTS OF ABBREVIATED SOLUTION - THOSE WITH RGF- )
   PUNCH 9,AO,WOMEGA,WMU,ALPHAM,BETAM,EPS
   PUNCH 2
3  FORMAT(1H 6H AO = F10.5,17H INCHES, OMEGA = F10.5,11H RPM, MU = F1
10.5/11H ALPHA = F10.5,17H DEGREES, BETA = F10.5, 6H DEGRS )
   PUNCH 3,AO,WOMEGA,WMU,ALPHAM,BETAM
4  FORMAT( 6F10.5)
   PUNCH 7,EPS
5  ALPHA = ALPHAM*3.1416/180.0
   BETA = BETAM*3.1416/180.0
   A=AO*WOMEGA**2*0.00028403*SINF(ALPHA-BETA)/COSF(BETA)
   PHI=(WMU+1.0/TANF(ALPHA-BETA))/(WMU+TANF(BETA))
   ZETA=WMU/(WMU+TANF(BETA))
   PSI=(WMU+TANF(BETA))*SINF(ALPHA-BETA)
   PUNCH 6,A,PHI,ZETA,PSI
6  FORMAT(/ 5H A = F10.5, 7H PHI = F10.5, 8H ZETA = F10.5, 7H PSI =
1 10.5)
7  FORMAT(1X,29H IMPACT LUBRICATION FACTOR = F10.5)
   TFL = ASINF(1.0/A)
   DISFAK=AO*PSI
   VELFAK=DISFAK*.10472*WOMEGA
   PLAVEL=VELFAK*(PHI-ZETA)
   PLADIS=DISFAK*(PHI-ZETA)
   PUNCH 8,PLAVEL,PLADIS
8  FORMAT(17H PLANE MAX X VEL= E12.5,13H MAX X DISPL= E12.5 )
9  FORMAT(//6F10.5)
   BE = -1.0/(2.0*A)
   CE = TFL/A+COSF(TFL)
   DE = -TFL**2/(2.0*A)-TFL*COSF(TFL)+1.0/A
   TI=1.57+SQRTF(11.0*(A-1.0))
10 TINEW=TI-(-SINF(TI)+BE*TI**2+CE*TI+DE)/(-COSF(TI)+2.0*BE*TI+CE)
   TEST=ABSF(TI-TINEW)
   IF(TEST-.00005)12,11,11
11 TI=TINEW
   GO TO 10
12 PUNCH 13,TFL,TINEW
   TI=TINEW
13 FORMAT( 21H FINAL VALUES TFL = F10.5, 9H TI = F10.5)
   DXDS=ZETA*((TI-TFL)/A+COSF(TI)-COSF(TFL))
   AIPH=1.0/(A*PHI)
   TBGD=ASINF(AIPH)
   TEGD=3.14159-TBGD
   XDSBGD=(PHI-ZETA)*COSF(TBGD)
   XDSTFL=(TBGD-TFL)/A-ZETA*(COSF(TFL)-COSF(TBGD))+XDSBGD
   XDSTI=(ZETA-1.0)*(TI-TFL)/A+XDSTFL
   XDSPTI=(PHI-ZETA)*COSF(TI)
   XDBGD=VELFAK*XDSBGD
   XDSTFL=VELFAK*XDSTFL

```

FORTRAN PROGRAM FOR SOLUTIONS WITH RIDES

```

XDTI=VELFAK*XDSTI
XTFL=0.
XTI=DISFAK*(.5/A*(ZETA-1.)*(TI-TFL)**2+XDSTFL*(TI-TFL))+XTFL
IF(XDSTI-XDSPTI+EPS*DXDS)14,14,16
14 PUNCH 15
15 FORMAT(44H FAILURE- PART VELOCITY TOO LOW AT IMPACT )
GO TO 400
16 IF(TEGD-TI)20,20,17
17 PUNCH 18
18 FORMAT(39H FAILURE SGD ZONE PERSISTS AFTER IMPACT )
GO TO 400
20 IF((1.-2.*ZETA)/A+PHI-2.*ZETA)25,25,22
22 AIPHP=(2.*ZETA-1.)/(A*(2.*ZETA-PHI))
TBLD=3.14159-ASINF(AIPHP)
TELD=6.28319+ASINF(AIPHP)
GO TO 30
25 PUNCH 26
26 FORMAT(/20H NO SLIDE L POSSIBLE )
TBLD=0.
30 IF(XDSTI -EPS*DXDS-XDSPTI)150,150,31
31 XDSTIS=XDSTI-EPS*DXDS
XDTIS=VELFAK*XDSTIS
TTG=4.712
C1=1./(A*PHI)
C2=(TI/A+ZETA*COSF(TI)+XDSTIS)/PHI
DO 35 I=1,10
F=COSF(TTG)+C1*TTG-C2
FP=C1-SINF(TTG)
TTGNEW=TTG-F/FP
TEST=ABSF(TTGNEW-TTG)
IF(TEST-.00005)40,35,35
35 TTG=TTGNEW
PUNCH 36,TTG
36 FORMAT( /43H FAILURE COULDN'T CONVERGE ON TTG, STOP ON E12.5 )
GO TO 400
40 TTG=TTGNEW
IF(TTG-TI)41,41,43
41 PUNCH 42,TTG
42 FORMAT( /29H FAILURE TTG UNDER TI, TTG= E12.5 )
GO TO 400
43 IF(TTG-TBGD-6.28319)45,45,44
44 PUNCH 47,TTG,TBGD
GO TO 400
45 XDSTTG=(PHI-ZETA)*COSF(TTG)
46 XDTTG=VELFAK*XDSTTG
47 FORMAT(38H FAILD IN GENL, TTG MORE THAN TBGD+2PI 2E12.5 )
XTTG=DISFAK*(-.5/A*(TTG-TI)**2-ZETA*(SINF(TTG)-SINF(TI)))+(ZETA*COS
1F(TI)+XDSTIS)*(TTG-TI))+XTI
IF(TBLD)123,123,48
48 IF(TTG-TBLD)50,90,90
50 XDSBLD=(PHI-ZETA)*COSF(TBLD)
XDBLD=VELFAK*XDSBLD
XBLD=DISFAK*(PHI-ZETA)*(SINF(TBLD)-SINF(TTG))+XTTG
TTL=6.28

```

FORTRAN PROGRAM FOR SOLUTIONS WITH RIDES

```

C1=(2.*ZETA-1.)/(A*(2.*ZETA-PHI))
C2=((1.-2.*ZETA)*TBLD/A-ZETA*COSF(TBLD)+XDSBLD)/(2.*ZETA-PHI)
DO 55 I=1,10
F=COSF(TTL)+C1*TTL+C2
FP=C1-SINF(TTL)
TTLNEW=TTL-F/FP
TEST=ABSF(TTLNEW-TTL)
IF(TEST-.00005)60,55,55
55 TTL=TTLNEW
PUNCH 56,TTL
56 FORMAT( /52H FAILURE COULDN'T CONVERGE ON TTL, IN RGFGR L STUPT AT
1 E12.5)
GO TO 400
60 TTL=TTLNEW
IF(TTL-TELD)62,65,65
62 PUNCH 63,TTL
63 FORMAT( /37H FAILURE, TTL IN RGFGR L UNDER TELD,= E12.5)
GO TO 400
65 IF(TTL-TBGD-6.28319)69,69,66
66 PUNCH 67,TTL,TBGD
67 FORMAT( /39H FAILURE IN RGFGR L,TTL MORE THAN TBGD, 2E12.5)
GO TO 400
69 XDSTTL=(PHI-ZETA)*COSF(TTL)
XDSTTL=VELFAK*XDSTTL
XTTL=DISFAK*(.5/A*(2.*ZETA-1.)*(TTL-TBLD)**2+ZETA*(SINF(TTL)-SINF(
TBLD)))+(XDSBLD-ZETA*COSF(TBLD))*(TTL-TBLD))+XBLD
PUNCH 70
70 FORMAT( /23H THIS IS AN RGFGR L SOLN )
PUNCH 72
72 FORMAT(29H TBGD,TEGD,TBLD,TELD,TTG,TTL )
PUNCH 73, TBGD,TEGD,TBLD,TELD,TTG,TTL
73 FORMAT(6E12.5)
PUNCH 74
74 FORMAT(42H XDBGD,XDSTFL,XDTI,XDTIS,XDSTTG,XDBLD,XDSTTL, )
PUNCH 75,XDBGD,XDSTFL,XDTI,XDTIS,XDSTTG,XDBLD,XDSTTL
75 FORMAT(6E12.5)
XBGD=DISFAK*(PHI-ZETA)*(SINF(TBGD)-SINF(TTL))+XTTL
X2TFL=DISFAK*(-.5/A*(TFL -TBGD)**2-ZETA*(SINF(TFL)-SINF(TBG
D)))+(ZETA*COSF(TBGD)+XDSBGD)*(TFL -TBGD))+XBGD
PUNCH 78
78 FORMAT(37H XTFL,XTI,XSTTG,XBLD,XTTL,XBGD,X2TFL )
PUNCH 79,XTFL,XTI,XSTTG,XBLD,XTTL,XBGD,X2TFL
79 FORMAT(6E12.5)
XDAVG=X2TFL*WOMEGA/60.
PUNCH 81, XDAVG
81 FORMAT(25H AVERAGE VELOCITY (IPS)= E12.5 )
GO TO 400
90 IF(TTG-TELD)91,118,118
91 TTL=6.28
C1=(2.*ZETA-1.)/(A*(2.*ZETA-PHI))
C2=((1.-2.*ZETA)*TTG/A-ZETA*COSF(TTG)+XDSTTG)/(2.*ZETA-PHI)
DO 94 I=1,10
F=COSF(TTL)+C1*TTL+C2

```

FORTRAN PROGRAM FOR SOLUTIONS WITH RIDES

```

FP=C1-SINF(TTL)
TTLNEW=TTL-F/FP
TEST=ABSF(TTLNEW-TTL)
IF(TEST-.00005)97,94,94
94 TTL=TTLNEW
PUNCH 95,TTL
95 FORMAT( /47H FAILURE COULDN'T CONVERGE ON TTL IN RGFGL,TTL= E12.5)
GO TO 400
97 TTL=TTLNEW
IF(TTL-TELD)98,102,102
98 PUNCH 99,TTL
99 FORMAT( /33H FAILD,TTL IN RGFGL UNDER TELD, = E12.5)
GO TO 400
102 IF(TTL-TBGD-6.28319)106,106,103
103 PUNCH 104,TTL,TBGD
104 FORMAT(34H FAILD IN RGFGL, TTL EXCEEDS TBGD, 2E12.5)
GO TO 400
106 XDSTTL=(PHI-ZETA)*COSF(TTL)
XDSTTL=VELFAK*XDSTTL
XTTL=DISFAK*(.5/A*(2.*ZETA-1.)*(TTL-TTG)**2+ZETA*(SINF(TTL)-SINF(
1 TTG)))+(XDSTTG-ZETA*COSF(TTG))*(TTL-TTG))+XTTG
PUNCH 107
107 FORMAT( /23H THIS IS AN RGFGL SOLN )
PUNCH 108
108 FORMAT(29H TBGD,TEGD,TBLD,TELD,TTG,TTL )
PUNCH 109,TBGD,TEGD,TBLD,TELD,TTG,TTL
109 FORMAT(6E12.5)
PUNCH 110
110 FORMAT(35H XDBGD,XDTFL,XDTI,XDTIS,XDTTG,XDTTL )
PUNCH 109,XDBGD,XDTFL,XDTI,XDTIS,XDTTG,XDTTL
XBGD=DISFAK*(PHI-ZETA)*(SINF(TBGD)-SINF(TTL))+XTTL
X2TFL=DISFAK*(-.5/A*(TFL -TBGD)**2-ZETA*(SINF(TFL)-SINF(TBG
1 D)))+(ZETA*COSF(TBGD)+XDSBGD)*(TFL -TBGD))+XBGD
PUNCH 115
115 FORMAT(30H XTFL,XTI,XTTG,XTTL,XBGD,X2TFL )
PUNCH 109,XTFL,XTI,XTTG,XTTL,XBGD,X2TFL
XDAVG=X2TFL*WOMEGA/60.
PUNCH 81, XDAVG
GO TO 400
118 PUNCH 119
119 FORMAT(/37H L POSS,BUT SLID G RIGHT THRU LD ZONE )
123 PUNCH 124
124 FORMAT(/21H THIS IS AN RGFG SOLN )
PUNCH 125
125 FORMAT(19H TBGD,TEGD,TBLD,TTG )
PUNCH 126,TBGD,TEGD,TBLD,TTG
126 FORMAT(4E12.5)
PUNCH 127
127 FORMAT(29H XDTFL,XDTI,XDTIS,XDTTG,XDBGD )
PUNCH 128,XDTFL,XDTI,XDTIS,XDTTG,XDBGD
XBGD=DISFAK*(PHI-ZETA)*(SINF(TBGD)-SINF(TTG))+XTTG

```

FORTRAN PROGRAM FOR SOLUTIONS WITH RIDES

```

X2TFL=DISFAK*(-.5/A*(TFL      -TBGD)**2-ZETA*(SINF(TFL)-SINF(TBG
1D)))+(ZETA*COSF(TBGD)+XDSBGD)*(TFL      -TBGD))+XBGD
PUNCH 129
128 FORMAT(5E12.5)
129 FORMAT(25H XTFL,XTI,XTTG,XBGD,X2TFL  )
PUNCH 128,XTFL,XTI,XTTG,XBGD,X2TFL
XDAVG=X2TFL*WO/IEGA/50.
PUNCH 81, XDAVG
GO TO 400
150 XDSTIS=(PHI-ZETA)*COSF(TI)
XDTIS=VELFAK*XDSTIS
IF(TBLD)180,180,151
151 IF(TI-TBLD)154,15?,152
152 IF(TI-TELD)153,178,178
153 PUNCH 300
XDBLD=0.
XBLD=XTI
XDSINP=XDSTIS
TINP=TI
GO TO 155
154 PUNCH 171
XDSBLD=(PHI-ZETA)*COSF(TBLD)
XDBLD=VELFAK*XDSBLD
XBLD=DISFAK*(PHI-ZETA)*(SINF(TBLD)-SINF(TI))+XTI
XDSINP=XDSBLD
TINP=TBLD
155 TTL=6.28
C1=(2.*ZETA-1.)/(A*(2.*ZETA-PHI))
C2=((1.-2.*ZETA)*TINP/A-ZETA*COSF(TINP)+XDSINP)/(2.*ZETA-PHI)
DO 156 I=1,10
F=COSF(TTL)+C1*TTL+C2
FP=C1-SINF(TTL)
TTLNEW=TTL-F/FP
TEST=ABSF(TTLNEW-TTL)
IF(TEST-.00005)160,156,156
156 TTL=TTLNEW
PUNCH 157,TTL
157 FORMAT(41H FAILD NO CONVERGE IN RGFRL ON TTL, TTL=  E12.5)
GO TO 400
160 TTL=TTLNEW
IF(TTL-TELD)162,165,165
162 PUNCH 163,TTL,TELD
163 FORMAT(44H FAILD, TTL IN RGFRL UNDER TELD, TTL,TELD=  2E12.5  )
GO TO 400
165 IF(TTL-TBGD-6.28319)169,169,166
166 PUNCH 167,TTL,TBGD
167 FORMAT(44HFAILD IN RGFRL,TTL EXCEEDS TBGD, TTL,TBGD=  2E12.5  )
GO TO 400
169 XDSTTL=(PHI-ZETA)*COSF(TTL)
XDSTTL=VELFAK*XDSTTL
XTTL=DISFAK*(.5/A*(2.*ZETA-1.)*(TTL-TINP)**2+ZETA*(SINF(TTL)-SINF(
1TINP)))+(XDSINP-ZETA*COSF(TINP))*(TTL-TINP))+XBLD
171 FORMAT(/24H THIS IS AN RGFRL SOLN  )

```

FORTRAN PROGRAM FOR SOLUTIONS WITH RIDES

```

PUNCH 172
172 FORMAT(24H TBGD,TEGD,TBLD,TELD,TTL )
PUNCH 173,TBGD,TEGD,TBLD,TELD,TTL
173 FORMAT(5E12.5)
PUNCH 174
174 FORMAT(37H XDTFL,XDTI,XDTIS,XDBLD,XDTTL,XDBGD )
PUNCH 109,XDTFL,XDTI,XDTIS,XDBLD,XDTTL,XDBGD
XBGD=DISFAK*(PHI-ZETA)*(SINF(TBGD)-SINF(TTL))+XTTL
X2TFL=DISFAK*(-.5/A*(TFL -TBGD)**2-ZETA*(SINF(TFL)-SINF(TBG
1D)))+(ZETA*COSF(TBGD)+XDSBGD)*(TFL -TBGD))+XBGD
PUNCH 175
175 FORMAT(30H XTFL,XTI,XBLD,XTTL,XBGD,X2TFL )
PUNCH 109,XTFL,XTI,XBLD,XTTL,XBGD,X2TFL
XDAVG=X2TFL*WOMEGA/60.
PUNCH 81, XDAVG
GO TO 400
178 PUNCH 179
179 FORMAT(/25H L POSS BUT FLEW THRU IT )
180 PUNCH 181
181 FORMAT(/20H THIS IS AN RGF SOLN )
PUNCH 182
182 FORMAT(15H TBGD,TEGD,TBLD )
PUNCH 183,TBGD,TEGD,TBLD
183 FORMAT(3E12.5)
PUNCH 184
184 FORMAT(24H XDTFL,XDTI,XDTIS,XDBGD )
PUNCH 185,XDTFL,XDTI,XDTIS,XDBGD
185 FORMAT(4E12.5)
XBGD=DISFAK*(PHI-ZETA)*(SINF(TBGD)-SINF(TI))+XTI
X2TFL=DISFAK*(-.5/A*(TFL -TBGD)**2-ZETA*(SINF(TFL)-SINF(TBG
1D)))+(ZETA*COSF(TBGD)+XDSBGD)*(TFL -TBGD))+XBGD
PUNCH 187
187 FORMAT(20H XTFL,XTI,XBGD,X2TFL )
PUNCH 185,XTFL,XTI,XBGD,X2TFL
XDAVG=X2TFL*WOMEGA/60.
PUNCH 81, XDAVG
300 FORMAT(/24H THIS IS AN RGFL SOLN )
400 GO TO 1
END

```

Fortran Symbols Table

| | |
|------------|---|
| A | A |
| ALPHA | α (RPM) |
| ALPHAM | α in degrees |
| AO | a |
| BE, CE, DE | the constants from (16) |
| BETA | β (radians) |
| BETAM | β in degrees |
| C1, C2 | dummy constants |
| DELTA | δ |
| DELX | same type of constant as XO |
| DISFAC | a constant to convert nondimensional displacement to inches |
| DXDS | $\frac{\Delta \dot{X}}{\psi}$ |
| EE | a constant in (46) |
| EPS | ϵ |
| GAMMA | γ |
| PHI | ϕ |
| PLADIS | the maximum plane y displacement in inches |
| PLAVEL | the maximum plane y velocity in inches per second |
| PSI | ψ |
| R | dummy variable, not used |
| T | τ |
| TBGD | τ_{bgd} |

Fortran Symbols Table

| | |
|--------|--|
| TBLD | τ_{bld} |
| TEGD | τ_{egd} |
| TELD | τ_{eld} |
| TFL | τ_1 |
| TGL | τ_{gl} , a transition time from a Slide G to a Slide L |
| TGLNEW | new value of τ_{gl} |
| TI | τ_2 |
| TINDEX | index |
| TINEW | the new value of τ_2 |
| TLG | τ_{lg} , a transition time from a Slide L to a Slide G |
| TTG | τ_{tg} |
| TTGNEW | new value of τ_{tg} |
| TTL | τ_{tl} |
| WMU | μ |
| WOMEGA | ω (RPM) |
| XBLD | $x(\tau_{\text{bld}})$ |
| XBGD | $x(\tau_{\text{bgd}})$ |
| XDAV | \dot{x}_{avg} |
| XDAVG | average x velocity (inches per second) |
| XDBGD | $\dot{x}(\tau_{\text{bgd}})$ |
| XDBLD | $\dot{x}(\tau_{\text{bld}})$ |
| XD(I) | velocity at $\tau = I \pi/10$ |
| XDLAV | average x velocity in inches per second |
| XDLTFL | $\dot{x}(\tau_1)$ |

Fortran Symbols Table

| | |
|--------|---|
| XDLTLG | $\dot{x}(\tau_{1g})$ |
| XDLTGL | $\dot{x}(\tau_{g1})$ |
| XDLTI | $\dot{x}(\tau_2)$ |
| XDLTIS | $x(\tau_2^*)$ |
| XDSAV | average non dimensional x velocity |
| XDSBGD | $\dot{X}(\tau_{bgd})/\psi$ |
| XDSBLD | $\dot{X}(\tau_{bld})/\psi$ |
| XDSPFL | $\dot{X}'(\tau_1)/\psi$ |
| XDSPTI | $\dot{X}'(\tau_2)/\psi$ |
| XDSTFL | $\frac{\dot{X}(\tau_1)}{\psi}$ |
| XDSTGL | $\dot{X}(\tau_{g1})/\psi$ |
| XDSTI | $\frac{\dot{X}(\tau_2)}{\psi}$ |
| XDSTIS | $\dot{X}(\tau_2^*)/\psi$ |
| XDSTLG | $\frac{\dot{X}(\tau_{1g})}{\psi}$ (x dot over ψ at τ_{1g}) |
| XDSTTG | $\dot{X}(\tau_{tg})/\psi$ |
| XDSTTL | $\dot{X}(\tau_{tl})/\psi$ |
| XDS2FL | $\dot{X}(\tau_1 + 2\pi)/\psi$ |
| XDS2LG | $X(\tau_{1g} + 2\pi)/\psi$ |
| XDTFL | $\dot{x}(\tau_1)$ |
| XDTI | $\dot{x}(\tau_2)$ |
| XDTIS | $\dot{x}(\tau_2^*)$ |

Fortran Symbols Table

| | |
|--------|---|
| XDTTG | $\dot{x} (\tau_{tg})$ |
| XDTTL | $\dot{x} (\tau_{tl})$ |
| X(I) | displacement at $\tau = I \pi/10$ |
| XLCYCL | Δx per cycle (inches) |
| XLDAV | \dot{x}_{avg} |
| XLTF1 | $x (\tau_1)$ |
| XLTGL | $x (\tau_{gl})$ |
| XLTLG | $x (\tau_{lg})$ |
| XLTI | $x (\tau_2)$ |
| XL2FL | $x (\tau_1 + 2 \pi)$ |
| XL2LG | $x (\tau_{lg} + 2 \pi)$ |
| XO | a constant used to make displacement zero at $\tau = 0$ |
| XSTFL | $X (\tau_1)$ |
| XSTI | $X (\tau_2)$ |
| XSTLG | $\frac{X}{\psi} (\tau_{lg})$ |
| XS2FL | $X (\tau_1 + 2 \pi)/\psi$ |
| XS2LG | $X (\tau_{lg} + 2 \pi)/\psi$ |
| XTFL | $x (\tau_1)$ |
| XTI | $x (\tau_2)$ |
| XTTG | $x (\tau_{tg})$ |
| XTTL | $x (\tau_{tl})$ |
| X2TFL | $X (\tau_1 + 2 \pi)$ |
| X2TFL | $x (\tau_1 + 2 \pi)$ |
| X2LG | $x (\tau_{lg} + 2 \pi)$ |
| ZETA | ζ |

APPENDIX A3
DETAILS OF EXPERIMENTAL APPARATUS

APPENDIX 3. 1

A DESCRIPTION OF THE MACHINE

Figures 10 and 11 show the machine. The plane is constructed of a 2 inch styrofoam core sandwiched between two 1/4 inch plywood sheets. The plane was one foot long and four feet wide. The plane is pivoted at its center of gravity to two arms extending out from the slider. This pivot made adjustment of the angle β possible. The slider is essentially a stiff wooden box with two arms on one end to support the plane, and a neck on the other end to receive motion from the connecting rod. On the undersurface of the slider two bronze bushing pillow blocks are attached in a straight line. These pillow blocks slide on a 3/4 inch diameter steel guide rod and guide the motion of the slider in a straight line. To eliminate roll and backlash, two ball bearings used as wheels are pressed up against the undersurface of the slider six inches either side of the centered pillow blocks. Steel plate tracks are bonded to the underside of the slider for the wheels to bear against. This is perhaps seen in better detail in Figure 11. The guide rod, on which the pillow blocks slide, is attached to a 24 inch long 4 inch square wooden beam. This beam also had the two ball bearing wheel assemblies cantilevered out from its center. The elevation of the two wheels could be raised or lowered to permit crosswise leveling of the slider and compensate for wear. One of the wheels could be forced tight with a tightening bolt to load the wheels and pillow blocks, thereby eliminating backlash. The beam was pivoted to a large wooden base, which permitted adjustment of the angle α . The base was essentially a tripod of three wooden "two-by-fours," bonded to a triangle of "four-by-fours." This triangle was in turn bolted securely to a massive T-slotted bed plate. The tripod of "two-by-fours," was completely skirted with 1/4 inch plywood bonded on all its edges to the "two-by-fours" and the "four-by-fours"; this was essential to provide torsional stiffness to the base.

Atop the tripod of "two-by-fours" was bonded a horizontal plate of three inch plywood. On the top surface of this plate two vertical triangular plates of two-inch plywood were bonded. These plates carried the bolt that pivoted the beam. An attempt was made to keep everything as stiff as possible, in order to assure pure translation of the plane.

The slider was driven by a 45 inch connecting rod, bolted to the neck of the slider. On the other end of the connecting rod was a bracket to contain a 3/8 inch ball bearing, which was in turn bolted to a crank plate. The connecting rod was fabricated out of 1 inch diameter, .049" wall, aluminum tubing.

The 1/2" thick steel crank plate contained a series of tapped holes (to receive the connecting rod bearing) so that the amplitude could be varied from 3/4 to 3 inches. It was welded to a hub which was bolted to a 3/4 inch steel idler shaft. This shaft was supported by two cast iron ball bearing pillow blocks. The pillow blocks were bolted to two vertical one inch thick steel plates, and these plates in turn were bolted to a large one inch steel base plate. This steel base plate was supported on large wooden blocks so that the elevation of the idler shaft could be adjusted for different angles, α . By using pipes and long bolts, as shown in the figure, this whole idler assembly was securely bolted to the bed plate. The idler shaft also contained a 14 inch V-pulley and a perforated disc. The perforations were 3/16 inch holes and the disk was 1/4 inch thick aluminum. The perforations were drilled in a circle of three inch radius and were spaced 12° apart. These perforations triggered a fast blinking strobe light. The V-pulley was driven by a large 1/2 HP variable speed electric motor, that was mounted on wooden beams so that it could be bolted to the bed plate in any desired position.

The channel used for the testing of granular material was constructed out of 1/4 inch plywood (see Figures 12 and 13). The transparent front was plexiglass. The channel was attached to the plane with fiberglass pressure sensitive tape. The width of the channel could be changed by adjusting a movable wall which was attached with screws and wing nuts.

All of the wooden joints were bonded with epoxy resins, which proved a very satisfactory fabrication technique.

An equipment list is included as Appendix A3.3.

Particular construction details are not always apparent. For example, the upper surface of the plane was made of standard lumber yard grade of 1/4 inch fir plywood. Effort was being made to construct light yet stiff plane. This surface was out of flat in excess of .020 inch, making appreciable hills and valleys on the surface. This situation was remedied by moulding a flat surface onto the top of the wood. A thin layer of unfilled epoxy resin (Sears Roebuck and Company Cat.No. 6H62851) was poured on a large piece of 1/4 inch plate glass; the upper surface of the plane was placed upon this layer of liquid epoxy and left in position until the epoxy had cured. Some bubbles resulted and these were filled with an automotive body putty. The surface was painted black with two coats of enamel, and then thoroughly rubbed with powdered pumice to obtain smoothness and uniformity. Careful measurements with a long straightedge and a feeler gage showed the resulting surface flat throughout within .002 inch.

Another example is the connecting rod. The anticipated maximum driving frequency was 7 cps (420 RPM), the natural frequency of the rod was approximately 16.5 cps (calculated) (Ref. 20.p, 432). The maximum anticipated acceleration of the slider was 10 g's; the weight of the slider plus the plane was approximately 20 lbs. Hence a 200 lb.

load was anticipated. This load gave a direct compressive stress of 1200 psi in the rod. The critical buckling load for this pin ended column was calculated in excess of 900 lbs. Thus, the design was adequate.

As to the effectiveness of the sandwich construction of the bed, natural frequency calculations, utilizing beam theory, give favorable results. The lowest mode of the plane supported in the center as it is, would be a kind of a symmetric umbrella mode. Since the table is four feet long, this mode would have the same frequency as a cantilever or clamped-free beam 2 feet long. Using the formula from Ref. 20 (p. 432) the frequency is calculated to be in excess of 150 cps, quite far above the maximum driving frequency of 7 cps.

The 45 inch connecting rod was necessary to assure essentially sinusoidal motion. Ref. 18 shows that the error in acceleration of sine wave produced by a slider-crank mechanism is approximately equal to the ratio of eccentric distance to the connecting rod length. Thus when the displacement amplitude was one inch, the error in acceleration of the plane was approximately 2%.

APPENDIX A3.2

THE TRIGGERING OF THE STROBOSCOPIC LAMP

This was accomplished by causing a lamp to shine on a black perforated disk, which caused an interrupted beam of light to strike a photocell. The photocell drastically and quickly drops in resistance from about 20 megohms in darkness to about 130,000 ohms when excited by the light. The configuration and circuit is diagramed in Figure A3.1.

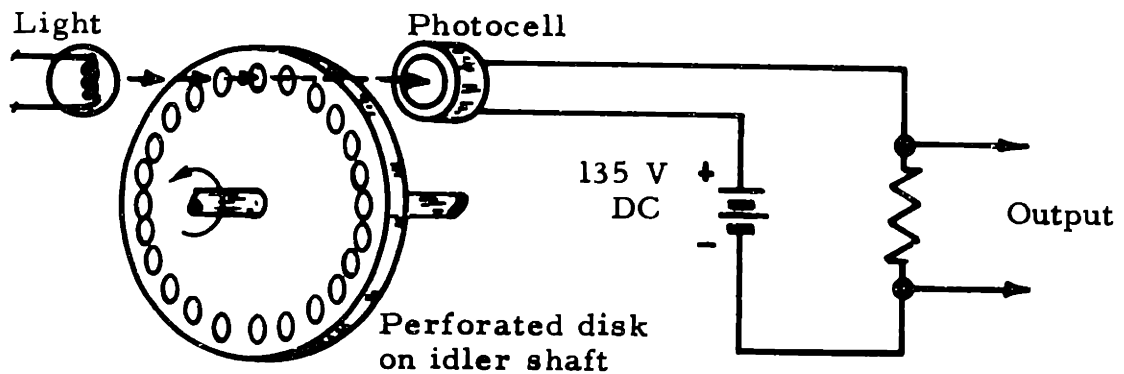


Figure A3.1 Stroboscopic Lamp Trigger

The resistor is of the order of 2 megohms; thus when the cell is dark, there is essentially no voltage drop across the resistance, but in the presence of light almost the full battery voltage is across the resistance. The two leads from the resistance give a pulse of voltage each time a hole in the disk permits light to strike the photocell. This voltage pulse was used to trigger the stroboscopic lamp. Ref. 16, describes the voltage pulse requirements and is quite helpful in the design of these triggering circuits. The lamp (a six volt pilot lamp, powered by a filament transformer) was encased in a small tube and emitted a tiny ray of light out of a pin hole. The ray was aimed at the photocell. All parts were painted flat black. When it was desired to

cover certain holes in the disk, to alter the number of flashes per cycle, black plastic electrical insulating tape was placed over the holes. The specifications of the various components are contained in the equipment list following this section.

APPENDIX A3. 3

EQUIPMENT LIST

Motor: Master Electric Company - Style 112773
115 V. A. C. ; 1725 RPM (Equipped with
Master "Speed Ranger"; RPM (180-2760)).

Stroboscopic Lamp: General Radio Company; "Type 1531A Strobotac"

Tachometer: Foxboro Company; S-6/3. 4000; # 85772

Camera: Yashica Model 635 - Twin Lens Reflex Type

Camera Rotator Motor: Bodine Type KYC-22RC, Synchronous Motor
4946194; 110 V. A. C. ; 4 RPM

Enlarger: Omega Model D II

Photocell: Clairex # CL 703

Counter: Lafayette Radio Corporation # 99R 9011; 110 V. A. C.

Timer: Dimco-Gray Company; GRALAB Model # 168.

BIBLIOGRAPHY

1. Blekhman, I. I., and Dzhanelidze, G. Iu. "Vibratsionnoe Peremeshchenie" (Vibrational Transporting). Izdatel'stvo Nauka (Publishing house, science), Moskva (Moscow) 1964.
2. Taniguchi, O., Sakata, M., Suzuki, Y., and Osanai, Y.; "Studies on Vibratory Feeder", Bulletin of the Japan Society of Mechanical Engineers; Vol. 6, No. 21; 1963.
3. Paz, Mario. "Conveying Speed of Vibrating Equipment", ASME Paper Number 64-WA/MH-1.
4. Bolz, H. A., ed. "Vibrating and Oscillating Conveyors". Materials Handling Handbook, Section 29, Ronald Press Company, New York.
5. Booth, J. H., and McCallion, H. "On Predicting the Mean Conveyor Velocity of a Vibratory Conveyor". Proc. Instn. Mech. Engrs., v 178, pt 1, n 20, pp. 521-538, 1963-64.
6. Berry, P. E. "Research on Oscillating Conveyors". Journal of Agricultural Engineering Research, v 3, n 3, pp. 249-259, 1953.
7. Troitskii, V. A. "On the Optimization of a Vibration Transporter Process". PMM; Applied Mathematics and Mechanics, v 27, n 6, pp. 1715-26, 1963.
8. Schertz, C. E., and Hazen, T. E. "Predicting Motion of Granular Material on an Oscillating Conveyor". Am. Soc. Agric. Engrs. Trans. v 6, n 1, pp. 6-10, 1963.
9. Wolff, E. "The Motion of Bulk Materials on Vibratory Conveyors". ASME Paper Number 62-WA-41, 1962.
10. Gutman, I. "Vibratory Conveyors". Engineers' Digest, v 24, n 5, pp. 93-100, May 1963.
11. Burton, D. W. "Movement of Material on Oscillating Trays". Rept. No. K-1186, Union Carbide Nuclear Company; Oak Ridge, Tenn., 1954.
12. Wehmeier, K. H. "Schwingfoerderrinnen-Eine Systematik der Bauformen und ihrer Eigenarten" (Vibrating Conveyors - Calculation, Design and Operation). Foerdern u Heben, v 14, n 3, pp. 155-161, March 1964.

BIBLIOGRAPHY (CONTINUED)

13. Rachner, H. G., and Jungk, L. "Schwingfoerderer in Giessereien" (Vibrating Conveyors in Foundries). *Giesserei*, v 51, n 7, pp. 172-182, Apr. 2, 1964.
14. Rabinowicz, E. "The Intrinsic Variables Affecting the Stick-Slip Process". *Proceedings of the Physical Society*, Vol. 71, p. 668, London, 1958.
15. Burrington, R. S. "Mathematical Tables and Formulas". Handbook Publishers, Inc., Sandusky, Ohio, 1955.
16. "Handbook of High Speed Photography", General Radio Company, West Concord, Mass., 1963.
17. Pipes, L. A. "Applied Mathematics for Engineers and Physicists", McGraw-Hill Book Company, New York, 1958.
18. Biezeno, C. B., and Grammel, R. "Engineering Dynamics, Vol. IV-Internal Combustion Engines". Translated from German by M. P. White, Blackie and Sons, Limited; London, 1954.
19. Jenike, A. W. "Steady Gravity Flow of Frictional-Cohesive Solids in Converging Channels". *Trans. ASME, J. App. Mechs., Series E*, Vol. 31, p. 5, March 1964.
20. Den Hartog, J. P. "Mechanical Vibrations". 4th edition, McGraw-Hill Book Company, Inc., New York, 1956.
21. Guthrie, J. J., Jr., and Morris, J. M. "Electromechanical Feeding and Proportioning of Bulk Solids". ASME Paper Number 65-MH-6, 1965.

BIOGRAPHICAL NOTE

The author was born in Detroit, Michigan, on April 11, 1931. He attended school in Dearborn, Michigan, graduating from Fordson High School in 1949. He began his college education at Wayne State University in Detroit, and later transferred to the University of Michigan in Ann Arbor, where he was awarded the degree of Bachelor of Science in Mechanical Engineering in 1955. He was then awarded a Teaching Assistantship at the Massachusetts Institute of Technology where he pursued graduate study and was awarded the degree of Master of Science in Mechanical Engineering in 1957.

He then accepted a position as a Mechanical Engineer in the field of Applied Mechanics at the Raytheon Corporation in Wayland, Massachusetts. In 1959 he accepted a position as an Assistant Professor of Mechanical Engineering at the Lowell Institute of Technology, and in 1960 he accepted a position as an Assistant Professor of Mechanical Engineering at Boston University, where he remained until 1964. At that time he was awarded a Science Faculty Fellowship by the National Science Foundation which permitted him to resume graduate study. Throughout his five years of teaching, he was employed part time by many engineering firms in the area, including Lessells and Associates, Brewer Engineering Laboratories, The Woods Hole Oceanographic Institute, and the Instrumentation Laboratory at M. I. T. He also spent two summers in Los Angeles as Staff Engineer in Applied Mechanics for Space Technology Laboratories and North American Aviation Company.

He is a member of Tau Beta Pi, Sigma Xi, The American Society of Mechanical Engineers, The National Society of Professional Engineers, The American Society of Engineering Education, and the Society for Experimental Stress Analysis. He is a registered professional engineer in Massachusetts and Michigan.